FOSSIL

DOE/PC/89806-T1
(DE91009051)

CONFINED VORTEX SCRUBBER

Final Technical Report

December 1990
Date Prepared

Work Performed Under Contract No. AC22-89PC89806

For
U.S. Department of Energy
Pittsburgh Energy Technology Center
Pittsburgh, Pennsylvania

By
Avco Research Laboratory, Inc.
Everett, Massachusetts

DISCLAIMER

This report has been reproduced directly from the best available copy.

Available to DOE and DOE contractors from the Office of Scientific and Technical Information, P.O. Box 62, Oak Ridge, TN 37831; prices available from (615)576-8401, FTS 626-8401.

Available to the public from the National Technical Information Service, U. S. Department of Commerce, 5285 Port Royal Rd., Springfield, VA 22161.

Printed in the United States of America. Office of Scientific and Technical Information, Oak Ridge, Tennessee

CONFINED VORTEX SCRUBBER

FINAL TECHNICAL REPORT

Date Prepared

December 1990

prepared for
U.S. DEPARTMENT OF ENERGY
Pittsburgh Energy Technology Center
P.O. Box 10940
Pittsburgh, Pennsylvania 15236

by
AVCO RESEARCH LABORATORY, INC.
a subsidiary of Textron Inc.
2385 Revere Beach Parkway
Everett, Massachusetts 02149

Under Contract No. DE-AC22-89PC89806

DOE/PC/89806--T1

DE91 009051

CONFINED VORTEX SCRUBBER

FINAL TECHNICAL REPORT

Date Prepared

December 1990

Prepared for

U.S. DEPARTMENT OF ENERGY

Pittsburgh Energy Technology Center
Pittsburgh, Pennsylvania 15236

by

AVCO RESEARCH LABORATORY
a subsidiary of Textron Inc.

2385 Revere Beach Parkway
Everett, Massachusetts 02149

Under Contract No. DE-AC22-89PC89806

TABLE OF CONTENTS

LIST OF ILLUSTRATIONS

LIST OF TABLES

EXECUTIVE SUMMARY

A novel fine particulate control concept based on a Confined Vortex Scrubber (CVS) has been proven in an experimental program. The overall program objective was to demonstrate efficient removal of fine particulates to sufficiently low levels to meet proposed small-scale coal combustor emission standards. This objective has been met for a simulated coal flue gas at ambient temperature: greater than 99 percent capture of extremely fine fly ash (mean particle size of 3 microns) has been demonstrated in the CVS at low pressure drops and low liquid flow rates. Projected particulate emissions from a small-scale coal combustor equipped with a Confined Vortex Scrubber would be well below the proposed emissions limit of 0.02 lbs/MM Btu.

The Confined Vortex Scrubber, which is illustrated schematically in Figure E-1, consists of a cylindrical chamber with multiple tangential flue gas inlets. The clean gas exit is via two vortex finder outlets, one at either end of the tube. Liquid is introduced into the chamber and is confined within the chamber by the centrifugal force generated by the gas flow itself. This confined liquid forms a layer through which the flue gas is then forced to bubble, producing a strong gas/liquid interaction, high inertial separation forces and efficient particulate cleanup. In effect, each of the sub-millimeter diameter gas bubbles traversing the liquid layer acts as a micro-cyclone, inertially separating particles into the surrounding liquid. The CVS thus obtains efficient particle removal by forcing intimate and vigorous interaction between the particle laden flue gas and the liquid scrubbing medium. The end wall secondary flows which occur in all cyclonic type flows are explicitly used as a removal path for water laden with solids inertially separated from the bulk flow.

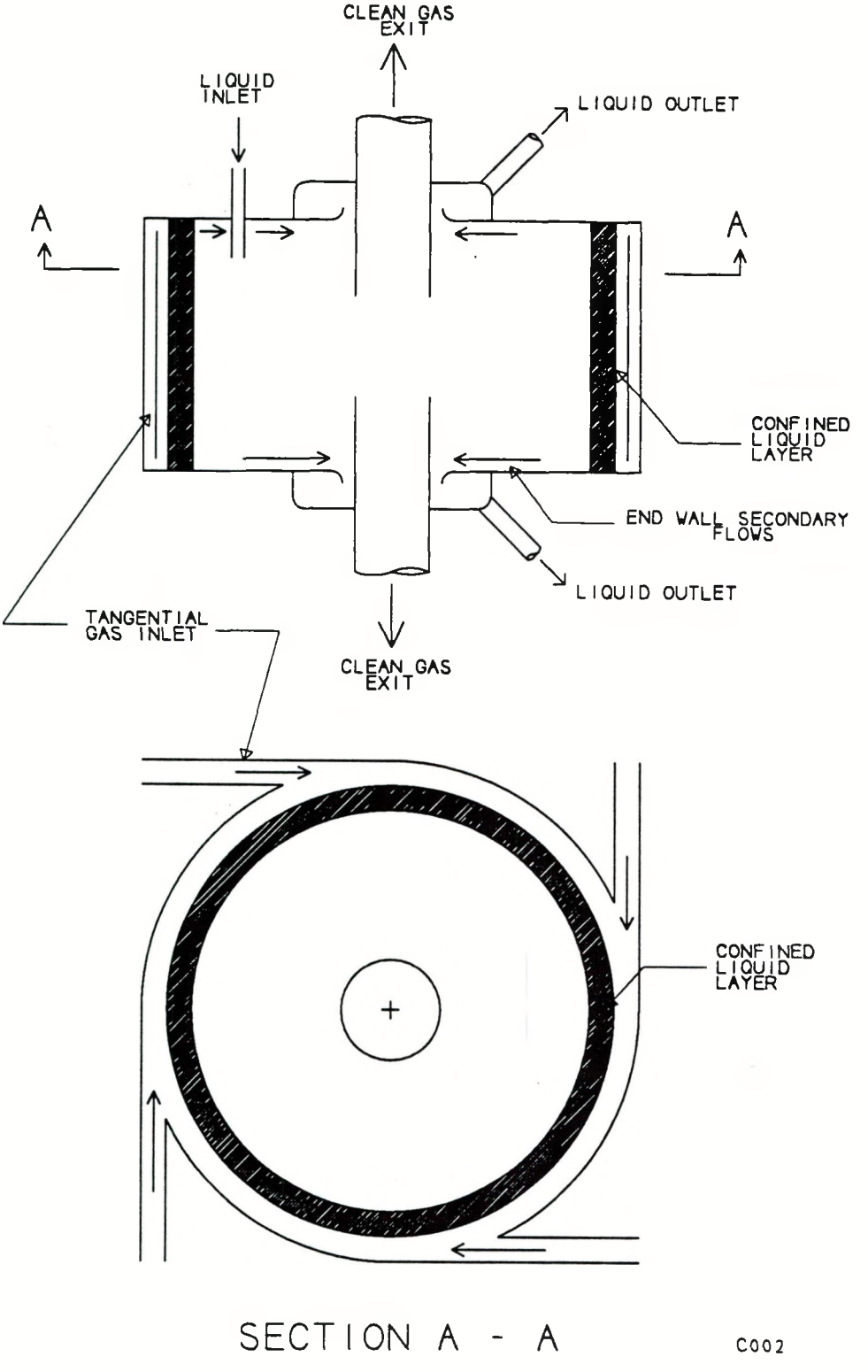

Figure E-1 Schematic Diagram of Confined Vortex Scrubber Concept

A twelve month experimental program was carried out in order to demonstrate and optimize the cleanup performance of the CVS. Tests were conducted on a model CVS at a mass flow equivalent to the exhaust gas flow of a 1 MM Btu/hr combustor. The test gas was essentially at ambient temperature and pressure. A modular design approach was adopted in order to allow rapid and simple modification of the CVS chamber geometry and of the air and water inlet and outlet geometries. The experimental hardware was assembled and installed at Avco Research Laboratory's Haverhill, Massachusetts test facility.

The experimental work was divided into two main areas: two-phase flow experiments and cleanup experiments. A comprehensive series of two-phase flow experiments were conducted on a variety of CVS configurations prior to performing fly ash cleanup tests. The goal of these experiments was to develop a CVS configuration with a stable flow field, high radial acceleration, good liquid confinement and an acceptable pressure drop. Initial testing concentrated on CVS geometry optimization from the point of view of pressure drop. Two principal CVS designs, the dual-inlet CVS and the squirrel cage CVS, were tested. The former gave adequate radial accelerations and pressure drops, but low liquid containments. The latter design met all performance goals.

Results for the initial dual-inlet CVS design, which has two tangential air inlet slots, indicated that a sheet of water could indeed be established and contained within the CVS chamber and that the water removal mechanism via the chamber end wall secondary flows was effective. However, subsequent experiments indicated several areas of concern, principal among which was a low level of liquid containment (3 to 4 percent of chamber volume). The liquid layer in the CVS was thin and the inlet air jets penetrated the liquid layer completely, leading to relatively poor air/liquid interaction. In other words, the inlet jets were not submerged, as desired. The lack of submerged inlet jets and of a vigorous air/liquid interaction suggested that

the desired level of particulate removal may not be obtained.

These problems were corrected in a revised CVS design. The modified design has 24 tangential slot inlets as opposed to the two in the initial CVS design. Two-phase flow tests of the new design (the "squirrel cage" design) indicated that a very different flow field existed in the squirrel cage chamber compared to that in the dual-inlet CVS chamber. The inlet air jets were now clearly submerged beneath a much thicker liquid layer than had been observed for the initial design. There was an extremely vigorous interaction between the air and the liquid: the liquid layer appeared thick and frothy in nature. The liquid mass contained within the CVS increased dramatically to a maximum of approximately 20 percent of chamber volume. The device pressure drop was found to be lower with a liquid layer present than without such a layer. The squirrel cage CVS design exceeded the performance objectives established for these experiments.

The objective of the cleanup experiments were to verify the CVS cleanup concept and to demonstrate efficient removal of fine particulates to sufficiently low levels to meet proposed small-scale combustor emission standards. A variety of dust size distributions and materials were tested. Dust and ash were fed to the CVS using a fluidized bed particle feeder at flow rates such that the CVS inlet gas simulated flue gases from the combustion of coal with ash contents in the range 1 to 5 percent. Shakedown experiments were made using fine silica and alumina dusts. Most of the cleanup tests were made with ultra-fine fly ash for which d_{10}, d_{50}, d_{90} = 1, 3, 8 microns as fed (10 percent of the mass of the dust is contained in particles of diameter d_{10} or smaller, 50 percent in particles of diameter d_{50} or smaller and 90 percent in particles of diameter d_{90} or smaller). This ultra-fine fly ash was generated by classifying fly ash in a cyclone separator. Three CVS configurations, all of the squirrel cage design, were tested. All three demonstrated extremely efficient capture of the ultra-fine fly ash: typical collection efficiencies

are greater than 99 percent and have been measured at up to 99.8 percent. Tests have also been made with fine silica and alumina dust, as well as larger grinds of fly ash (200 and 325 mesh). The CVS is also extremely efficient at capturing sub-micron particles: 98 percent collection for 0.3 micron alumina particles has been demonstrated.

The final CVS configurations tested produced greater than 99 percent capture of extremely fine fly ash (mean particle size of 3 microns) at low pressure drops (10 - 20 in. water) and low liquid flow rates (0.3 l/m^3). Device operation was simple and reliable: the two-phase flow field in the device proved to be very stable. The collection efficiency of the device was found to increase with increasing air mass flow (and hence tangential inlet velocity). This trend agrees with that predicted from a first order inertial separation analysis: increasing the radial gas injection velocity increases the radial acceleration field, leading to smaller gas bubbles with higher internal velocities, thereby leading to a smaller particle cut diameter and increased separation efficiency. Provided that the liquid flow rate is sufficient to establish a thick liquid layer, the collection performance was found to be insensitive to liquid flow rate. The CVS collection performance was also found to be insensitive to inlet particulate loading, unlike venturi scrubber collection performance. In order to control deposition in the plenum which feeds the inlet slots, liquid can be introduced via the plenum instead of directly into the CVS chamber. This has no effect on ash collection performance. Reducing the surface tension of the liquid in the chamber by introducing surfactants was found to produce a drop in both collection efficiency and pressure drop. These two effects appear to be correlated.

The size distributions of the ash entering the CVS, the ash collected in the water and the ash collected in the downstream filter were found to be very similar. This suggests that the CVS does not have a classic inertial separator-type grade efficiency curve, with high collection efficiency for larger particles and progressively lower collection efficiency for smaller particles.

Rather, it suggests that the CVS has a uniformly high collection efficiency for particles of all sizes (in the range exhibited by the fly ash used) and the mechanism by which a very small fraction of the inlet ash is passed through the CVS is connected with either failure to contact all the inlet air with the water or with re-release of a small fraction of the separated ash from the water. At present there is insufficient evidence to determine the precise mechanisms involved.

Results from the cleanup experiments show an exponential relationship between the cleanup performance and the radial acceleration in the device. This relationship correlates measured cleanup data from three different diameter scrubbers over a wide range of radial accelerations. This together with physical considerations of the two-phase flow field suggest that the bubble size in the liquid layer is a key parameter in obtaining highly efficiency fine particle removal. The bubble size is reduced as the radial acceleration field in the CVS is increased. The radial acceleration can be increased by either reducing the device radius or increasing the inlet tangential velocity. Both of these tend to increase the device pressure drop. This suggests that although the CVS has a much more favorable scaling characteristic than most inertial separation devices, there may be a physical limit to the flow that could be handled by a single CVS at a reasonable pressure drop. At flows greater than this multiple CVS units can be employed to given efficient cleanup at low pressure drop.

In summary, a 12 month experimental program has led to the proof of a novel fine particulate cleanup concept based on a Confined Vortex Scrubber. A program of two-phase vortex experiments led to the development of a CVS which produces high radial accelerations, good liquid containment, an extremely vigorous air/liquid interaction and low pressure drop. The CVS design retains the mechanical simplicity of conventional reverse flow cyclone separators, but has far superior collection performance for fine particulates. Results from cleanup experiments show collection efficiencies in excess of 99 percent for fine fly ash (mean

particle size 3 microns) at low pressure drops and liquid flow rates. A collection efficiency of 98 percent has also been demonstrated for 0.3 micron particles. The device also has the potential for controlling SO_x emissions by suitable choice of the liquid scrubbing medium.

Under this contract the CVS concept has been verified at room temperature conditions and at small scale using a simulated coal flue gas. In order to allow further development of the device, tests should be carried out both at realistic flue gas temperatures and at larger scales. In addition, the potential for SO_x and NO_x removal should be evaluated. Future development work could be divided into the following areas (1) Conduct cleanup tests at high temperature coal flue gas conditions at the same small scale as the tests reported here; (2) Develop and test a larger scale device (capable of cleaning 25 times the flow-rate of the small unit) to be tested initially at ambient conditions and subsequently at realistic flue gas conditions; and (3) Test the potential of the CVS for SO_x (and possibly NO_x) removal.

1.0 INTRODUCTION

This is the final technical report under this contract and describes the design, fabrication, testing of a novel fine particulate control device, the Confined Vortex Scrubber (CVS). The CVS is a simple yet highly efficient fine particle control device which is suited for application to small scale coal combustor flue gas cleanup.

1.1 PROGRAM OBJECTIVE AND BACKGROUND

The program objective was to demonstrate efficient removal of fine particulates to sufficiently low levels to meet proposed small-scale coal combustor emission standards. This was to be accomplished using a novel particulate removal device, the Confined Vortex Scrubber. This objective was met for a simulated coal flue gas at ambient temperature conditions.

Increased utilization of the extensive domestic coal reserves will reduce the United States' dependence on imported oil. Though total coal consumption has been increasing in the U.S., there has been a shift in usage: 85 percent of the coal burned today is accounted for by utility power generation. Natural gas and oil use in the industrial, commercial and residential sectors currently accounts for approximately one quarter of the total US energy consumption. In order to increase its utilization in these markets, coal must be burnt in an environmentally and economically acceptable manner at small scales. This requires significant advances in the areas of coal preparation, small-scale combustor design and flue gas cleanup. Research is currently ongoing in the areas of coal preparation techniques and advanced combustor designs. Practical limitations to advances in these areas in the near term require the development of improved flue gas cleaning methods for small-scale coal combustors. In order to be acceptable at smaller scales, flue gas cleaning devices must be simple and reliable, with a minimum maintenance

requirement.

Particulate emission from coal burning can cause a variety of deleterious effects, both on man and in his environment. Fine particles can be particularly damaging: particles larger than 10 microns in diameter tend to be deposited in the nose on inhalation, those between 5 and 10 microns tend to be deposited in the bronchii, while those smaller than 2 microns can penetrate efficiently into the lower lung and alveoli. Depositions in the lung can lead to bronchitis, emphysema and, in the case of severe build up, silicosis. Prolonged exposure to fine particulates can also lead to heart disease, due to the reduced oxygenation capability of the lung. Particles between 0.4 and 0.8 microns tend to cause the greatest restrictions in visibility, while particles below 0.1 microns can induce nucleation of water droplets, and lead to weather modification. Fine particulates can also inhibit respiration and photosynthesis in plants. Thus control of fine particulate emission is now a significant concern in the development of advanced coal burning systems, and may in the future become a stringent limitation.

Some of the emission control approaches used at the utility scale may remain attractive at a small scale, provided that maintenance requirements are low. Others are not attractive for low maintenance, small-scale operation. Electrostatic precipitators, for example, are expensive, as well as being bulky, and are very sensitive to changes in flow rate. Inertial separation devices such as conventional cyclones are much more attractive. They are cheaper and simpler devices, and have high separation efficiencies for particles larger than approximately 10 microns in diameter. However, the separation performance of conventional inertial separators falls off very rapidly for particles smaller than this.

Typical small-scale coal combustor fuel sizes (whether supplied dry or as a coal-water slurry) are considerably smaller than in conventional pulverized coal fired boilers. Fuel size distributions are expected to be -325 mesh (22 micron mean diameter, 45 micron top size) or

smaller. The proposed particulate emission requirement is less than 0.02 lbs/MM Btu (Gyorke, 1987). Thus for coals with ash contents in the range 1 - 2 percent, total fly ash collection efficiencies in the range 97 - 99 percent are required. Removal of 99% of the fly ash produced from combustion of such fine fuels requires cleanup technologies significantly more effective then those currently employed or proposed. Control of emissions of fine particulates is particularly important for this class of combustors, given the very fine coal particles being burned. Another source of very fine particles in coal combustion is heavy metal condensates: this source exists in many coal combustion systems, not just those of small size. The proposed particulate cleanup device, the Confined Vortex Scrubber, has several novel features which lead to highly efficient fine particulate removal and is described below.

1.2 CLEANUP CONCEPT

The CVS, which is illustrated in Figure 1-1, consists of a cylindrical chamber with multiple tangential flue gas inlets. The clean gas exit is via two axial tubes or vortex finders. Liquid is introduced into the chamber and is confined within the vortex chamber by the centrifugal force generated by the gas flow itself. This confined liquid forms a layer through which the flue gas is then forced to bubble. Due to the high radial acceleration field, the bubbles generated are very small, leading to a strong gas/liquid interaction, high inertial separation forces and efficient particulate cleanup. In effect, each of the sub-millimeter diameter gas bubbles traversing the liquid layer acts as a micro-cyclone, inertially separating particles into the surrounding liquid.

The establishment of a simple, steady flow field, with maximum radial acceleration and low pressure drop is of key importance in obtaining good separation performance. The chamber geometry is chosen to allow such a flow field. The end wall secondary flows which occur in all

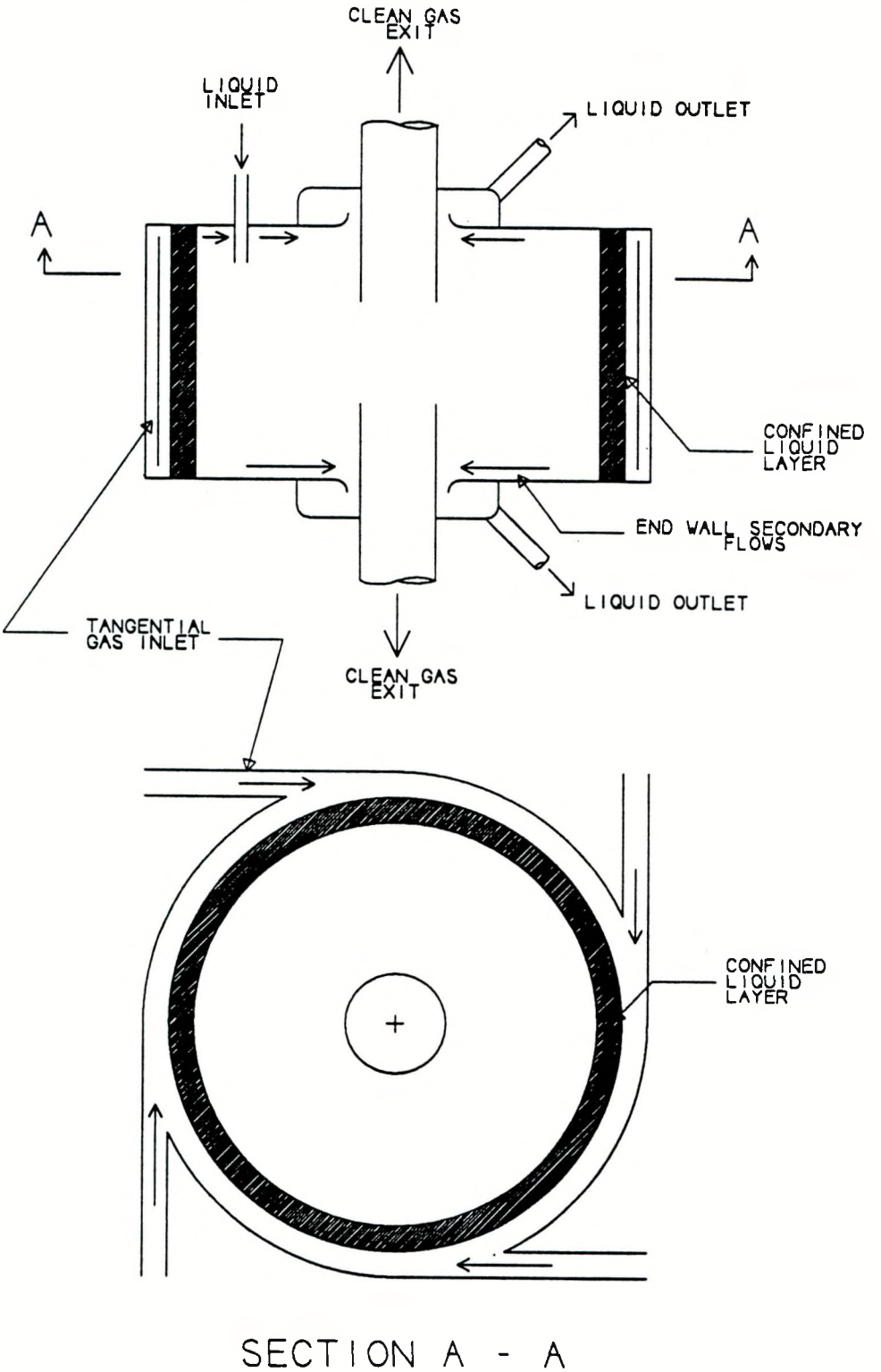

Figure 1-1 Schematic Diagram of Confined Vortex Scrubber Concept

cyclonic type flows are explicitly used as a removal path for water laden with solids inertially separated from the bulk flow. This water is cleaned using conventional fiber filter technology and then recycled to the CVS.

The combination of design features described above leads to very high separation efficiencies for fine particulates, while maintaining a simple, compact geometry. The CVS retains the inherent mechanical simplicity of cyclonic-type separators. The lack of moving parts should lead to reliable, low maintenance operation. The CVS also has the potential for enhancing SO_x removal from coal combustor product streams. This could be accomplished by suitable choice of the liquid scrubbing medium.

1.3 PROJECT SCOPE

The overall objective of the program was to develop an efficient fine particle removal technology based on a confined vortex scrubber particulate control device applicable to small-scale coal combustors. In order to meet this objective, an experimental program supported by analytical efforts was conducted. Specific objectives were to (1) verify the proposed particulate cleanup concept by laboratory experiments, (2) investigate and optimize performance by varying design and operating parameters in the experiments, (3) investigate the scaling of the proposed cleanup concept, and (4) demonstrate efficient removal of fine particulates to sufficiently low levels to meet proposed small-scale combustor emission standards.

The experimental tests were divided into two main areas: (1) investigation of the single and two-phase vortex flow field in the CVS and (2) investigation of the cleanup performance of the CVS. The experiments were conducted at a scale and in a method appropriate for proof of concept. The analytical effort was mainly related to the correlation of experimental data and to the questions of scaling of the device to larger sizes.

The scope of the work was broken into tasks as follows:

Task 1: Project Work Plan

Task 2: Design Experiment

Task 3: Fabricate Experiment

Task 4: Vortex Flow Experiments

Task 5: Cleanup Experiments

Task 6: Data Analysis

Task 7: Reporting and Management

The emphasis in all the experiments was on development of an optimized CVS configuration. The project was thus designed to accommodate feedback between design and experiment. Accordingly, the CVS design work (Task 2: Design Experiment) and fabrication work (Task 3: Fabricate Experiment) overlapped with the early part of CVS testing (Task 4: Vortex Flow Experiments): this allowed design modifications and improvements to be made in the light of the initial CVS performance and allowed the rapid development of an optimum CVS configuration before commencing cleanup experiments (Task 5: Cleanup Experiments).

This introduction is Section 1 of this Final Report. The test facility that was designed and fabricated for the CVS proof of concept experiments is described in Section 2. Sections 3 and 4 discuss the two-phase flow experiments and the cleanup experiments, respectively, that were conducted. Conclusions are presented in Section 5.

2.0 CVS AND TEST FACILITY DESIGN

2.1 CVS DESIGN CONCEPT

In the late 1960s and early 1970s, the confinement of both liquids and solid particles in vortices was studied at MIT for application in nuclear rocket propulsion (Stickler et al., 1974, Lewellen and Stickler, 1972). In the early 1980s, Avco Research Laboratory performed experiments, under IR&D funding, directed towards development of a hot gas cleaning system based upon a similar concept (Avco Research Laboratory, 1982). The results of these two studies provide a theoretical and experimental base for the current flue gas cleaning concept. Both of these experiments were performed at atmospheric pressure using essentially similar geometries. In developing the design of the CVS, the geometries and configurations of these earlier devices were studied.

Key to the separation performance of the CVS is the establishment of a stable vortex flow with strong radial acceleration. The geometry of the CVS was chosen with this aim in mind. The gross flow field in the CVS is used to confine a layer of liquid in the chamber. The microscale flows in this liquid layer then force transfer of fine particles from the gas to the liquid. The gas is injected into the chamber tangentially, and after passing through the confined liquid layer, exits through two central cylindrical tubes, see Section A-A, Figure 1-1. The vortical flow field produced is thus much simpler and more stable than that produced in a conventional cyclone separator. In a conventional cyclone, the downward-spiralling flow is forced to reverse direction in order to spiral back up the center of the tube and reach the exit: this reversal of axial flow direction represents a fundamental source of instability. Though a detailed understanding of the complex flow in a reverse flow cyclone separator is lacking, a number of the salient

features which lead to its performance weaknesses have long been known. Visualization of cyclone separator flows (Smith, 1962) revealed the sudden and unpredictable onset of periodicity in the flow. This was associated with the precessing of the vortex attachment point on the cyclone barrel wall. The CVS geometry eliminates the possibility of this type of instability. Smith also describes a mechanism for the re-mixing of separated particles in a conventional cyclone, which occurs because of the instability of the outer wall boundary layer to radially inward displacement. Due to the deceleration of the fluid by viscous forces, the thickness of the wall boundary layer grows. The breaking away of parts of this thickened, low-momentum fluid layer and its radially inward flow are the sources of the high turbulence in the cyclone separator and are responsible for the remixing of previously separated particles.

A number of studies have been made of the performance of modified cyclone geometries (Yellott and Broadley, 1955, Smith, 1962, Schmidt, 1986) in order to address this problem. General Electric (1980) identified the principal cause of poor cyclone performance as "short-circuiting", i.e. the direct passage to the exit duct of a portion of the inlet flow. Design modifications made as a result of recognizing this mechanism led to significant improvement in performance of a development cyclone.

A more recent paper (Schmidt, 1986) addresses the same problem in a different way. The conventional cyclone vortex finder exit tube was replaced by a pipe with a closed bottom end and a twisted entrance slot with a diffuser channel around the periphery. The objective was to provide a linearly distributed sink in the cyclone barrel, as opposed to the strong local sink provided by a conventional cyclone exit. The addition of the outlet tube halved the cyclone pressure drop and significantly improved the collection efficiency, the 99 percent cut diameter (i.e. the particle diameter for which 99 percent collection was obtained) being reduced from 9 microns to 3.3 microns. Further investigation of the cyclone flow field determined that a

significant part of the performance improvement could be attributed to the elimination of large radially inward velocities in the vicinity of the exit pipe opening.

Unlike the geometries investigated in the MIT liquid containment studies and the ARL IR&D work described above, one of the CVS exit geometries tested, Figure 2-3, provides a uniformly distributed sink outlet along the whole length of the vortex chamber. This has two advantages: firstly, the need for the flow to reverse direction in order to exit the chamber is removed, leading to a more stable flow field; secondly, this choice of exit geometry allows the use of both end wall secondary flows as dust removal paths. The considerably reduced pressure drop obtained with this kind of outlet is expected to be preserved.

The end wall secondary flows which occur in all cyclonic type flows are explicitly used as a removal path for water laden with solids inertially separated from the bulk flow. Having utilized the end wall secondary flows as the dust removal mechanism, there exists the possibility of controlling these flows by selectively altering the exit back pressures in the clean and dirty gas outlets. The geometry of the CVS therefore provides a much greater degree of control over the flow field than does that of a conventional cyclone. Thus the separation performance of the device may be optimized for a given set of operating conditions.

2.2 CVS DESIGN DETAILS

The initial CVS configuration was designed and fabricated to provide as much flexibility as possible in testing. A modular design was adopted, in order to allow rapid variation of CVS geometry. The initial CVS design has two tangential inlet slots. This proved not to be an optimum configuration. However, the initial design is described in some detail below so as to provide a reference for future discussion of geometry optimization, see Section 3.

Chamber Dimensions. The initial CVS design developed is illustrated in Figure 2-1 and

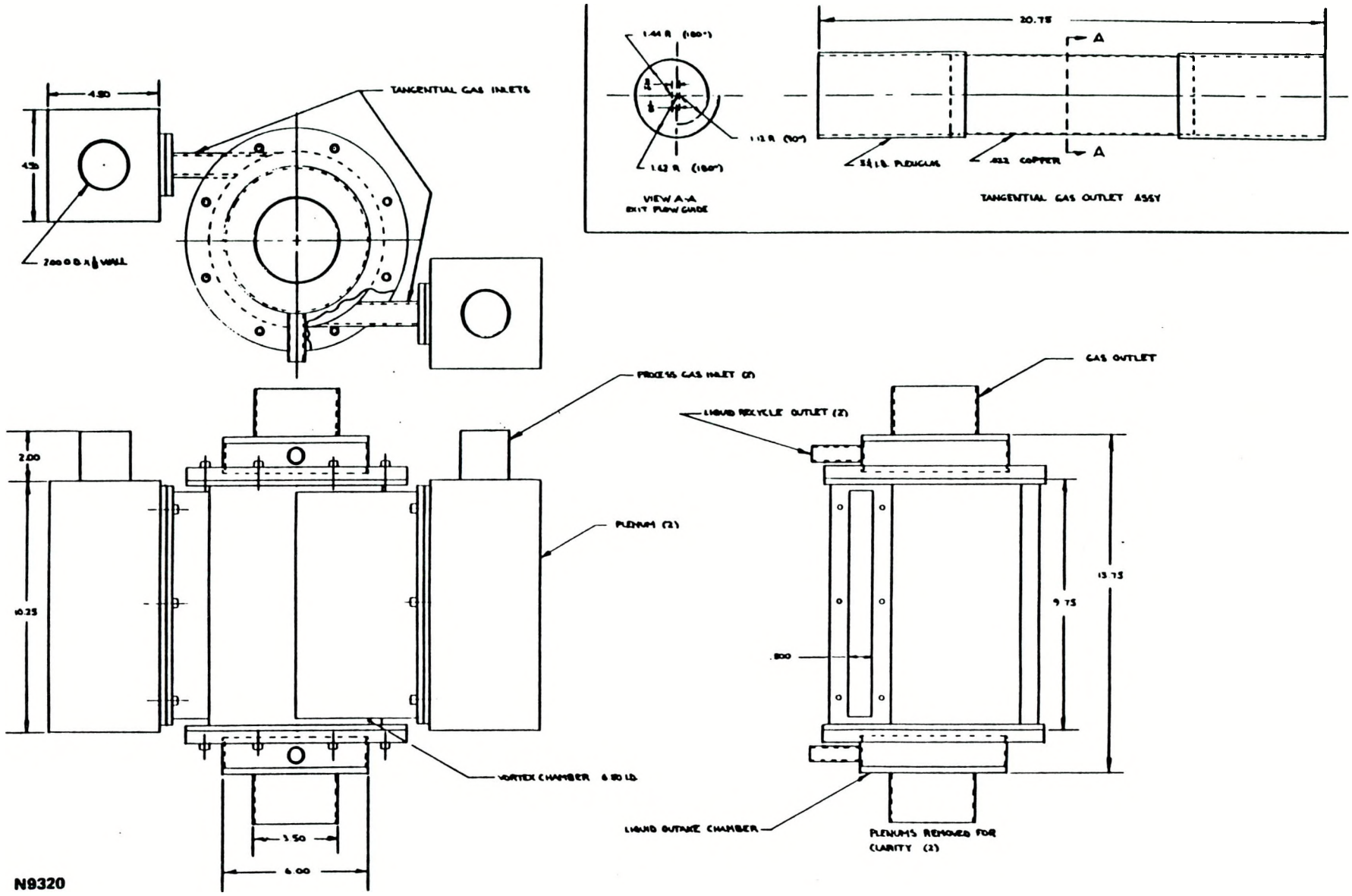

Figure 2-1 Dual-Inlet CVS Configuration, Showing Principal Dimensions

the main design parameters and their parametric variations are listed in Table 2-1. The chamber diameter was established by considering the nominal design mass flow. The CVS was designed for a nominal mass flow equivalent to that of the exhaust gas from a 1 MM Btu/hr coal combustor. This is approximately 0.25 lb/s at 10 percent excess air conditions. The MIT chamber was run at mass flows of up to 0.13 lb/s and the ARL IR&D experiment was run at mass flows up to 1.1 lb/s. Thus in terms of size and flow rate the CVS falls between these two previous experiments. The diameters of the MIT and ARL IR&D chambers were 4 inches and 11 inches respectively. The CVS chamber internal diameter was fixed at 6.5 inches. This is appropriate from a mass flow scaling point of view and also meant that readily available Plexiglas tube material could be used for construction.

TABLE 2-1

CVS GEOMETRY AND PARAMETRIC VARIATIONS

Parameter	Design Value	Parametric Variation
Chamber Internal Diameter	6.5"	-
Aspect Ratio (L/D)	1.5	1.0
Air Inlet Type	Slots	Jets
Air Outlet Type	Slot	Vortex Finder
Air Outlet Diameter	0.50	0.25
Water Outlet Type	Single Tube	Multiple Tubes

Aspect ratios (chamber length/diameter) in the range 1.0 to 1.5 are of interest. From a construction standpoint, it was simpler and more cost effective to manufacture two chambers of different lengths rather than one chamber of variable length. Chambers of aspect ratio 1.0 and 1.5 were constructed.

Air Inlet Geometry. The nominal air inlet geometry chosen was two diametrically opposite tangential slots. The air inlet slot geometry was designed to accept inserts of differing thicknesses, see Figure 2-2, in order to allow separate control of mass flow and inlet velocity in the experiments. Two inserts were manufactured, giving three possible slot heights. The minimum slot height was chosen to give approximately 120 ft/s tangential inlet velocity at the design mass flow rate. In addition, a jet insert was also designed. This insert, see Figure 2-2, allows a change of air inlet geometry from tangential slots to rows of tangential jets.

Air Outlet Geometry. The nominal design air outlet geometry was based on the Schmidt flow guide described above (Section 2.1), but instead of having a twisted slot, a straight slot was provided. At either end, the slotted tube was connected to an open ended tube which passes through the water out-take chamber to the air exit duct, see Figure 2-3. Two slotted exit tubes were designed, one having a diameter of half the chamber internal diameter and one of one quarter the chamber internal diameter. In addition, conventional vortex finder air exits were provided: these are simply open ended tubes which protrude into the vortex chamber at either end, see Figure 2-3. Again, two vortex finder exit tubes were manufactured, of diameters one half and one quarter the CVS chamber internal diameter.

Water Inlet. The initial water inlet arrangement consisted simply of two small stainless steel tubes, 0.125 in. internal diameter, which protrude axially into the main chamber close to the walls, see Figure 2-4. The ends of the tubes were sealed and the water entered the chamber through a series of holes. Thus the water was sprayed into the chamber in the same direction as the tangential air inlet flow.

Water Outlet. The initial water outlet arrangement is shown in Figure 2-4. The water leaves the main chamber in the end wall secondary flows and passes through an annulus into the water out-take chamber. A 0.372 in. ID water outlet tube located at the bottom of this

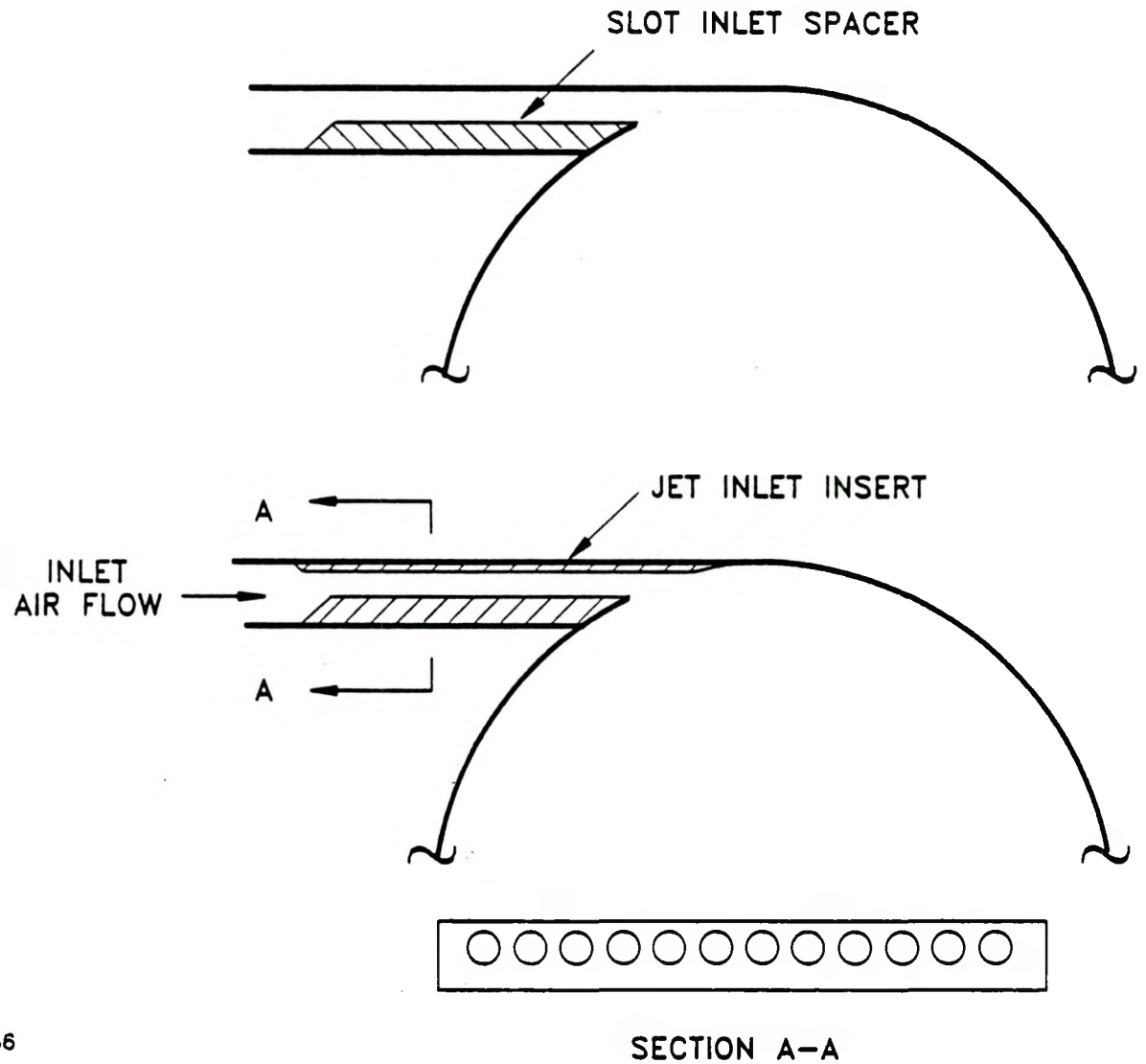

Figure 2-2 Dual-Inlet CVS Air Inlet Geometries

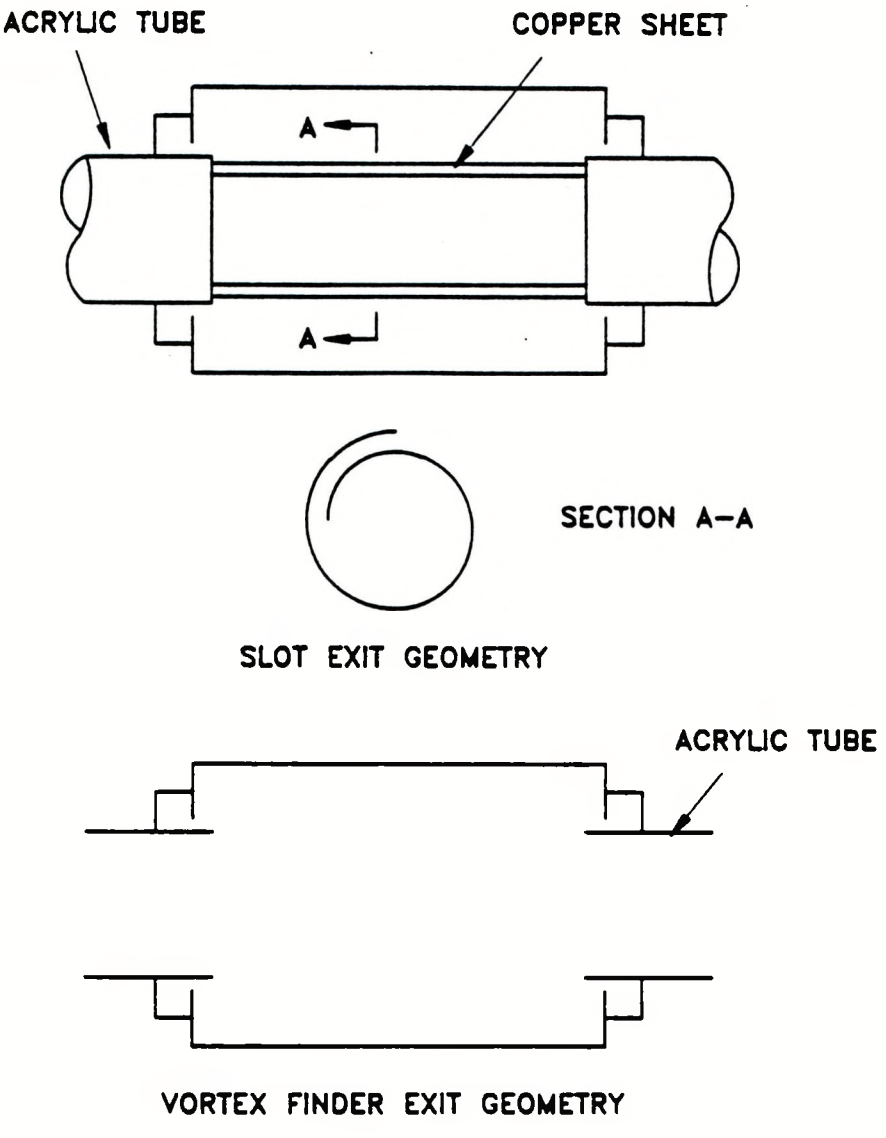

Figure 2-3 CVS Air Outlet Geometries

chamber allowed the water to leave the CVS entirely.

Porous Walls. Porous chamber walls were considered at the outset of the design effort, for the following reasons. In the MIT liquid containment studies, gas was introduced into the vortex chamber through six tangential ports and also through a porous cylindrical sidewall. The radial flow through the sidewall provided transpiration cooling of that wall, an important requirement to the application then being considered. In addition, however, it was noted that the radial inflow provided a beneficial effect on both pressure drop and liquid containment. In the CVS the inlet flow contains fine fly ash particles, so inclusion of a porous wall poses a variety of problems, not least of which is the potential for complete plugging of the pores with fly ash. Given the anticipated pressure drop benefits of the CVS outlet geometry and in the interests of simplicity, it was decided to avoid the added complexity of a porous chamber wall.

2.3 EXPERIMENTAL ARRANGEMENT

The experimental arrangement used is illustrated schematically in Figure 2-5. The test gas was supplied by a regenerative blower (Rotron Model DR-P7). This blower is capable of supplying some 200 scfm at 90 in. water and approximately twice this airflow at 40 in. water. A butterfly valve in the air supply by-pass line allowed control of the mass flow of test gas to the CVS. The by-pass air was exhausted outside the building. The test gas was fed to the CVS via a sharp-edged orifice plate, for mass flow measurement, and two inlet manifolds. The manifolds connected directly to the CVS slot inlets. The two exhaust air streams from the CVS were merged before being filtered and exhausted outside the building. Standard pressure and temperature instrumentation was used to obtain inlet air mass flow measurements. The water for most tests was from the city water supply. For tests using liquids other than water, a separate pressurized liquid feed system was assembled. A photograph of the experimental

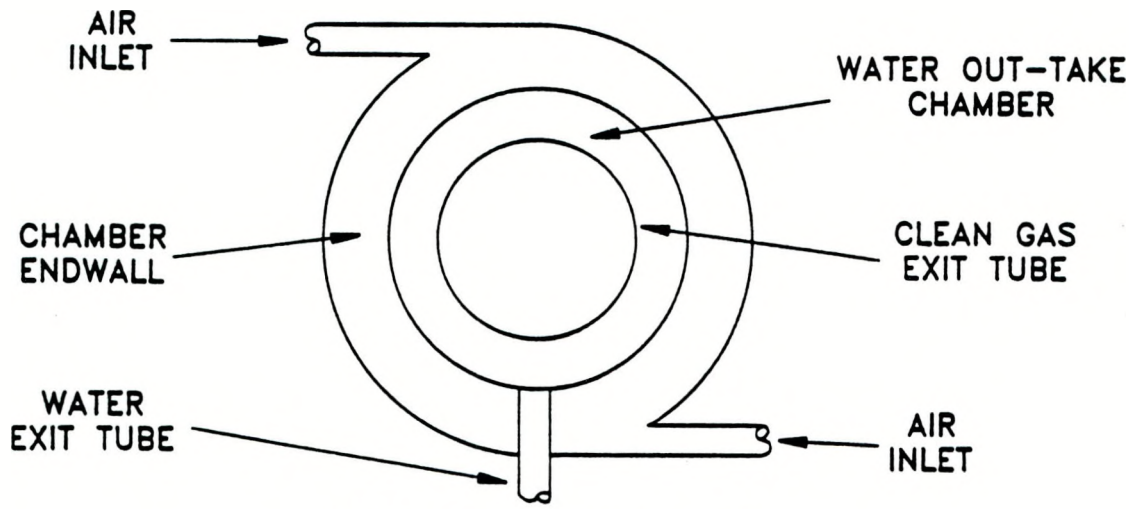

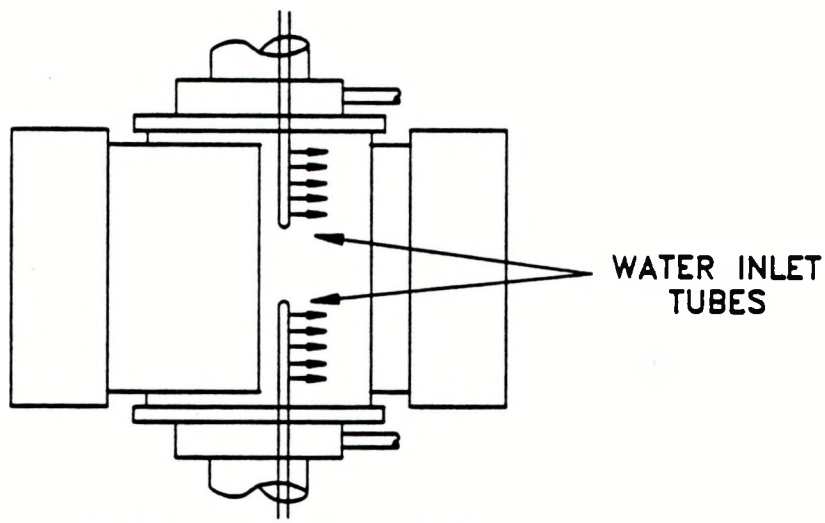

Figure 2-4 CVS Water Inlet and Outlet Arrangements

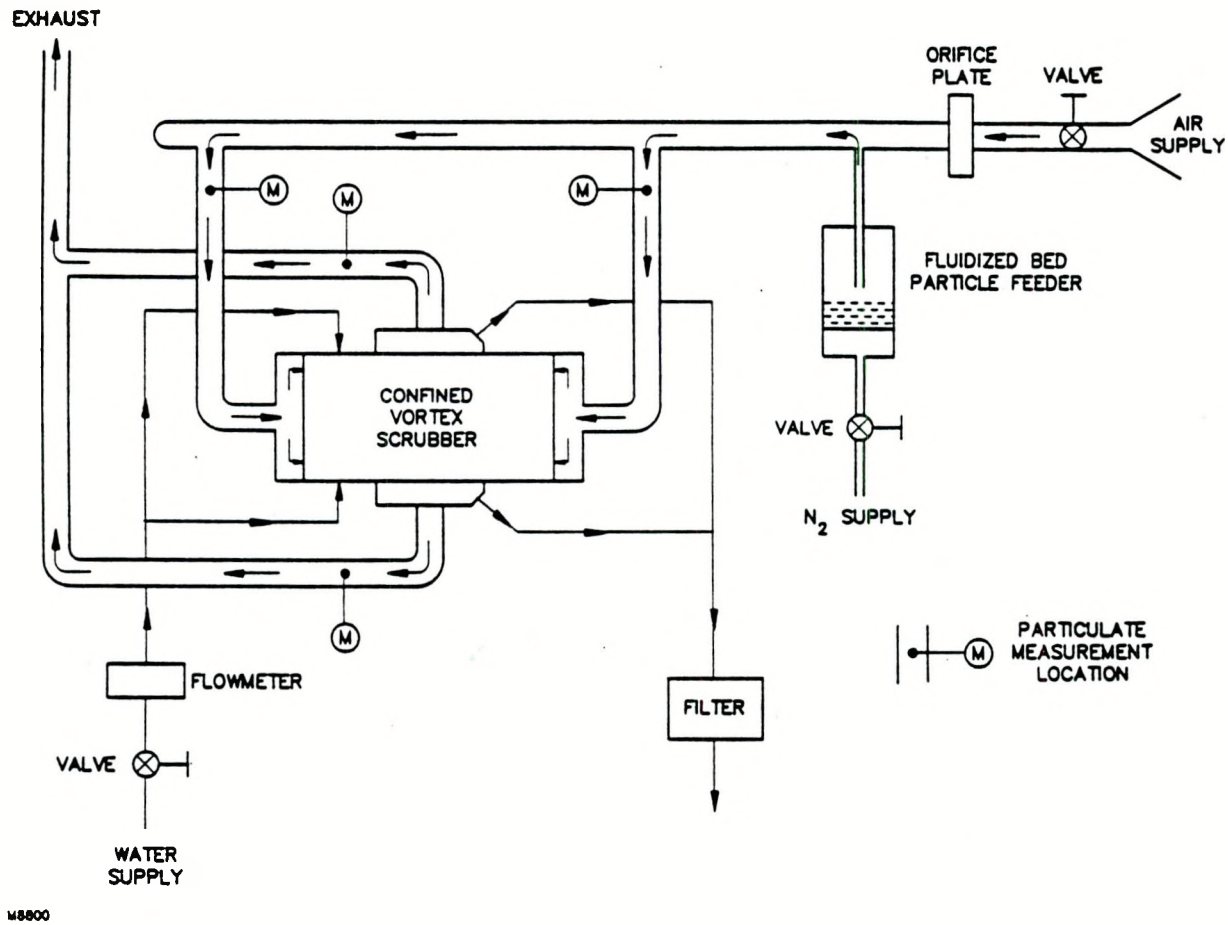

Figure 2-5 Schematic Diagram of CVS Experimental Arrangement

installation is shown in Figure 2-6.

Fabrication of all CVS hardware was carried out at ARL. The CVS chamber, end-walls, air inlet arrangement and water out-take chamber were fabricated from transparent acrylic (Plexiglas). This was to aid visualization of the internal flow field. The slot exits were fabricated from copper sheet, which was formed to the correct contour. The copper sheet was then attached to an acrylic tube at either end.

The air inlet and outlet piping system was fabricated from Schedule 40 PVC piping and fittings. Flexible PVC hoses were used to connect the inlet manifolds and the outlet tubes to the PVC supply and exhaust pipes. Tygon tubing was used to connect the water supply and exhaust. The experiment was assembled in Test Cell #2 at ARL's Haverhill, Massachusetts test facility. No significant problems were encountered in fabricating and installing the CVS experiment as designed, though small changes in dimensions and geometry were necessary in order to simplify machining and assembly.

A fluidized bed particle feeder was used to supply dust to the CVS during the cleanup experiments. A schematic diagram of the fluidized bed feeder is shown in Figure 2-7. The feeder consists of a 4 inch diameter chamber into which is fitted a porous plate close to one end. The region beneath the porous plate is filled with wire wool. The powder to be fed is loaded onto the top of the porous plate. Fluidizing nitrogen is supplied beneath the porous plate and flows upwards through the plate and then through the powder bed, fluidizing it. An offtake tube is located at a variable distance above the top of the fluidized powder. The fluidized powder is thus entrained into the offtake tube and conveyed to the CVS main air inlet pipe. The entire feeder was attached to an electronic balance, in order to allow feed rate measurements to be made.

It proved impossible to obtain sufficient fluidizing nitrogen flow through the porous plate

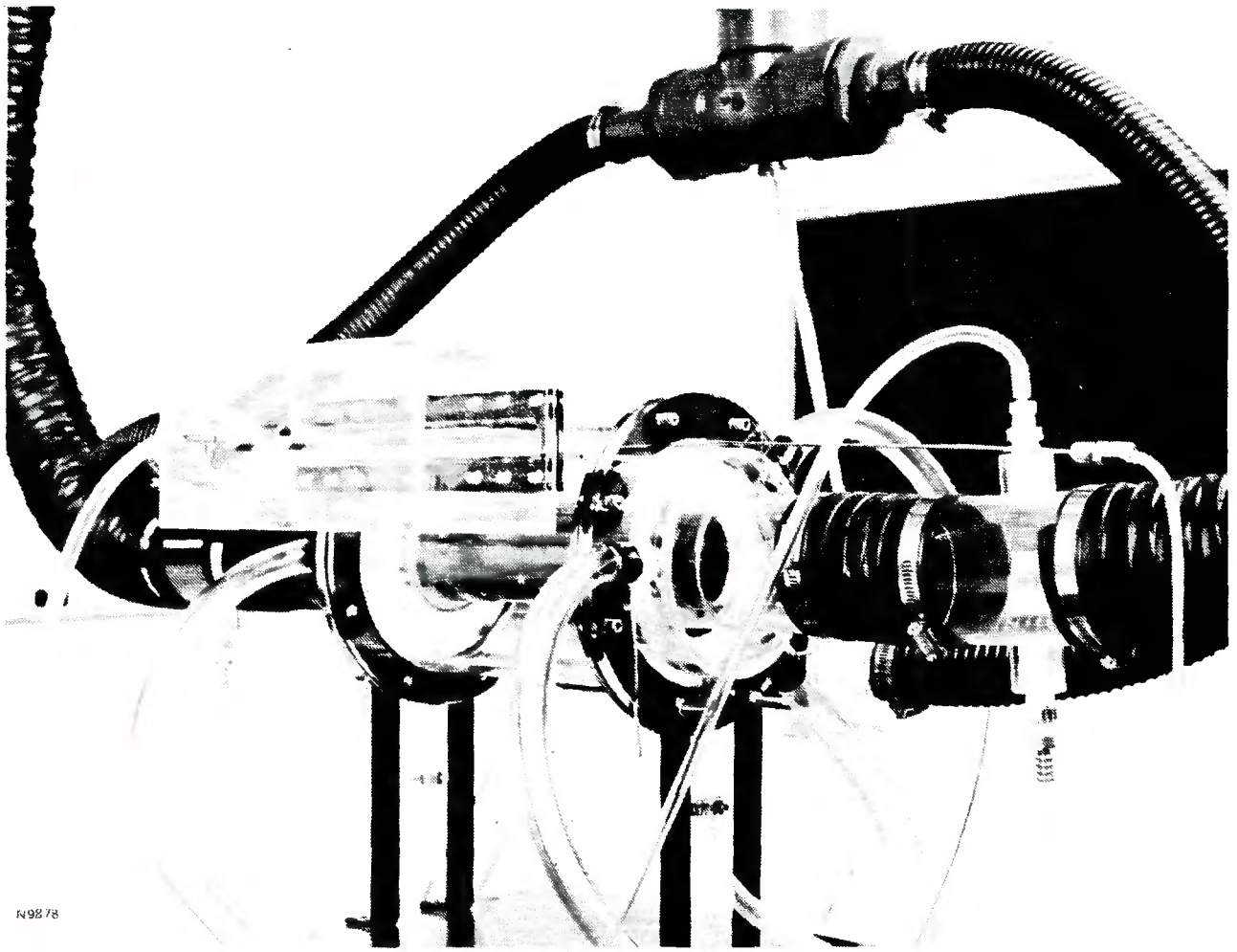

Figure 2-6 Photograph of CVS Experimental Installation at ARL Haverhill

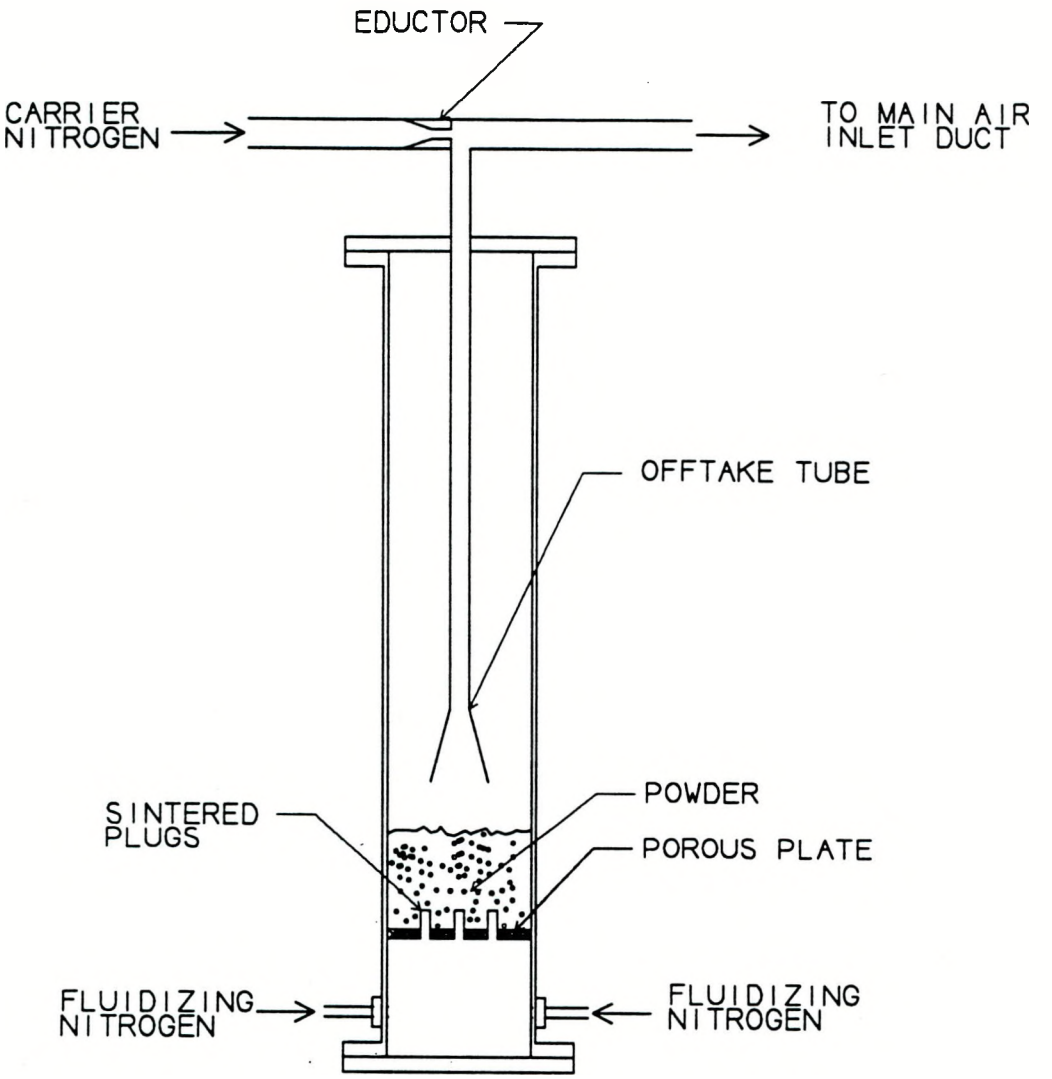

Figure 2-7 Schematic Diagram of Fluidized Bed Dust Feeder

to fluidize the finest powders used in the cleanup experiments without over-pressuring the feeder chamber. In order to overcome this problem five sintered plugs were installed in the feeder. The fluidizing nitrogen was then supplied through the sintered plugs. A small vibrator was also attached to the feeder wall, below the top of the bed. This proved to be an effective method of feeding very fine dusts at a reasonable nitrogen mass flow rate and feeder chamber pressure.

2.4 INSTRUMENTATION AND CONTROL

Control of the experiment was entirely manual. The blower was started and the main air bypass valve adjusted until the desired air mass flow rate was established. Then the liquid feed was started and controlled manually to the desired flow rate. Particulate feed was commenced by starting the supply of fluidizing nitrogen to the particle feeder. The feed rate was monitored by recording manually the rate of change of the weight of the feeder. During the period of particle feed, the air supply pressure and temperatures as well as the CVS chamber pressure drop and temperatures were also recorded manually. After a known quantity of particulate had been supplied to the CVS, the particle feed was stopped. Soon thereafter the liquid and air flows were stopped. The air and, if appropriate, liquid filters were then removed and weighed.

Inclined tube manometers and dial gauges were used for pressure measurements. Type E thermocouples with digital readouts were used for temperature measurement. An electronic balance was used to measure the particle feeder weight change. A triple beam balance was used to measure the air filter weight change. A Malvern laser diffraction particle size analyzer was used for all particle size measurements, both on-line and off-line. A stroboscope was used as a flow visualization aid.

Given the extremely high collection efficiency of the CVS, the mass of dust input to the system and the mass of dust collected in the CVS are large quantities (of order 100 g for a typical test) while the mass of dust passed by the CVS and collected in a downstream filter is a small quantity (of order 0.5 g). Thus the measurement of input mass and passed mass leads to a much more accurate efficiency measurement than measurement of the input mass and the collected mass. A further complicating factor here is the fact that a fraction of the fly ash used was water soluble (this is typical of fly ash). Thus measurements of the mass of ash collected by the CVS are difficult to make. For a small number of tests a complete dust mass balance was made by measuring the input, collected and passed ash masses. However, unless stated to the contrary, all efficiency data reported here are based on measurements of the input and passed masses of dust.

3.0 VORTEX FLOW EXPERIMENTS

As discussed in Section 1, above, the emphasis in this program was on the experimental development of an optimized CVS configuration. The goal of the Vortex Flow Experiments was to develop a CVS configuration with a stable flow field, high radial acceleration, good liquid confinement and low pressure drop. Specific performance goals were agreed with DOE program management. These goals were as follows: (1) Pressure drop comparable to conventional cyclone separator (approximately 10 - 12 inlet dynamic heads); (2) Mass of liquid confined in chamber equivalent to approximately 10 percent of chamber volume; (3) Controllable end-wall outlet flows; and (4) Stable two-phase flow field. Technical issues of interest in these experiments include the degree of radial acceleration possible, the pressure drop, the degree of liquid containment, the stability of the two-phase flow field, the water loss rate, the pressure drop and the control of the dirty water exit flow using the end wall secondary flows.

A series of shakedown experiments were conducted before commencing the investigations of the two-phase flow in the CVS. These experiments proceeded smoothly and took only a few days to complete. At the start of testing, a shell and tube heat exchanger was installed in the CVS air supply system, between the blower and the CVS. This was done to prevent the possibility of over-heating the acrylic components of the CVS. Acrylic is only rated to 140°F, and the blower air can reach temperatures greater than 150°F when operated at high pressure rise (80 - 90 in. water) and low mass flow. Overall air flow characteristics, mass flow rates, system pressure drops and operating temperatures were evaluated. Initial observations were that the blower was operating at close to maximum pressure rise and minimum flow rate, but that the bulk of the system pressure drop was across the heat exchanger itself. The

maximum mass flow rate which could be obtained through the CVS was only approximately 85 percent of design mass flow. At this maximum mass flow rate the CVS tangential inlet velocity was 40 ft/s. Without the heat exchanger operating, the temperature of the test gas at the orifice plate reached 130°F after the blower had been operating for only 12 minutes.

The heat exchanger was removed and another test was run. The system pressure drop was much lower, consequently the blower operated at a lower outlet temperature and there was no need for the heat exchanger. The air temperature at the orifice plate stabilized at approximately 120°F. With the heat exchanger removed the design mass flow rate through the CVS could easily be achieved.

Two principal CVS geometries were tested and assessed from the point of view of flow field stability, pressure drop and liquid confinement. These were (1) the initial CVS design or Dual-Inlet CVS, described in Section 2.2 above and (2) a modified version of this, the Squirrel Cage CVS, which is described below. The former gave adequate radial accelerations, stability and pressure drops, but low liquid containments. The latter design met all performance goals. The results for each design will be discussed in turn.

3.1 DUAL-INLET CVS

3.1.1 Aerodynamic Tests

Initial tests were made without water addition and were primarily concerned with flow field stability and device pressure drop. The CVS configurations tested are specified in Table 3-1. The aspect ratio (chamber length/diameter) was fixed at 1.50. Two slot exit tube diameters, two air exit types (slot and vortex finder) and two water exit arrangements (single and multiple tubes) were tested.

Measured pressure drop results for the six configurations detailed in Table 3-1 are

TABLE 3-1

CVS CONFIGURATIONS FOR AERODYNAMIC TESTS

Configuration	L/D	D_e/D	S/D	Air Exit	Water Exit
A	1.50	0.25	0.077	SE	W1
B	1.50	0.25	0.077	VF	W1
C	1.50	0.50	0.077	SE	W1
D	1.50	0.50	0.045	SE	W1
E	1.50	0.50	0.045	SE	W2
F	1.50	0.50	0.035	SE	W2

Legend

L = Chamber Length D = Chamber Diameter
D_e = Exit Tube Diameter S = Inlet Slot Height

Air Exit:
SE = Slot Exit
VF = Vortex Finder Exit

Water Exit:
W1 = One 0.372" ID Exit Tube
W2 = One 0.372" Exit Tube + Three 0.627" Exit Tubes

presented in Figure 3-1. The measured pressure drop is expressed as a percentage of the chamber inlet total pressure and is shown as a function of the chamber tangential inlet velocity. Configurations A and B (small exit diameter) demonstrated high pressure drops. These tests were performed with the heat exchanger installed, consequently the system mass flow, and hence inlet velocity, was limited. Nonetheless, the dramatic increase in pressure drop produced by changing from the slot exit (Configuration A) to the vortex finder exit (Configuration B) is evident. At the same inlet mass flow and velocity, the vortex finder exit produced a 50 percent higher pressure drop than the slot exit.

The effect of exit diameter may be seen by comparing Configuration A and Configuration C. At the same inlet velocity and mass flow, the smaller exit tube gives approximately three

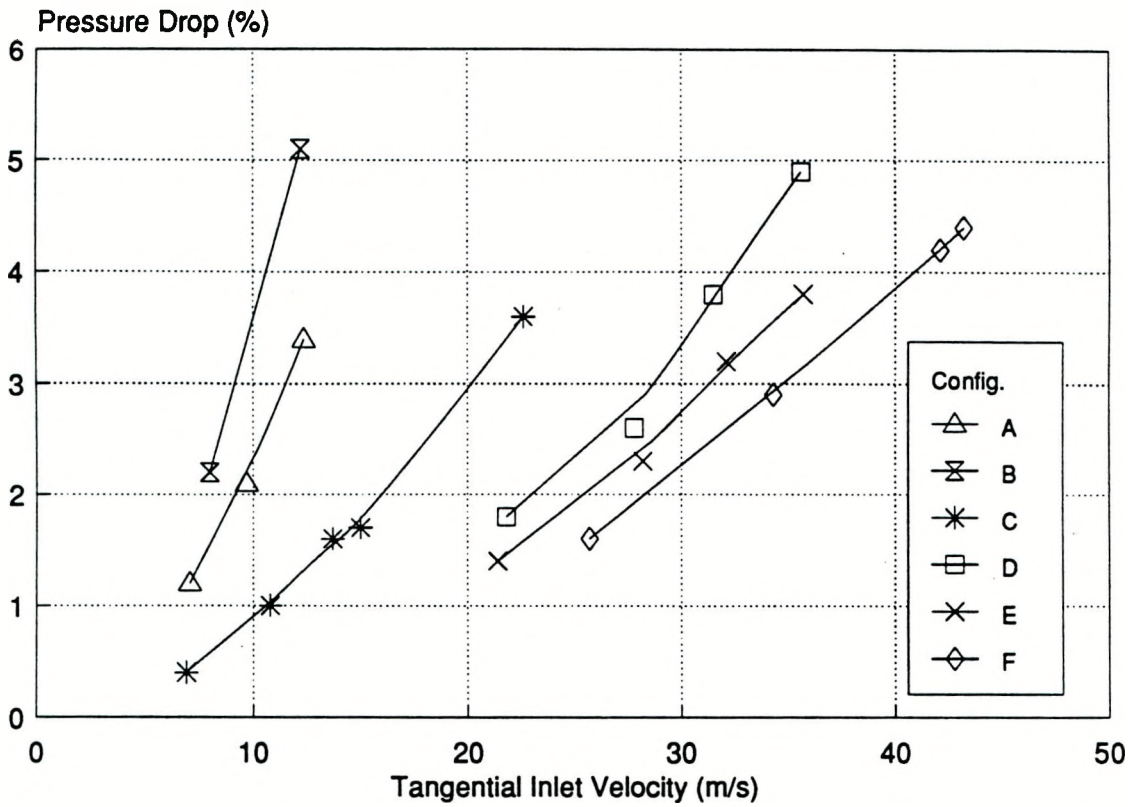

Figure 3-1 Measured Pressure Drop Data for Single Phase Flow. CVS Configurations as in Table 3-1

TABLE 3-2

CVS NON-DIMENSIONAL PRESSURE DROP - NO WATER ADDITION

Configuration	Number of Dynamic Heads Loss
A	40.7
B	62.0
C	13.2
D	6.6
E	5.5
F	4.4

times the pressure drop of the larger exit tube. Reduction of the inlet slot height allowed higher inlet velocities and hence the production of greater radial accelerations. For the final configuration (F), the slot height is 0.208". This gives inlet velocities of up to 50 m/s.

It is useful and conventional to express pressure drops for inertial separators in terms of the number of inlet dynamic heads. This allows direct comparisons to be made between devices of differing geometries and scales. For example, the pressure drop of a conventional reverse flow cyclone separator of "high efficiency" design is in the range 10 - 12 inlet dynamic heads. The non-dimensional pressure drop for the six configurations tested is shown in Table 3-2.

The initial CVS configuration with the small exit tube therefore has a non-dimensional pressure drop some four times greater than that of a conventional cyclone. The final CVS configuration has a non-dimensional pressure drop of less than half that of a conventional cyclone. Figure 3-2 shows the non-dimensional pressure drop for the last four configurations as a function of inlet velocity. It is interesting to note that as the inlet slot height is reduced, the non-dimensional pressure drop of the device was reduced (compare configuration C to D to F).

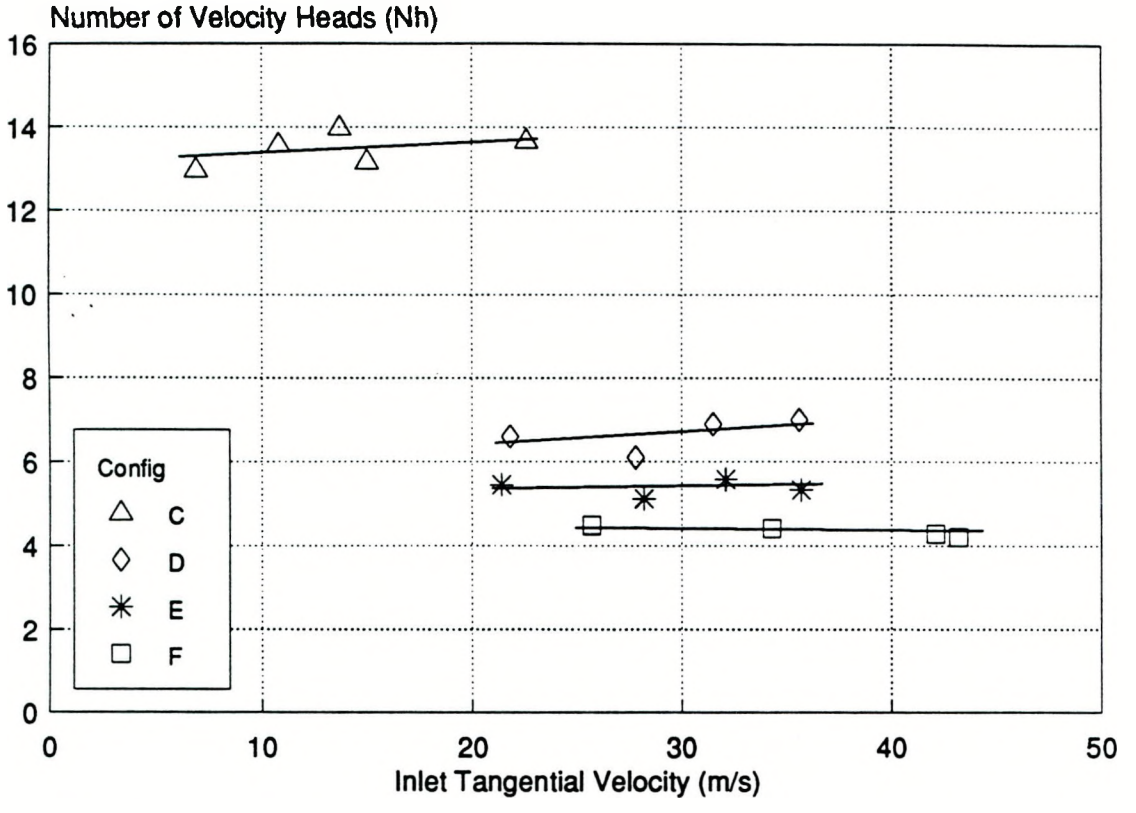

Figure 3-2 Measured Pressure Drop Expressed in Non-Dimensional Form. CVS Configurations as in Table 3-1

Increasing the water exit area had a much smaller effect on the device pressure drop (compare D to E).

Of prime concern from a practical point of view is the device pressure drop at the design mass flow rate. This is shown in Figure 3-3 as a function of the inlet slot height. While the non-dimensional pressure drop (i.e. number of dynamic heads) decreases as the slot height is reduced, the dynamic head at the design mass flow rate increases. As the pressure drop scales as velocity squared, the net result is an increase in absolute pressure drop as the slot height is reduced. For the highest inlet velocities tested to date (i.e. the smallest slot height), the system pressure drop at the design mass flow rate is just over 2.5 percent, which would correspond to approximately 10 in. water. This is less than half the pressure drop of a conventional cyclone separator operated at the same inlet velocity.

3.1.2 Two-phase Flow Tests

Initial water addition experiments were made for the L/D = 1.5 chamber with the flow guide slot exit tube ($D_e/D = 0.50$). The water was introduced initially via a single 0.125" OD stainless steel pipe located on the axial centerline of CVS chamber close to the chamber wall and subsequently through two such tubes, one being introduced from either end of the CVS chamber. Initial observations were that a liquid layer could indeed be contained within the chamber, but that a considerable fraction of the input water flow exited via the central clean gas exit tube. Initial estimates were that this fraction was as much as 50 percent of the input water. Careful visualization of the CVS central exit tube indicated that the water appeared to be entering the clean gas exit at either end of the slot. Use of pulses of water as a flow visualization agent revealed that the loss mechanism was actually water flowing back into main chamber from water out-take chamber, see Figure 3-4.

In order to address this problem, additional water outlet tubes were added to the water

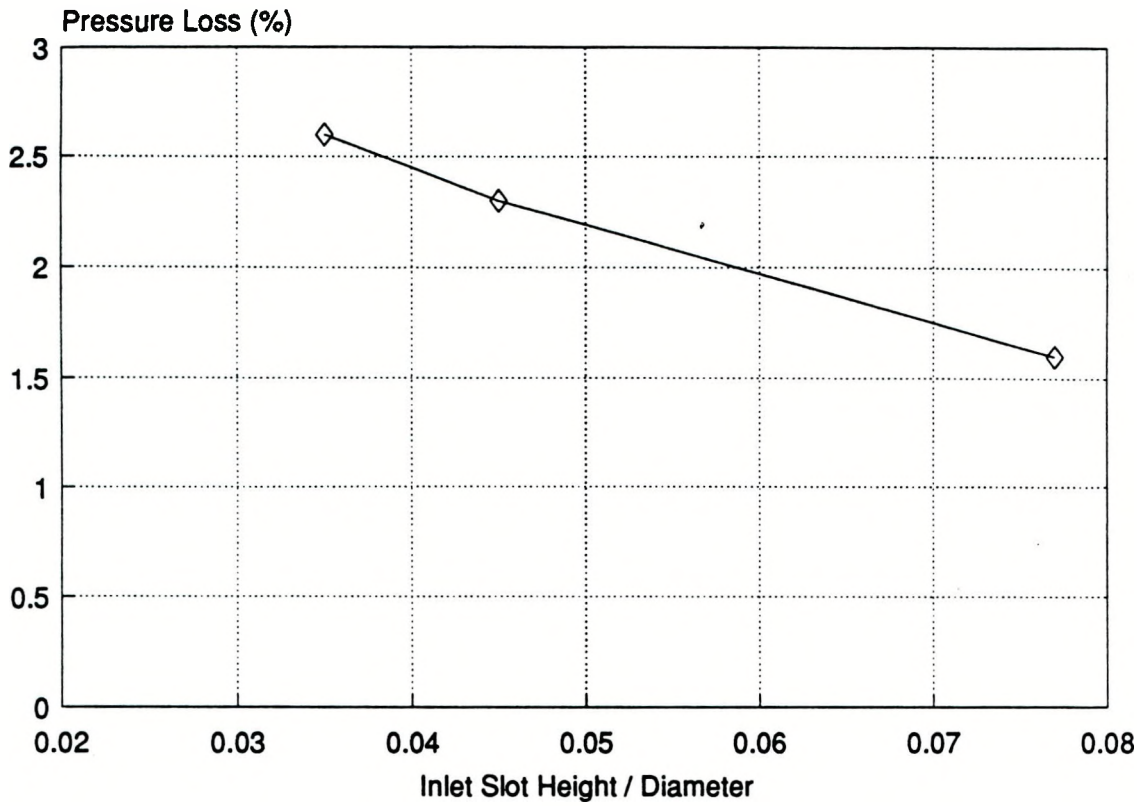

Figure 3-3 Pressure Drop at Design Mass Flow Rate as a Function of Air Inlet Slot Height for Dual-Inlet CVS

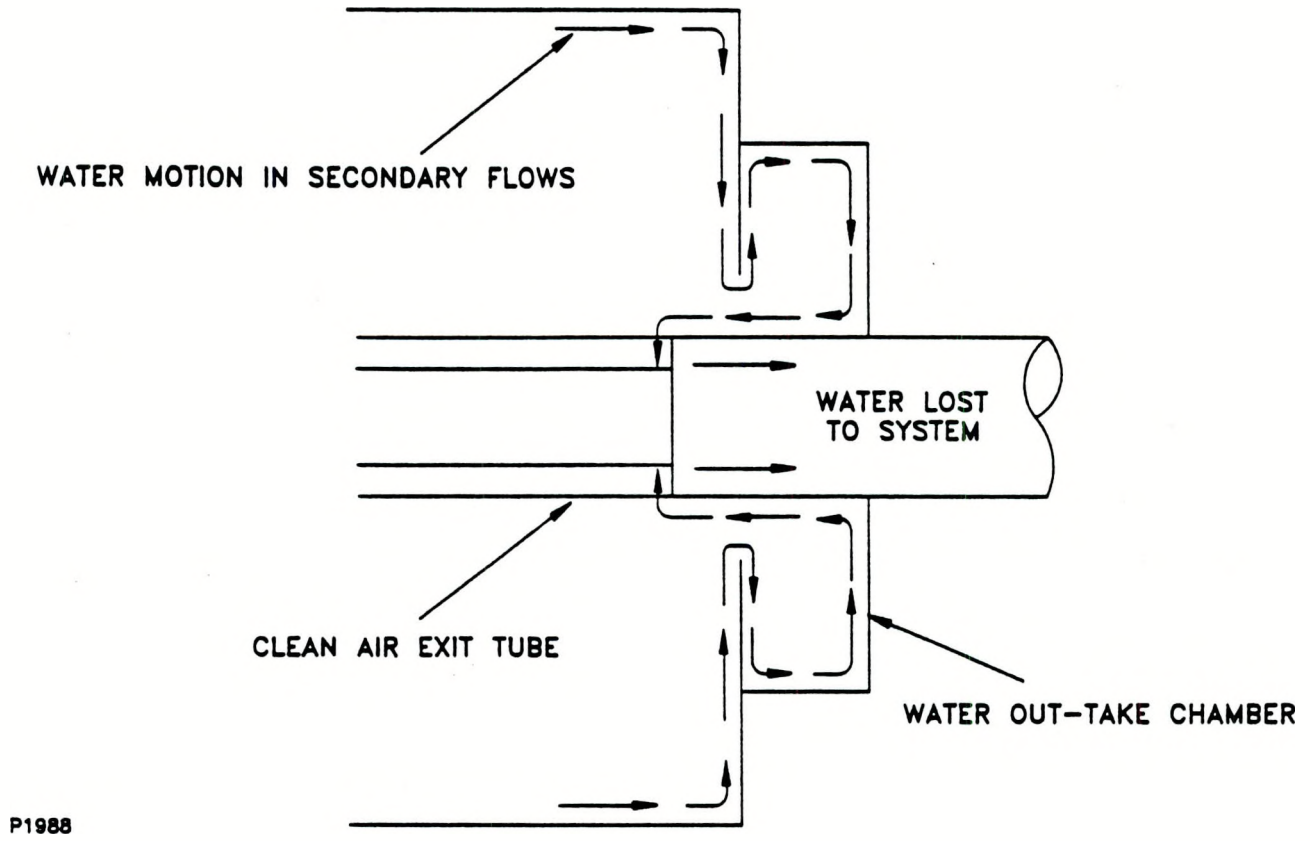

Figure 3-4 Schematic Diagram Showing Water Loss Mechanism via Clean Gas Exit in Dual-Inlet CVS

out-take chambers. The initial water exit design had one 0.372" ID exit tube per chamber (W1 exit). The revised water exit design (W2 exit) had three 0.627" ID exit tubes in addition to the single smaller tube. The effect of this change on the water loss can be seen in Figure 3-5. In this figure, the water loss, expressed as a percentage of the total water input, is plotted as a function of the input water flow rate for the two different water exit arrangements. A dramatic improvement in the water loss was achieved by adopting the W2 exit arrangement. At one condition, the loss was eliminated entirely. The reason for the improvement was that the water entering the out-take chamber is now removed from that chamber quickly before it has a chance to reach the outer surface of the center tube and hence re-enter the main chamber.

The mechanism for water removal from the main chamber via the endwall boundary layer secondary flows proved very effective. In fact, the removal mechanism was so effective that a greater input flow rate of water than expected was required in order to establish a stable liquid layer within the chamber. At input water flow rates lower than this minimum, two incomplete layers were established at either end of the chamber. The minimum flow rate required to establish a stable liquid layer is plotted as a function of the tangential air inlet velocity in Figure 3-6.

In general for a given air mass flow rate, the device pressure drop was lower with a stable liquid layer in the chamber than without such a layer. The pressure drop was typically reduced by 20 - 25 percent when the liquid layer was established.

Liquid containment is plotted as a function of water input flow rate in Figure 3-7. The liquid containment is expressed as a percentage of the chamber volume. At water flow rates at which the liquid loss is small, the containment is only 3 - 4 percent. This is considerably lower than the containment measured in related experiments at MIT (Lewellen and Stickler, 1972), where containments of order 10 - 12 percent were achieved. One major difference between the

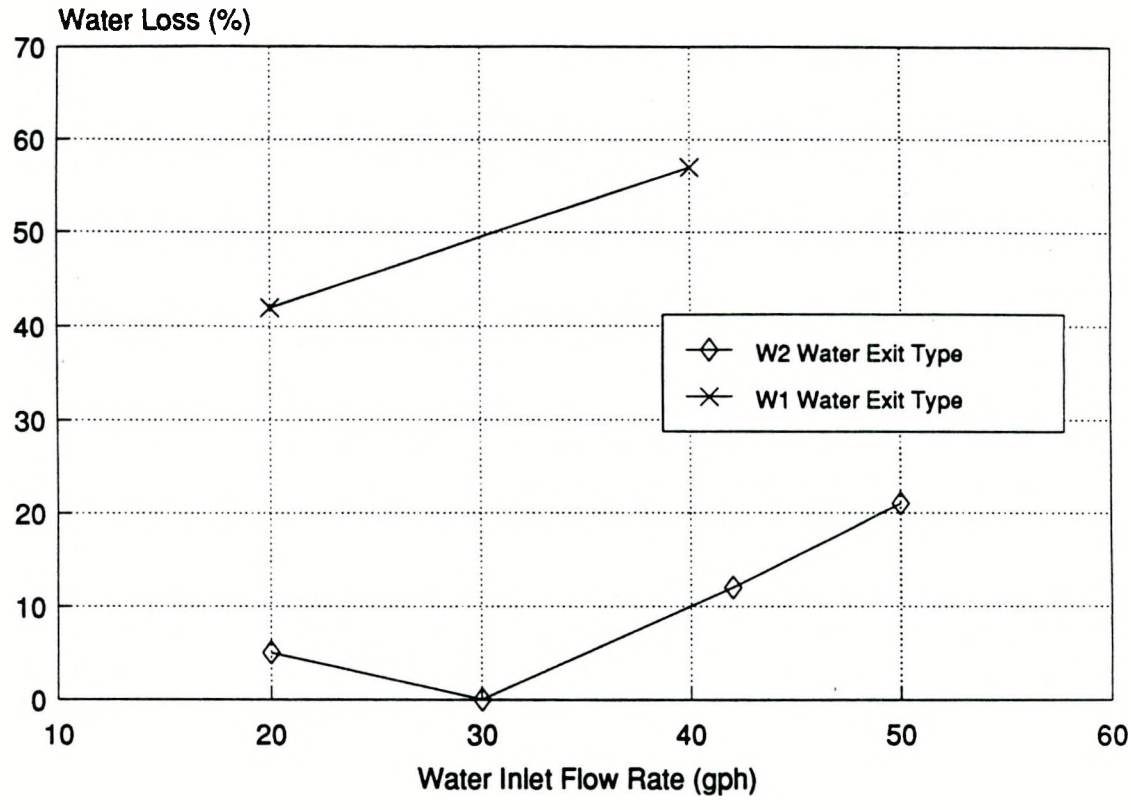

Figure 3-5 Effect of Water Outlet Area on Water Loss via Clean Gas Exit for Dual-Inlet CVS

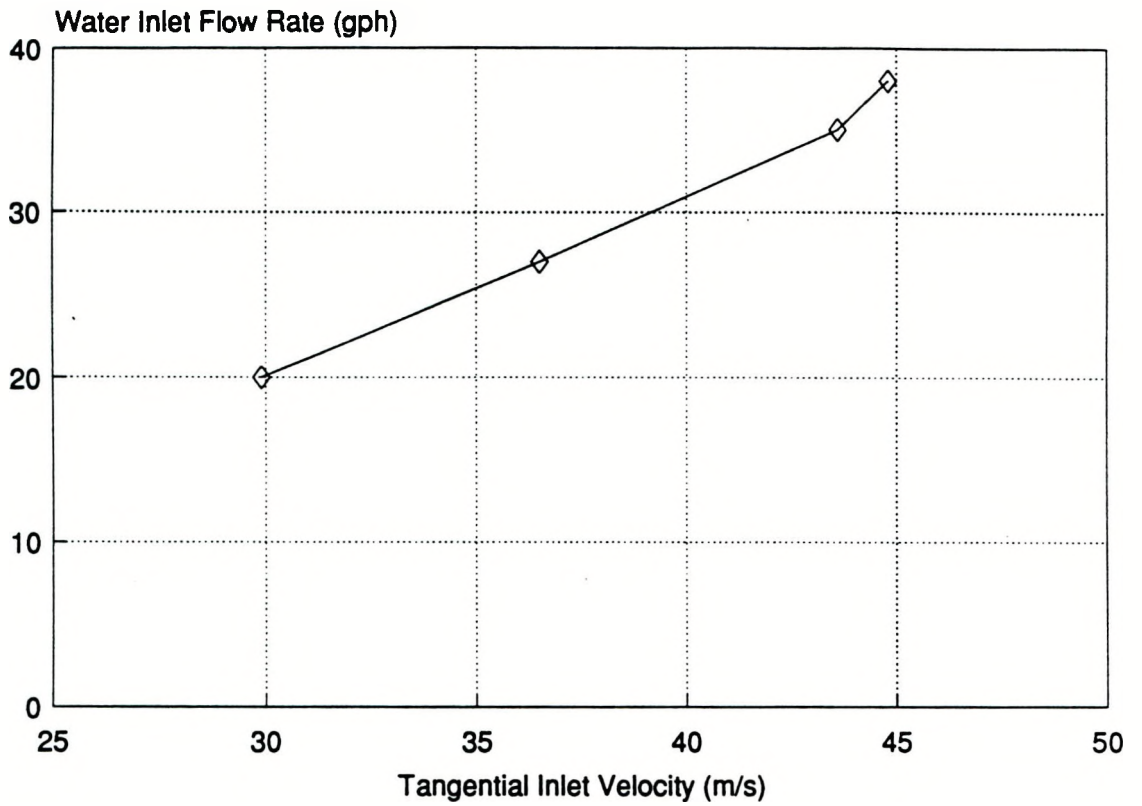

Figure 3-6 Minimum Input Water Flow Rate Required to Establish a Stable Liquid Layer as a Function of Air Inlet Velocity for Dual-Inlet CVS Design

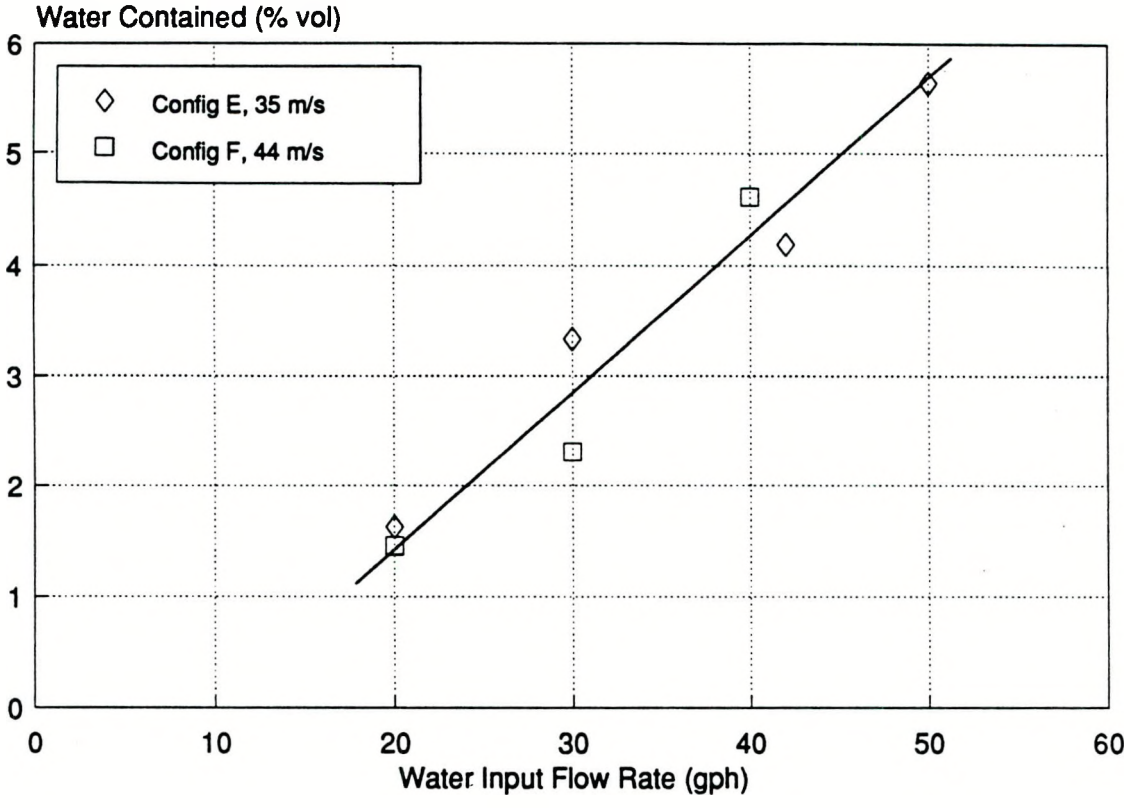

Figure 3-7 Mass of Liquid Contained, Expressed as a Percentage of Chamber Volume, as a Function of Water Input Flow Rate for Dual-Inlet CVS Design

CVS and the previous work at MIT is that in the CVS there is a net through-flow of liquid. In the MIT experiments the aim was to maximize the containment and prevent all liquid outflow. The requirement for a controllable through-flow adds significant complexity to the problem.

Thus two important issues to be resolved were (1) the low water containment and (2) the water loss via the clean gas exit. Both these issues were related to the high water through-flow. The containment was low because of the efficiency of the endwall liquid removal approach and the water loss problem was also related to the high rate of water flow through the out-take chambers, leading to some water re-entering the main chamber on the outside of the central exit tube and being lost to the system. A series of experiments were undertaken to investigate the control of the water outflow in order to increase the liquid containment and to control the water loss mechanism. These experiments and their results are described below.

Endwall Modifications. The approach taken to control the endwall water outlet flow was to energize the endwall boundary layer in order to reverse the direction of the endwall secondary flows (i.e. to drive the endwall boundary layer flow radially outward). This approach was utilized in the liquid containment experiments at MIT (Stickler et al., 1974): gas with high angular momentum was injected into the boundary layer on the exhaust port end wall in order to minimize the loss of water due to end wall secondary flow effects. In order to accomplish this, the CVS chamber endwalls were modified to include four tangential jets, as illustrated schematically in Figure 3-8. The jet diameter was 0.125", and the jets were located midway between the chamber walls and the inner edge of the water exit annulus. In the initial design the jets were supplied with air from the main inlet plenums, see Figure 3-9. Testing of this configuration showed no beneficial effect of the endwall jets. The momentum flux through the endwall jets was apparently insufficient to energize the endwall boundary layer.

The endwall jets were therefore disconnected from the main air inlet plenums and

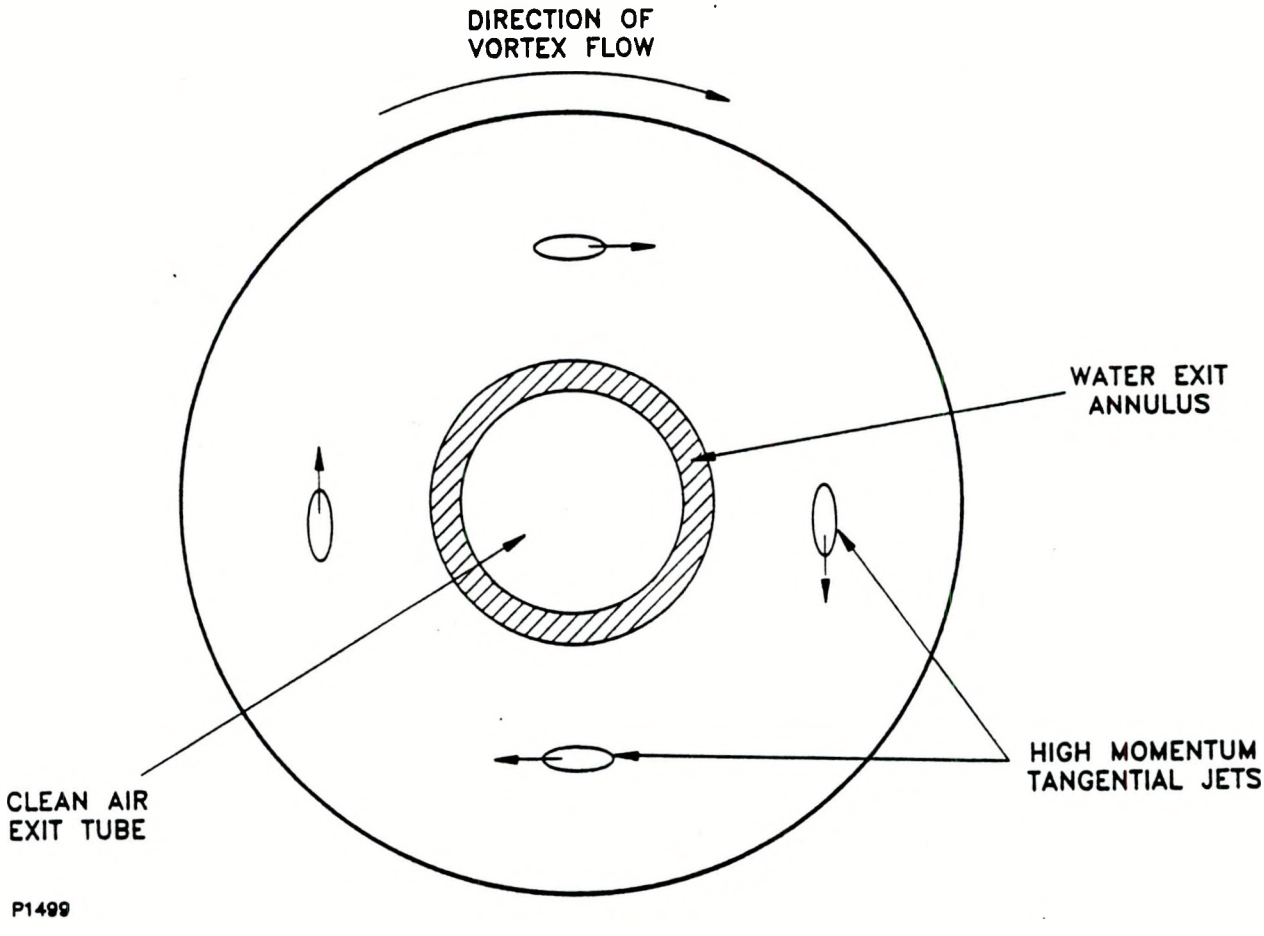

Figure 3-8 Schematic Diagram Showing Location of Jets on CVS Chamber End Walls

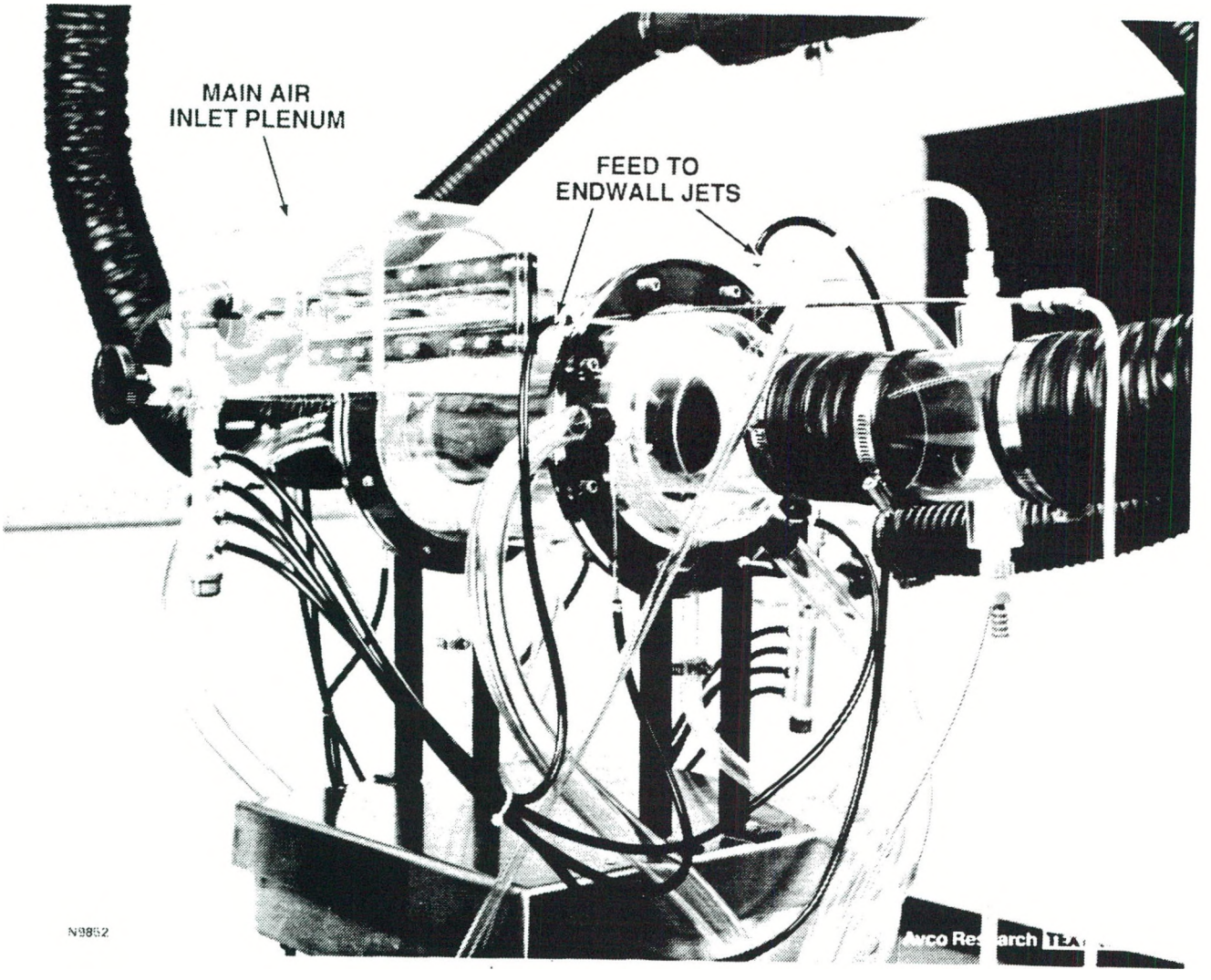

Figure 3-9 Photograph of Dual-Inlet CVS Design, Showing End Wall Jet Air Supplies

connected to a regulated shop air supply. Tests were conducted for steadily increasing endwall mass flows, until the endwall jets were choked. No improvement in water outflow characteristics, water loss, mass of water required to establish a stable liquid layer or mass of water contained was observed. In fact, at high endwall jet mass flows, the water loss at the endwalls increased significantly, due to liquid spraying where the high velocity jet impacted the liquid layer on the chamber walls. Tests were also conducted for both water outflow geometries (W1 and W2) in order to modify the net axial air flow through the water exit annulus. No effect was detected.

The poor performance of the endwall jets at modifying the secondary flows was unexpected, given the fact that the same technique had been used successfully in the MIT experiments. A significant difference between the two experiments, however, is the fact that there is a net through-flow of liquid in the CVS. A brief experiment was conducted in which the water outlet annulus at either end of the CVS chamber was closed off, by inserting a Plexiglas ring. In this manner the current experiment was made to simulate conditions in the MIT experiment. Under these conditions the endwall jets were seen to have a beneficial effect. The mass of liquid contained was increased over that for the normal CVS configuration. Therefore the failure of the endwall jets to improve the water containment in the CVS appears to be related to the fact that there is a liquid and an air outflow at the endwall.

Alternate Geometries. Tests were also conducted for the case of multiple jet air inlets. For the L/D = 1.5 model, the inlet arrangement consisted of two sets of eight inlet jets of diameter 0.358". Based on gas turbine film cooling practice (Goldstein, 1971) the jet centers were spaced at one and a half hole diameters in order to give optimum jet interaction and film coverage on the chamber wall. An aerodynamic test of this inlet arrangement (no liquid injection) showed that inlet velocities up to 53 m/s were obtained and the dimensionless

pressure drop was 3.7 inlet dynamic heads. This was the lowest dry pressure drop of any of the configurations tested.

Water addition experiments with the multiple jet inlet showed generally the same flow field characteristics, levels of water containment, pressure drop and water loss rates as for the slot inlets. However, there appeared to be a much stronger and more vigorous air/liquid interaction. Air bubbles in the liquid were clearly visible for the jet inlet case, whereas they were not for the slot inlet case.

TABLE 3-3

CONFIGURATION FOR CVS OF ASPECT RATIO = 1.0

Chamber Internal Diameter	6.50"
Aspect Ratio (L/D)	1.00
Air Inlet Type	Slots
Inlet Slot Height	0.312"
Air Outlet Type	Flow Guide Slot Exit
Air Outlet Diameter (D_e/D)	0.50
Water Outlet Type	Single Tube, 0.372" ID

Tests were also made with a CVS chamber of unity aspect ratio. The dimensions of this model are given in Table 3-3. An aerodynamic test of this inlet arrangement (no liquid injection) showed that inlet velocities up to 43 m/s were obtained and the dimensionless pressure drop was 6.1 inlet dynamic heads. Water addition experiments with the L/D = 1.0 model showed generally the same flow field characteristics, levels of water containment, pressure drop and water loss rates as for the higher aspect ratio model.

3.1.3 Dual-Inlet Conclusions

Based on the testing conducted, the following conclusions may be drawn about the performance of the dual-inlet CVS configuration. The pressure drop of the device was well controlled by suitable design modifications: refinements in system design progressively reduced the device pressure drop to approximately one third that of a conventional reverse flow cyclone separator operating at the same inlet velocity. The device pressure drop was also lower with a stable liquid layer confined within the chamber than without such a layer.

Water addition experiments indicated that a sheet of water could indeed be established and contained within the chamber and that the proposed water removal mechanism via the chamber end-wall secondary flows was effective. However, three areas of concern were identified:

1. The amount of liquid contained within the CVS was small - the layer of liquid in the CVS was thinner than desired and did not lead to the level of air/liquid interaction expected.
2. There was a relatively high through-flow of liquid, leading to flow handling problems in the water out-take chamber and liquid loss.
3. At higher air inlet velocities there was some atomization of the liquid layer at the air inlets, leading to liquid loss.

The first problem is illustrated in Figure 3-10. The observed liquid layer behavior (a) is compared with the desired behavior (b). The intention was to have a liquid layer which is not in contact with the wall and is 'supported' on a layer of air, the air bubbling through the liquid in order to exit the chamber. The actual layer was thin and did appear to be on the chamber wall. The inlet air jets penetrated the liquid layer completely (hence the atomization problem), leading to relatively poor air/liquid interaction. The inlet jets were not submerged, as desired.

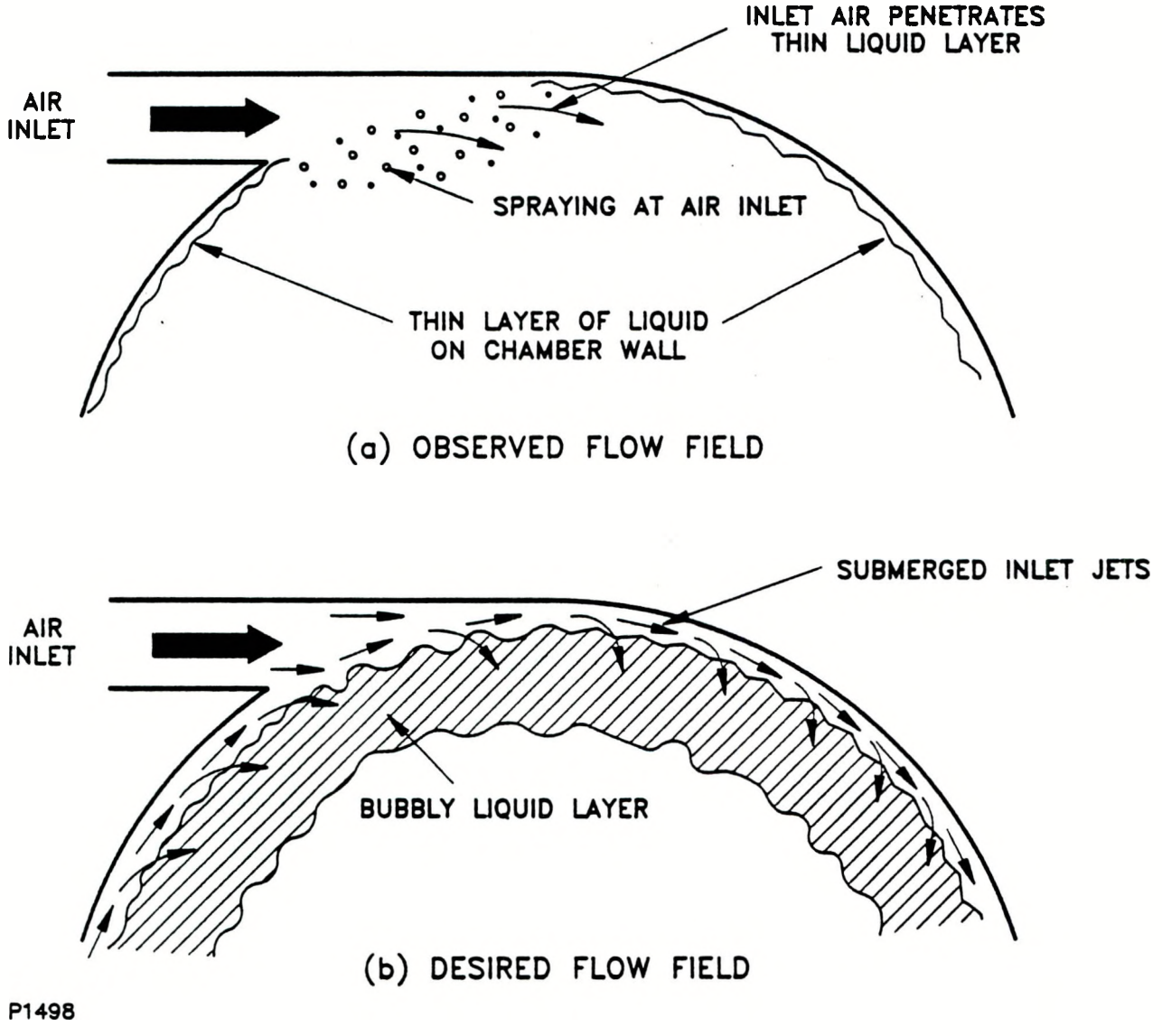

Figure 3-10 Schematic Diagram Showing (a) Observed Flow Field Within Dual-Inlet CVS Design and (b) Desired Flow Field

The problems described above apply to all dual-inlet configurations tested, though problems (1) and (2) could essentially be eliminated at certain conditions. However, the lack of submerged inlets jets and a vigorous air/liquid interaction suggested that the desired level of particulate removal may not be obtained.

The CVS chamber was therefore re-designed in order to establish a flow field with submerged inlet air jets, to increase the level of liquid containment and to enhance the air/liquid interaction.

3.2 SQUIRREL CAGE CVS

3.2.1 Design Details

The re-designed chamber, the Mark I Squirrel Cage CVS, is illustrated schematically in Figure 3-11. The number of tangential air inlets was increased from 2 to 24. A plenum was required in order to feed all 24 inlets. In order to facilitate progress, the revised CVS chamber was designed such that the existing 6.5" internal diameter, L/D=1.0 CVS model could be used as a plenum chamber to feed a 4.25" internal diameter, 24 inlet squirrel cage CVS, see Figure 3-11. This minimized the amount of machining and fabricating required before the new design could be tested. The key dimensions of the revised CVS design are given in Table 3-4. A photograph of the modified test arrangement is given in Figure 3-12.

3.2.2 Two-Phase Flow Tests

First tests with the 24 inlet squirrel cage configuration showed a dramatically different two-phase flow field than had been observed with the dual-inlet CVS configuration. The inlet air jets were now clearly submerged beneath a much thicker liquid layer than had been observed hitherto. There was a much more vigorous interaction between the air and the liquid: the liquid layer appeared thick and frothy in nature. The mass contained increased dramatically to a

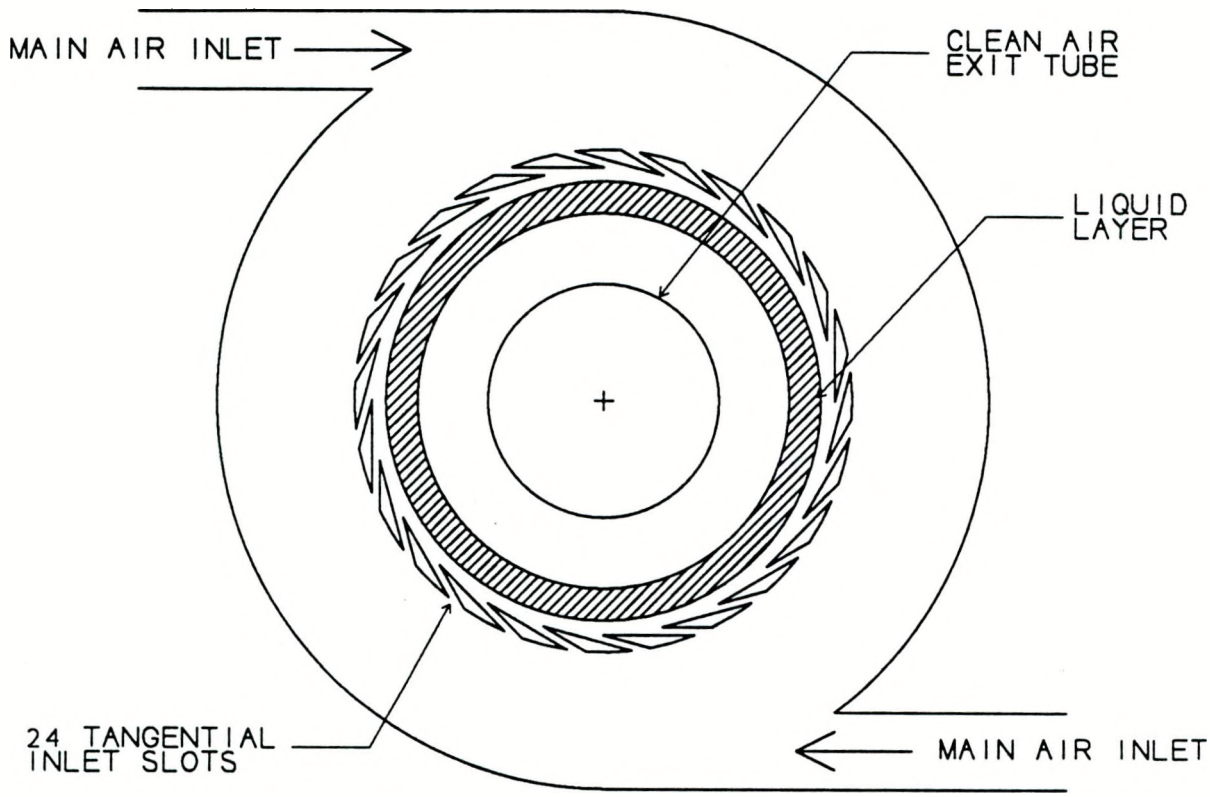

Figure 3-11 Schematic Diagram of Re-Designed CVS Chamber of "Squirrel Cage" Design

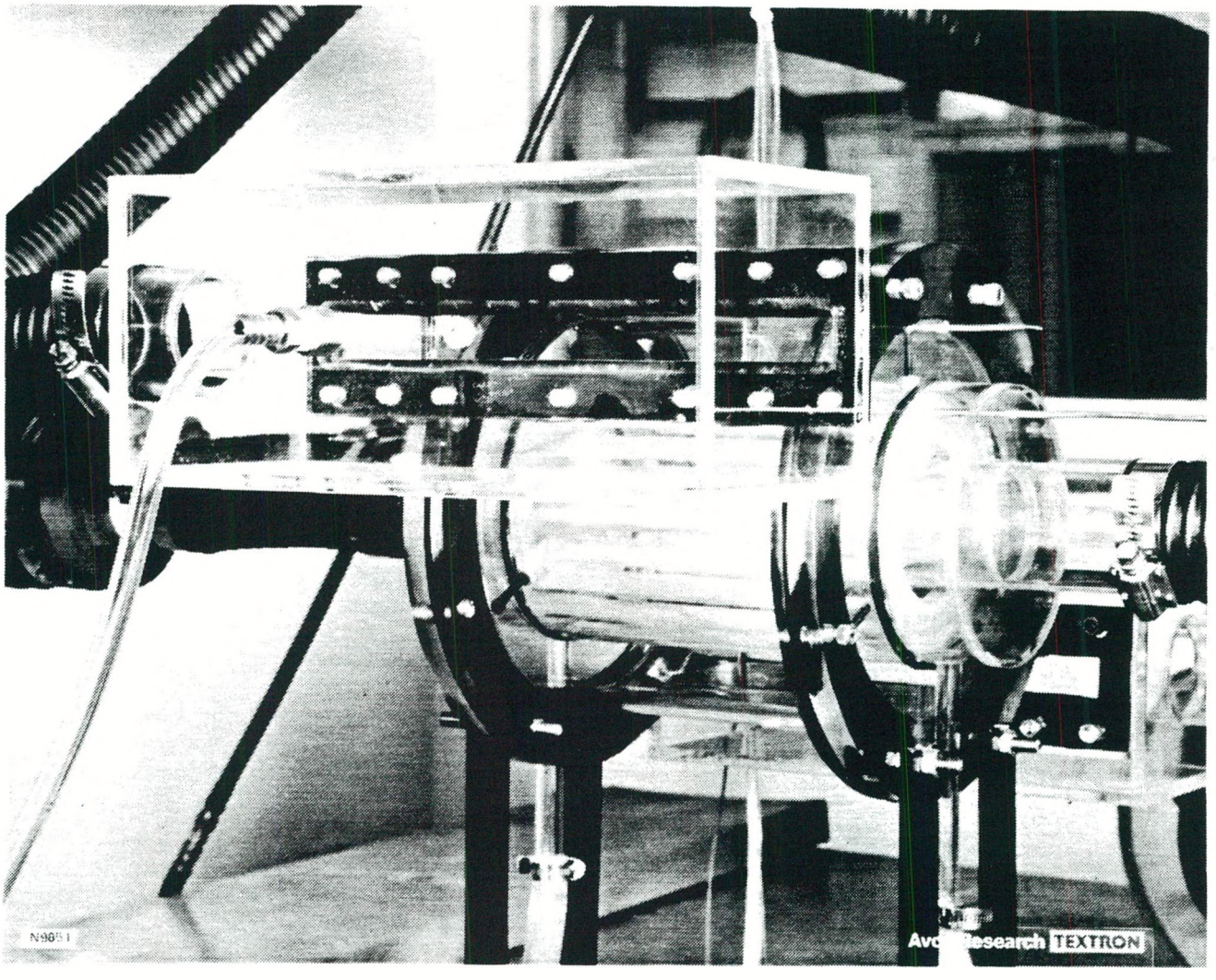

Figure 3-12 Photograph of Mark I Squirrel Cage CVS Installation

maximum corresponding to approximately 20 percent of chamber volume. Once again, the pressure drop was lower when a stable liquid layer was established than without such a layer. Other significant differences observed with the squirrel cage CVS were that the vortex finder outlet appeared to give superior performance to the flow guide slot outlet and the fact that a spray cloud was visible at the outer edges of the liquid layer, indicating some atomization and entrainment of liquid in this region. Two-phase flow experiment results for the squirrel cage CVS are described in more detail below.

TABLE 3-4

MARK I SQUIRREL CAGE CVS CONFIGURATION

Chamber Internal Diameter	4.25"
Aspect Ratio (L/D)	1.53
Air Inlet Type	Slots
No of Slots	24
Inlet Slot Height	0.040"
Air Outlet Type	Vortex Finder
Air Outlet Diameter (D_e/D)	0.41
Water Outlet Type	Single Tube, 0.372" ID

Figure 3-13 shows the liquid containment results for the squirrel cage CVS. Liquid containment, expressed as an equivalent percentage of chamber volume, is plotted against total air mass flow rate. Data for the two air outlet types (vortex finder (VF) and flow guide slot exit (SE)) are plotted. The vortex finder shows clearly superior performance, with a maximum containment of 18 percent of chamber volume. For comparison purposes, data from the original dual-inlet CVS tests is included. At the same air and water mass flow rates, the measured containment for the dual-inlet design is one sixth that for the squirrel cage design. The

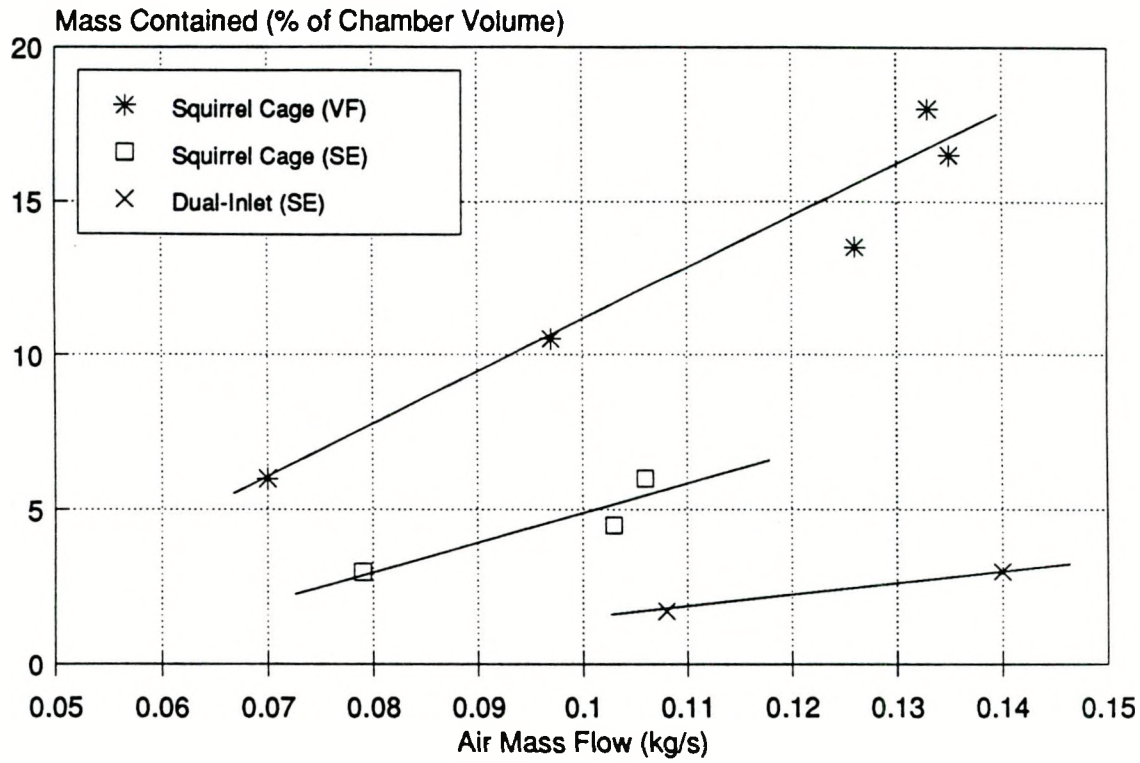

Figure 3-13 Mass of Liquid Contained, Expressed as a Percentage of Chamber Volume, as a Function of Air Mass Flow Rate for Mark I Squirrel Cage CVS Design with Vortex Finder (VF) and Slot Exits (SE) and for Dual-Inlet CVS Design

monotonic upward trend of containment with air mass flow observed for the squirrel cage design is as expected.

Significant qualitative flow field differences were observed between the vortex finder and the slot exit arrangements. As mentioned above, for the vortex finder exit the liquid layer was thick (of order 0.5" to 0.75") and appeared frothy. The layer was of uniform thickness along the length of the CVS chamber. For the slot exit it proved extremely difficult, if not impossible, to obtain a uniform liquid layer along the length of the CVS chamber. The liquid layer was always biassed to one end or another of the chamber. In addition, the layer was not as thick as for the vortex finder case, and did not appear as frothy.

It should be noted that the Mark I squirrel cage CVS was undersized for the design mass flow rate. As discussed above, the chamber was sized such that the existing 6.5" internal diameter, L/D=1.0 CVS model could be used as a plenum chamber to feed the 24 inlet squirrel cage CVS. Thus this design had a high pressure drop at the design mass flow. Pressure drop data for the Mark I squirrel cage CVS is presented in Figures 3-14 and 3-15, for the vortex finder and slot outlets, respectively.

Considering the vortex finder data first (Figure 3-14), a dramatic reduction in pressure drop is clearly seen once a stable liquid layer is established (the 'wet' pressure drop is less than half the 'dry' pressure drop). In non-dimensional terms, the dry pressure drop is approximately 22 inlet dynamic heads and the wet pressure drop is only 9 inlet dynamic heads. Possible mechanisms for this large reduction in pressure drop include: (1) reduction of angular momentum at vortex finder outlet due to momentum transfer between the inlet air and the liquid layer; (2) reduction of wall skin friction losses; and (3) turbulence suppression by liquid droplets. The first of these mechanisms is most likely responsible for most of the reduction, with effects (2) and (3) producing second order effects. The bulk of the pressure drop produced in

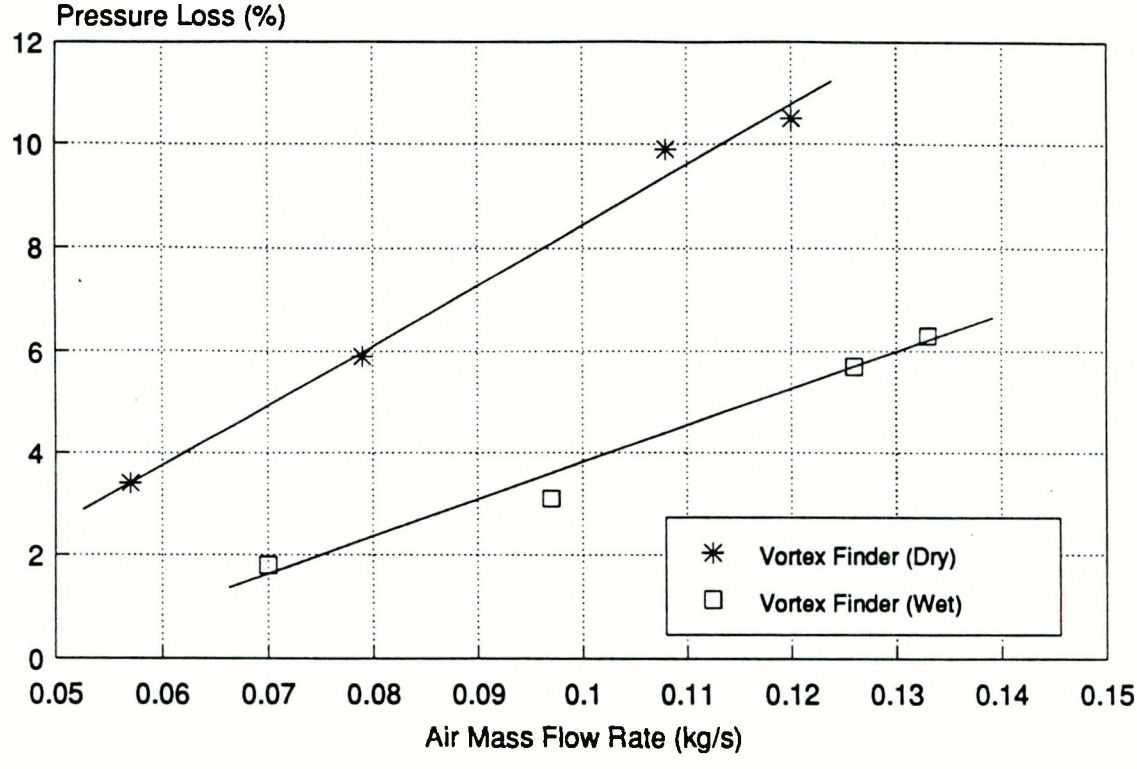

Figure 3-14 Pressure Loss, Expressed as a Percentage of CVS Inlet Total Pressure, for Mark I Squirrel Cage CVS with Vortex Finder Outlet With (Wet) and Without (Dry) Liquid Layer Present

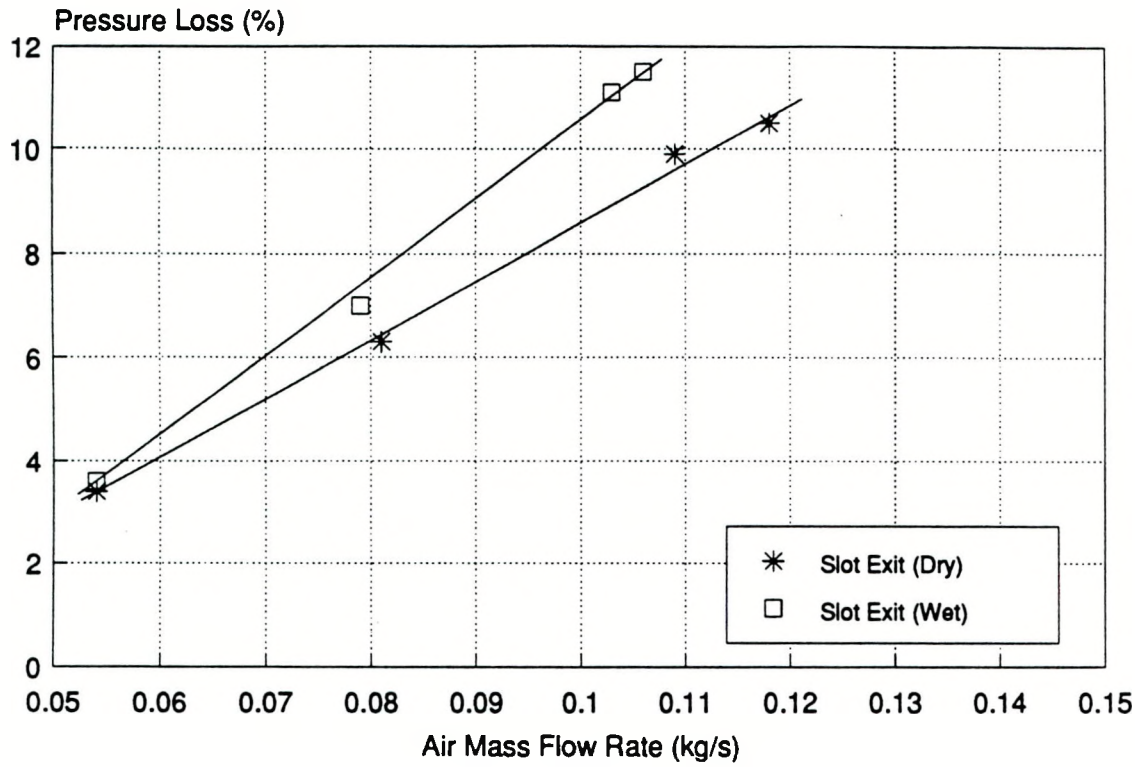

Figure 3-15 Pressure Loss, Expressed as a Percentage of CVS Inlet Total Pressure, for Mark I Squirrel Cage CVS with Slot Outlet With (Wet) and Without (Dry) Liquid Layer Present

devices with vortex finder type outlets is associated with the high angular momentum exit flow. It is possible that the presence of the liquid layer leads to reduced tangential velocities at the surface of the liquid layer, and consequently in the exit pipe itself, thereby reducing the radial pressure gradient and the pressure drop considerably.

Very different effects were observed for the slot exit, see Figure 3-15. In particular, the 'wet' pressure drop was higher than the 'dry' pressure drop, by approximately 20 percent. In non-dimensional terms, the dry pressure drop is approximately 22 inlet dynamic heads and the wet pressure drop is over 28 inlet dynamic heads. It should be remembered that with the slot exit, as discussed above, it was almost impossible to obtain a uniform liquid layer along the length of the CVS chamber: the liquid layer was biassed to one end of the chamber and was not as thick as for the vortex finder case, and did not appear as frothy. Using the arguments given above in reference to the vortex finder results, the presence of a liquid layer in only a portion of the CVS can be projected to lead to a variety of effects which could be responsible for the higher pressure drop. Assuming that the axial distribution of inlet mass flow is uniform (a significant assumption), the portion of the chamber which has no liquid layer will have a relatively high flux of angular momentum and a large radial pressure gradient. The portion of the chamber which has a liquid layer present will have a lower flux of angular momentum and a reduced radial pressure gradient. This, in turn, will lead to an axial pressure gradient near the center of the chamber, which will drive mass flow from the 'wet' portion of the CVS to the 'dry'. Thus the axial distribution of outlet mass flow will be decidedly non-uniform, potentially leading to the bulk of the inlet mass flow exiting via only a portion of the outlet slot, thereby leading to an increased pressure drop.

Given the paucity of flow field data, these arguments are speculative. Detailed measurement of the radial, tangential and axial velocity distributions in the chamber with and

without liquid injection would provide much insight into these effects. However, not only would detailed velocity mapping of the two-phase flow field be difficult and time-consuming (non-intrusive methods would be required), but it was also outside the scope of the present work.

Figure 3-16 shows the inlet water mass flow rate required for the establishment of a stable liquid layer within the CVS as a function of the air mass flow rate. For the slot exit, a stable liquid layer was only obtained for relatively low mass flow rates. Again, the vortex finder exit is clearly superior: these liquid flow rates are approximately half those required for establishment of a stable layer in the dual-inlet CVS.

Finally, Figure 3-17 shows the percentage of input water that exits via the clean gas exit, again plotted as a function of air mass flow rate. For the vortex finder, approximately one third of the water exited via this route at and above design mass flow. For the slot exit, approximately three-quarters of the water exited via the clean gas exit. In both cases, however, the liquid that left via the central clean gas exit tube was immediately inertially separated onto the walls of the two outlet tubes, making it very amenable to subsequent re-capture.

3.3 SUMMARY

A CVS test rig was designed and fabricated. Aerodynamic testing was conducted for a variety of CVS geometries. From the point of view of pressure drop, the slotted exit tube was found to be superior to the more conventional vortex finder type exit. The vortex finder tube produced 50 percent higher pressure drops than the slotted exit at the same mass flow. Further refinements in system design progressively reduced the device pressure drop to less than half that of a conventional reverse flow cyclone separator operating at the same air inlet velocity.

Two-phase flow experiments on the initial dual-inlet CVS design indicated three areas

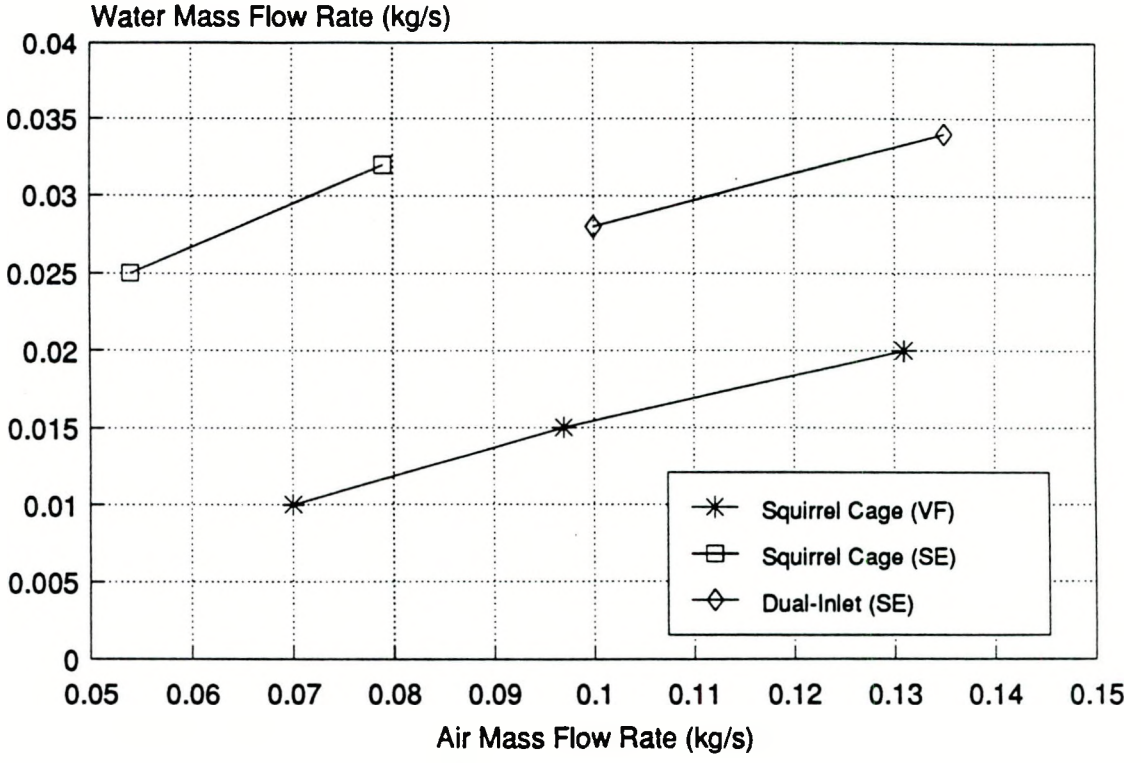

Figure 3-16 Minimum Input Water Flow Rate Required to Establish a Stable Liquid Layer as a Function of Air Inlet Velocity for Mark I Squirrel Cage CVS Design with Vortex Finder (VF) and Slot Exits (SE) and for Dual-Inlet CVS Design

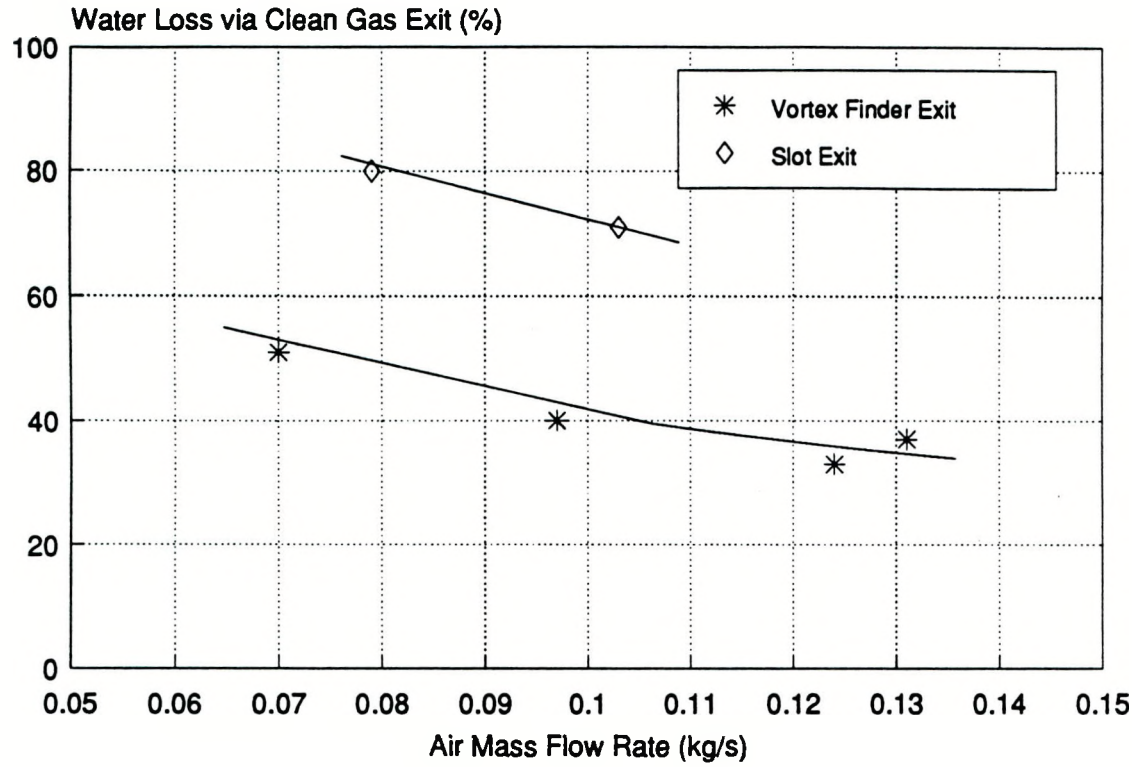

Figure 3-17 Water Loss via Clean Gas Exit for Mark I Squirrel Cage CVS as a Function of Air Mass Flow Rate

of concern: (1) a low levels of liquid containment; (2) a high through-flow of liquid, leading to flow handling problems in the water out-take chamber and liquid loss; and (3) atomization of the liquid layer near the air inlets at high air inlet velocities, leading to liquid loss. The first problem was considered the most significant of the three. The liquid layer was thin and the inlet air jets penetrated the liquid layer completely, leading to relatively poor air/liquid interaction. In other words, the inlet jets were not submerged, as desired. The lack of submerged inlets jets and a vigorous air/liquid interaction suggested that the desired level of particulate removal may not be obtained.

Accordingly, the CVS was re-designed. The re-designed squirrel cage CVS demonstrated clear superiority over the initial CVS design. Results obtained for the Mark I squirrel cage CVS indicated effective liquid containment and extremely vigorous air/liquid interaction at a reasonable pressure drop. This CVS design met the performance goals established for this task. In contrast to the observations made during the testing of the dual-inlet CVS, the two-phase testing of the squirrel cage CVS showed the vortex finder exit to be clearly superior to the slot exit in all areas of concern: pressure drop, liquid containment, liquid mass flow to establish liquid layer, level of air/liquid interaction and rate of liquid loss via clean gas exit.

A portion of the inlet water flow was found to exit the CVS chamber via the clean gas exit. All the liquid that enters the clean air exit is very effectively inertially separated onto the exit duct walls. This is to be expected, given the centrifugal forces present in the outlet ducts. This means that it was relatively simple to collect this water in a secondary device. This is discussed further in the next section.

4.0 CLEANUP EXPERIMENTS

This section is divided into two parts. The first part contains a chronology of the testing, starting with the rig modifications and shakedown testing. During the cleanup experiments the CVS design was optimized with respect to fine particulate collection efficiency, pressure drop and operability of the device. The three CVS designs that were developed and tested during this process are termed the Mark I, II and III CVS designs. The bulk of the cleanup experiments were conducted with the Mark III design. The second part of this section contains a discussion of the results obtained during the cleanup experiments. CVS performance data and operational observations will be presented.

4.1 TEST CHRONOLOGY

4.1.1 Shakedown Tests

The first cleanup experiments were carried out with the Mark I squirrel cage CVS configuration described above (Section 3.2). Its geometric parameters are given in Table 4-1. A photograph of the Mark I CVS as installed is shown in Figure 4-1.

A number of modifications were made to the experimental hardware before commencing the cleanup tests. These included adding two water knockout chambers and a filter section downstream of the CVS. The purpose of the knockout chambers is to collect any water which is entrained into the clean air leaving the CVS. The purpose of the filter section is to allow the mass of dust passed by the CVS to be determined in order to obtain measurements of cleanup efficiency. A schematic diagram of the revised arrangement is given in Figure 4-2. Figure 4-3 is a photograph of the complete experimental installation for the cleanup tests.

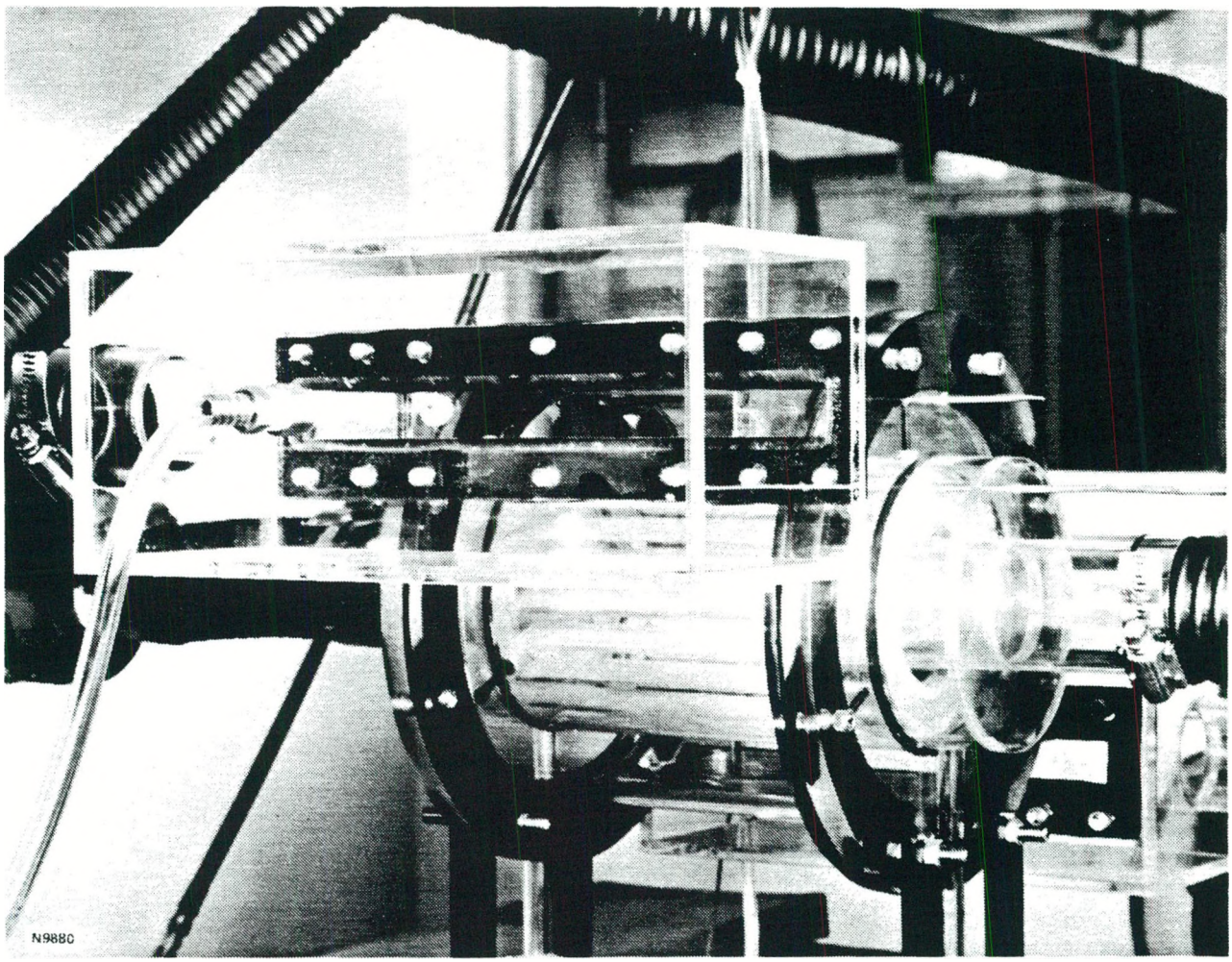

Figure 4-1 Photograph of Mark I Squirrel Cage CVS Installation

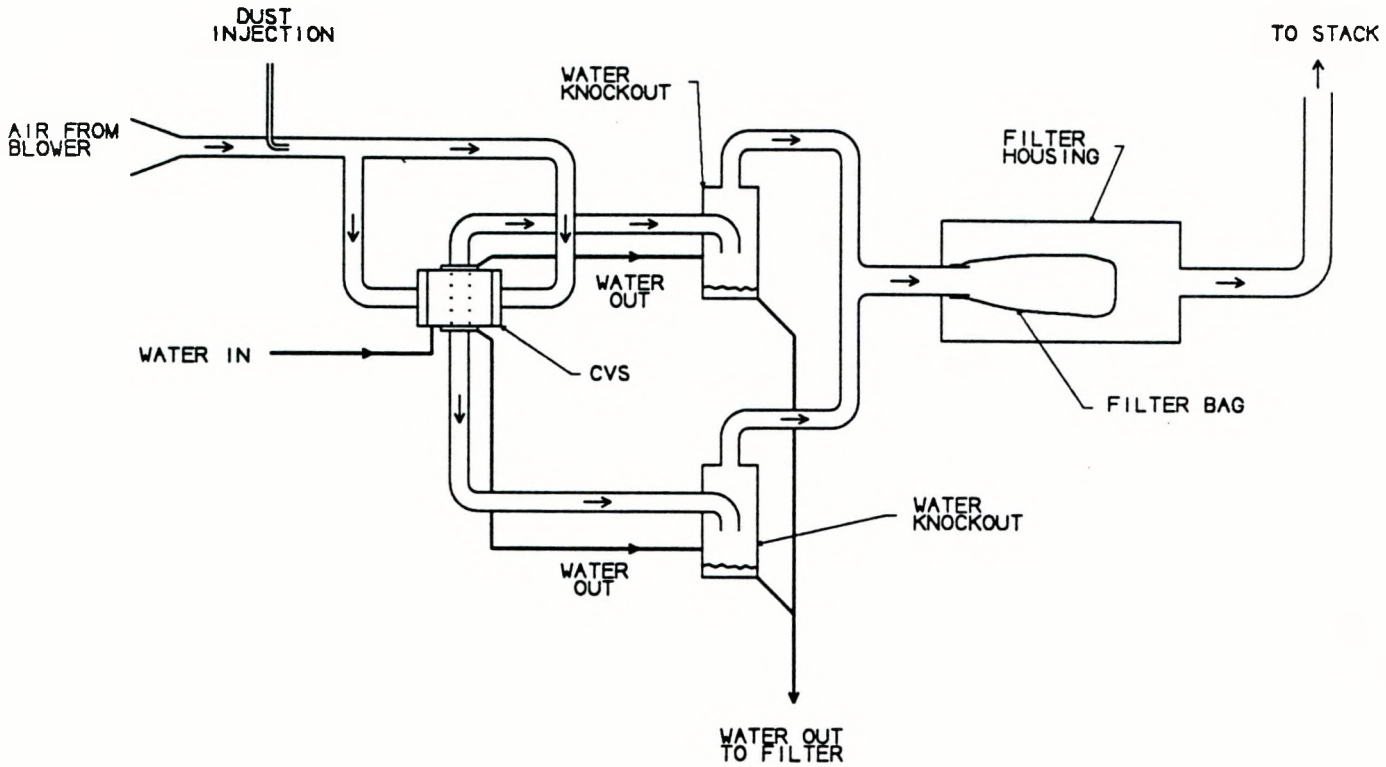

Figure 4-2 Schematic Diagram of Experimental Arrangement for Cleanup Experiments

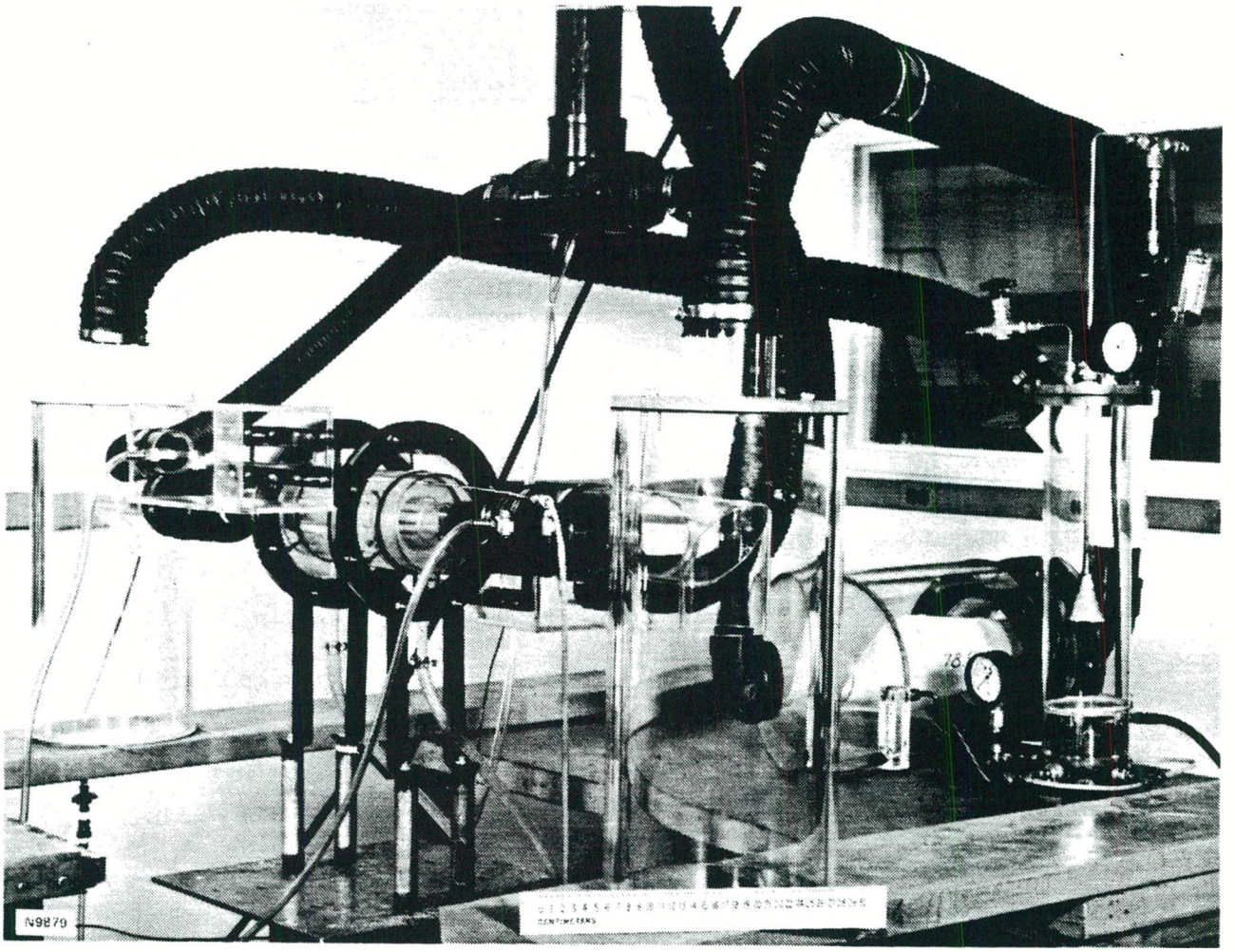

Figure 4-3 Photograph of Experimental Installation for Cleanup Experiments

TABLE 4-1

MARK I SQUIRREL CAGE CVS CONFIGURATION

Chamber Internal Diameter	4.25"
Aspect Ratio (L/D)	1.53
Air Inlet Type	Slots
No of Slots	24
Inlet Slot Height	0.040"
Air Outlet Type	Vortex Finder
Air Outlet Diameter (D_e/D)	0.41
Water Outlet Type	Single Tube, 0.372" ID

Shakedown of New Test Rig. Shakedown tests were conducted with the new experimental installation in order to evaluate the efficiency of the water removal arrangement in the clean air exits. A known quantity of water was introduced into the CVS and the mass of water collected from the both the CVS itself and the water knockout chambers was recorded. Complete recovery was made, within the measurement accuracy. The outlet filter weight change was also monitored. This showed a very small and consistent increase of approximately 0.1 g (in approximately 100 g). This increase was independent of the length of time the test was run and of the quantity of water flowed through the CVS. After approximately half an hour at room temperature, the filters consistently returned to their original weights, indicating that the weight gain was due to humidification of the filter material.

Fluidized Bed Feeder Tests. Fluidized bed feeder calibration tests were also made. A schematic diagram of the fluidized bed feeder used in these experiments is shown in Figure 4-4. The CVS nominal design airflow simulates the exhaust flow from a 1 MM Btu/hr combustor. Assuming that a 2 percent ash coal is burned, the exhaust ash mass flow rate is approximately 13 g/min. Tests were made to ensure that a stable dust feed in the range 10-15 g/min could be

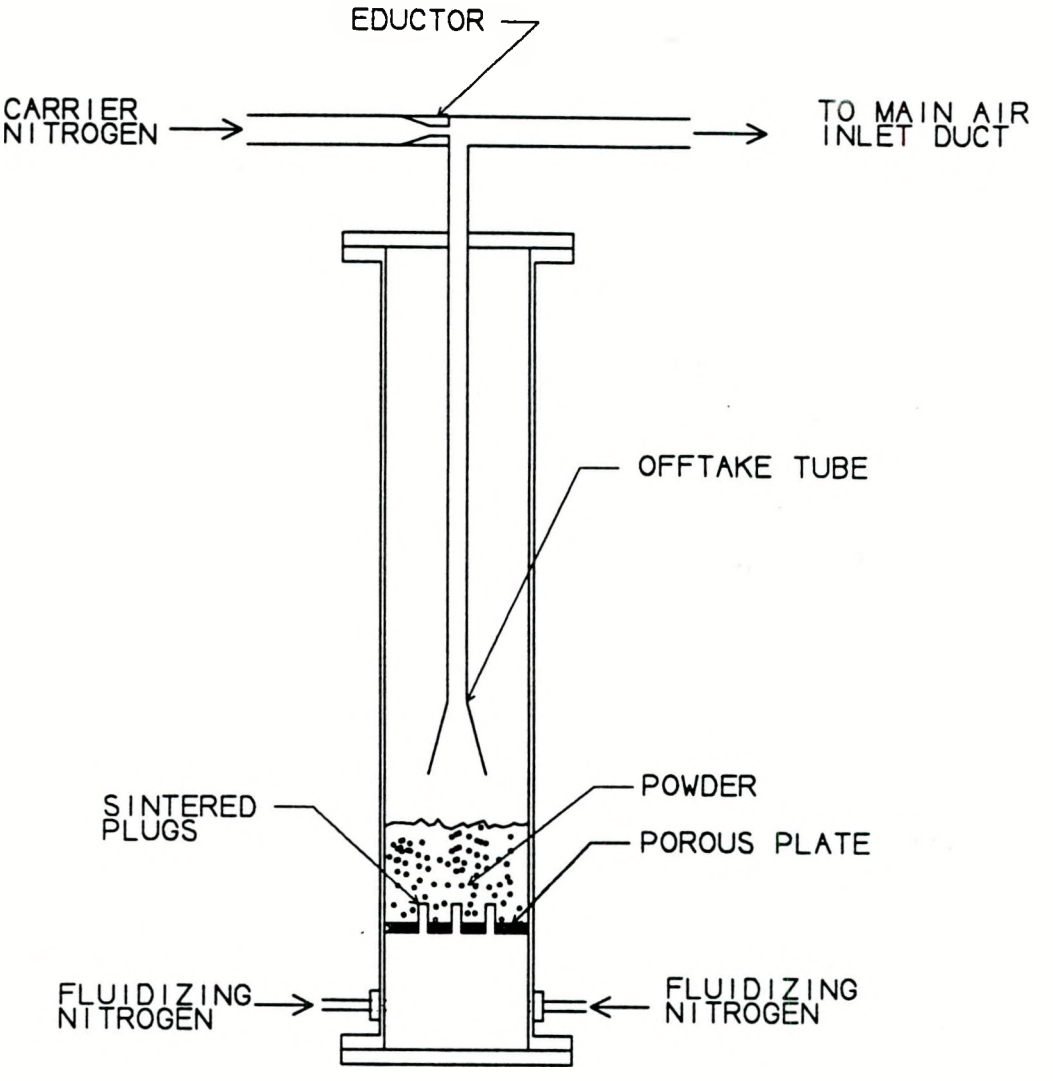

Figure 4-4 Schematic Diagram of Fluidized Bed Dust Feeder

obtained. In this report, dust size distributions will be given in terms of d_{10}, d_{50} and d_{90}, where 10 percent of the mass of the dust is contained in particles of diameter d_{10} or smaller, 50 percent in particles of diameter d_{50} or smaller and 90 percent in particles of diameter d_{90} or smaller. First tests were made with a relatively coarse silica dust for which d_{10}, d_{50} and d_{90} were 8, 19 and 34 microns respectively. The overall size distribution for the silica dust is shown in Figure 4-5. Satisfactory feed was obtained for this dust.

Preliminary Cleanup Tests. A preliminary cleanup test was conducted with the silica dust. The CVS airflow was set to the design mass flow rate and 218 g of silica dust were introduced into the main air inlet pipe over a period of 20 minutes. After the test the filter unit was disassembled and the filter weight gain was recorded. A gain of 0.1 g was measured, indicating a CVS collection efficiency of 99.95 percent.

Subsequently, further shakedown tests were conducted with much finer alumina dust, for which d_{10}, d_{50} and d_{90} = 2, 5 and 8 microns respectively, see Figure 4-5. Some difficulty was experienced in feeding this dust. In order to obtain reliable feed of this very fine material at the desired flow rates, a greater nitrogen flow rate through the fluidized bed was required than for the silica dust used previously. The feeder was modified so as to provide a greater bed flow and the carrier flow was dispensed with. The powder was thus fed directly through the bed offtake tube into the main air inlet and the bed nitrogen flow was used as the dust carrier flow.

Four cleanup tests were then made with the fine alumina dust, in the same manner as was described above. At the design air mass flow, collection efficiencies of 99.75, 99.87 and 99.82 percent were measured. One test was made with no water addition: a collection efficiency of 77.27 percent was measured. Thus with no water present the CVS chamber acts as a high efficiency cyclone separator, with separation due only to centrifugal forces. With a confined liquid layer present, however, the intimate and vigorous air/liquid interaction provides for

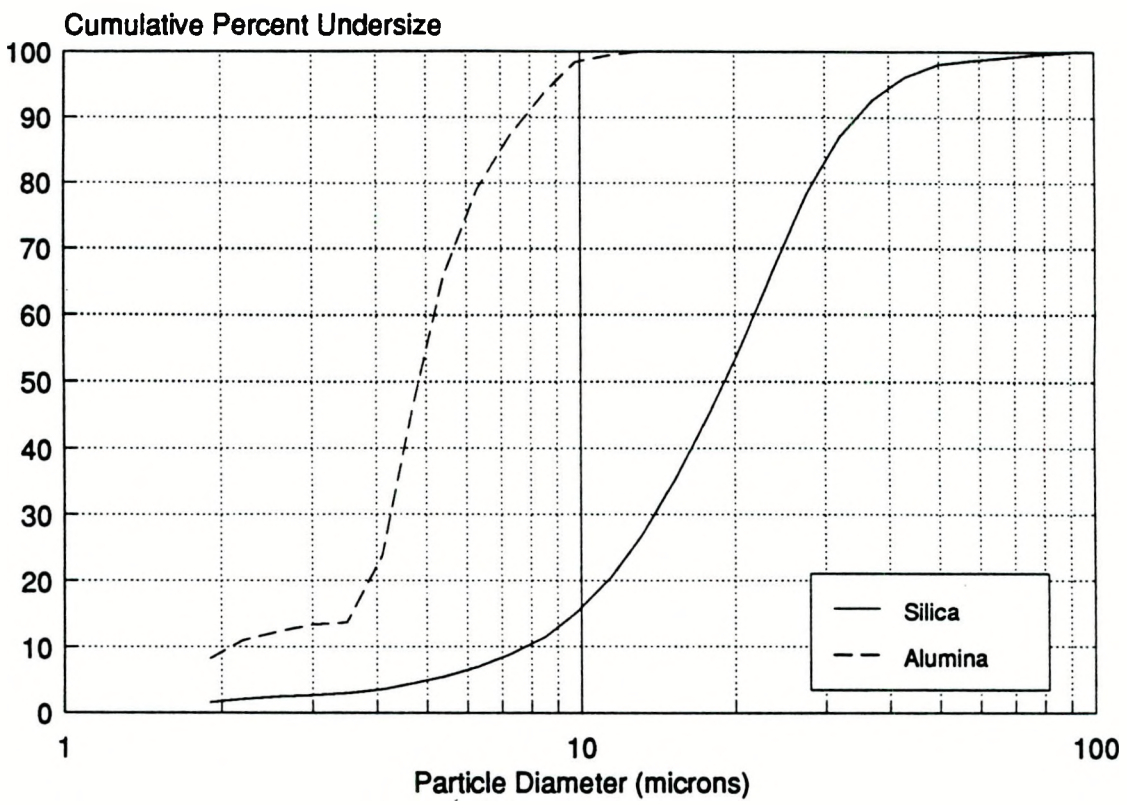

Figure 4-5 Size Distributions of Silica and Alumina Used in Shakedown Experiments

extremely high collection efficiencies.

During the last of the tests with fine alumina powder, the fluidized bed feeder was damaged by a chamber overpressure.[1] This caused the porous plate to become detached from the main feeder vessel, see Figure 4-4. Once the feeder was repaired it proved impossible to successfully fluidize the fine alumina powder. It transpired that before the feeder failure the bulk of the nitrogen flow through the bed was via leaks at the junction of the porous plate and the feeder vessel wall. When the feeder was re-built the leaks were fixed and it no longer proved possible to obtain sufficient fluidizing nitrogen flow through the porous plate to fluidize the fine powder. In order to overcome this problem five sintered plugs were installed in the feeder. The fluidizing nitrogen was then supplied through the sintered plugs. A small vibrator was also attached to the feeder wall, below the top of the bed. This proved to be an effective method of feeding the fine dust at a reasonable nitrogen mass flow rate and feeder chamber pressure.

The filter material used to filter the CVS outlet flow in these experiments is rated at 99.8 percent collection down to 1 micron particles. This was checked by feeding a known quantity of the fine alumina dust directly into the CVS outlet piping and hence into the filter, in order to determine the suitability of the filter material collection of these fine dusts. Greater than 99 percent collection was measured in the filter, with the discrepancy probably due to very small amounts of deposition in the lines.

4.1.2 Mark I CVS Cleanup Tests

The nominal fly ash to be tested in the CVS was utility fly ash sieved to below 20 microns in diameter. Tests were actually conducted with three different sizes of fly ash: 200 mesh, 325

[1] This caused an extremely high transient dust flow rate of 200 g in 1 - 2 seconds, some 500 times the design dust mass flow rate, yet the CVS collection efficiency was still measured at 99.82 percent for this test.

mesh and ultra-fine, sub-20 micron ash. An ash classifier was designed in order to produce such fine ash from as-supplied utility fly ash, see Section 4.2.1. While the ash classifier system was being commissioned, a number of cleanup tests were made with larger grinds of fly ash. Two tests were made with 200 mesh fly ash and seven were made with 325 mesh fly ash. Subsequently five tests were made with ultra-fine, sub-20 micron fly ash. Air mass flow rate, liquid/air ratio and ash mass flow rates were varied in these tests. In order to verify the suitability of the downstream air filter for measurement of the mass of ash passed by the CVS, downstream filter tests were also conducted for all three fly ash size distributions in the same manner as that described above. Better than 99 percent collection in the filter was measured for all three sizes of fly ash.

Through all these cleanup tests, the Mark I CVS demonstrated extremely efficient capture of fine fly ash, see discussion below (Section 4.2). However, it was felt that the same performance could be obtained at a lower pressure drop.

4.1.3 Mark II CVS Cleanup Tests

The squirrel cage CVS was re-designed in order to retain the same excellent fine particulate collection performance that had been demonstrated by the Mark I CVS, but at a lower pressure drop. The key geometric parameters of the Mark II CVS are given in Table 4-2

A series of two-phase flow experiments were made to assess the performance of the Mark II CVS. Initial results were encouraging: non-dimensional pressure drops for the Mark II CVS were considerably lower than those for the Mark I CVS. The dry and wet non-dimensional pressure drops (wet pressure drop is for stable liquid layer in CVS) for the Mark II CVS with vortex finder outlets were 7 and 4.5 inlet dynamic heads, respectively. The corresponding values for the Mark I CVS were 22 and 9 dynamic heads. Once again, the vortex finder exit was superior to the slot exit: the dry and wet non-dimensional pressure drops for the Mark II CVS

with slot outlets were 10 and 15 inlet dynamic heads, respectively. The corresponding values for the Mark I CVS were 22 and 28 dynamic heads.

TABLE 4-2

MARK II SQUIRREL CAGE CVS CONFIGURATION

Chamber Internal Diameter	6.50"
Aspect Ratio (L/D)	1.00
Air Inlet Type	Slots
No of Slots	24
Inlet Slot Height	0.040"
Air Outlet Type	Vortex Finder
Air Outlet Diameter (D_e/D)	0.50
Water Outlet Type	Single Tube, 0.372" ID

The liquid layer was not as stable in the Mark II CVS as in the Mark I, and considerably higher liquid flow rates were required in order to establish an acceptable liquid layer in the chamber. Consequently, the liquid injection velocity in the Mark II CVS was much higher than in the Mark I CVS. The high liquid inlet momentum led to a disruption of the liquid layer in the vicinity of liquid injectors. The diameter of the liquid inlet tubes was increased from 0.125" to 0.250" in order to decrease the liquid inlet momentum at a given flow rate. This change resulted in a much more stable liquid layer, but once again the water flow required (60-120 gph) was significantly higher than that for the Mark I CVS (10-30 gph).

It was also noticed that the airflow in the annular plenum feeding the squirrel cage slots was asymmetric. This was due to the fact the two plenums feeding this annulus were only fed from one side each. In order to rectify the situation, the inlet air supply was further split and

each main inlet plenum was fed from both sides. This eliminated the asymmetric flow in the annular plenum.

A further change was made to the fluidized bed feeder in order to increase the stability of the feed of the ultra-fine fly ash. As ash is fed from the feeder the bed tended to settle and an increasingly large nitrogen flow was required in order to obtain the desired ash flow. An electrically driven stirring bar which rotates at 1 rpm was installed within the powder bed. The interaction between the nitrogen flow and the stirrer successfully prevented the bed from settling.

Six cleanup tests were made with the Mark II CVS using the ultra-fine fly ash. Air mass flow rates and liquid/air ratios were varied. In general, the results obtained were as desired: at the same collection efficiency the Mark II CVS had a substantially lower pressure loss, see Section 4.2 below.

Considerably ash deposition occurred in the annular plenum feeding the squirrel cage slots. After some 15 minutes of testing the deposits had begun to obstruct some of the inlet slots. This problem did not occur in the Mark I CVS tests. The deposits started in strong re-circulation zones which were established in the annulus just upstream of each main air slot inlet. The CVS was re-designed to eliminate this problem.

4.1.4 Mark III CVS Cleanup Tests

The re-designed CVS was designated the Mark III CVS. Its principal geometric parameters are given in Table 4-3. The squirrel cage diameter was reduced, while keeping the annular plenum and outlet tube diameters fixed. The annular plenum velocities were thus reduced by a factor of four.

Non-dimensional pressure drops for the Mark III CVS were similar to those for the Mark II CVS and were again considerably lower than those for the Mark I design. The Mark III CVS

was tested only with vortex finder outlets. The dry and wet pressure drops for the Mark III CVS were very similar to those for the Mark II design. Pressure drops for all three CVS designs are plotted against the square of the tangential inlet velocity in Figure 4-6. The liquid flow rates required to obtain a stable, thick liquid layer in the Mark III design were comparable to those for the Mark I CVS and were considerably lower than those required for the Mark II design. The re-circulation zones in the annular plenum feeding the squirrel cage inlet slots were much smaller and less intense than in the Mark II design, as intended.

TABLE 4-3

MARK III SQUIRREL CAGE CVS CONFIGURATION

Chamber Internal Diameter	5.50"
Aspect Ratio (L/D)	1.18
Air Inlet Type	Slots
No of Slots	24
Inlet Slot Height	0.040"
Air Outlet Type	Vortex Finder
Air Outlet Diameter (D_e/D)	0.59
Water Outlet Type	Single Tube, 0.372" ID

A comprehensive series of cleanup tests were made with the ultra-fine fly ash. Once again the air, liquid and ash mass flows were varied. In addition a series of experiments were conducted in order to assess the effects of liquid surface tension on collection performance. Solutions of three different surfactants were assessed. The deposition problem that had been observed with the Mark II CVS was again noticed with the Mark III design. A variety of liquid inlet arrangements were studied and the problem was eliminated by introducing some of the liquid to the CVS via the main inlet plenum, see Section 4.2 below. A liquid filtration system

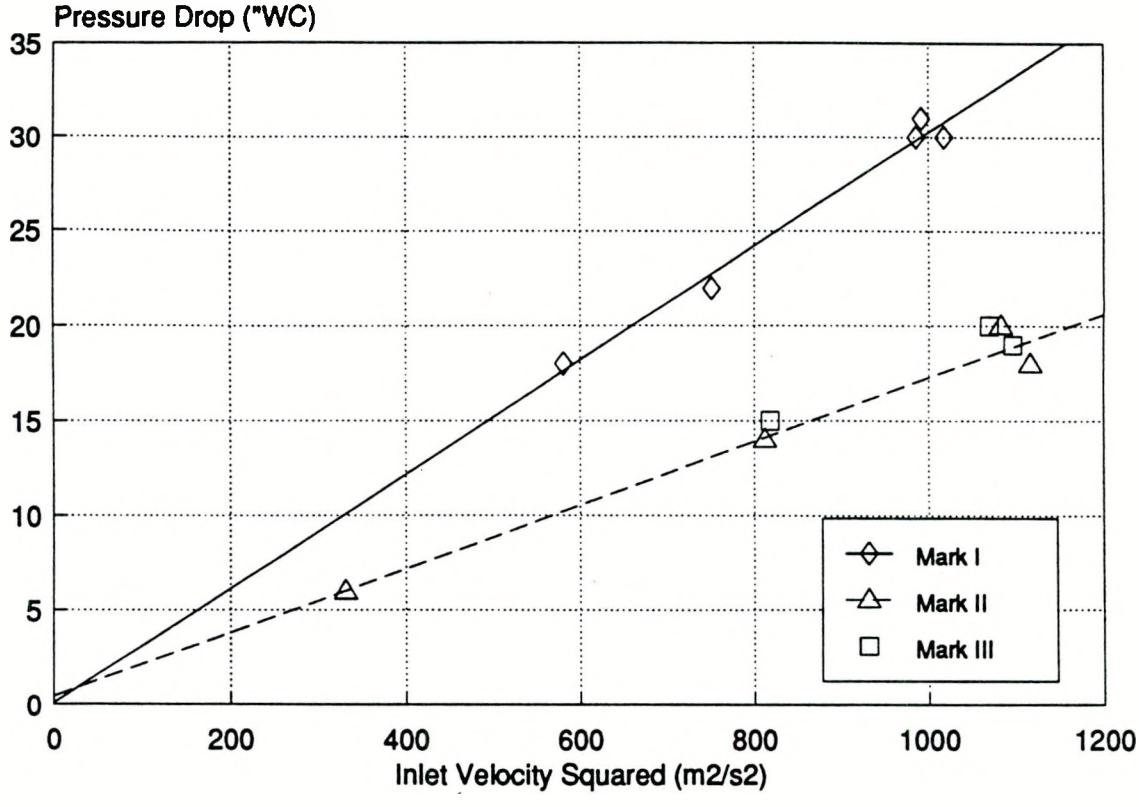

Figure 4-6 Comparison of Pressure Drop with Liquid Layer Present for Three CVS Designs as a Function of the Square of the Inlet Velocity

was installed during these tests in order to allow for a complete ash mass balance to be obtained for the system.

In addition to tests with 200 mesh, 325 mesh and ultra-fine fly ash, a number of tests were made with sub-micron alumina powder. The CVS retained its excellent particulate collection performance even for these sub-micron particles.

4.2 DISCUSSION OF CLEANUP RESULTS

4.2.1 Fly Ash Size Distributions

The nominal design dust to be cleaned in these experiments was fly ash sieved to below 20 microns in size. Tests were actually conducted with three different sizes of fly ash: 200 mesh, 325 mesh and ultra-fine. The 200 mesh and 325 mesh fly ashes were generated simply by sieving the as-supplied fly ash (Pozzolanic Fly Ash Class C & F, meets ASTM C-618, obtained from the Quality Concrete Co., Billings, Montana). The as-sieved size distributions for these ashes are shown in Figure 4-7. The 200 mesh ash has d_{10}, d_{50}, d_{90} = 4, 11, 41 microns, respectively and the 325 mesh fly ash has d_{10}, d_{50}, d_{90} = 3, 10, 26 microns, respectively.

Sieving to below 20 microns proved to be extremely time-consuming, so in order to generate such fine fly ash a cyclone based classifier was developed. This system is illustrated in Figure 4-8. Fly ash was first sieved to below 80 mesh and then loaded into a screw feeder. Air was supplied to the cyclone by a fan. The ash was fed by the screw feeder into the cyclone inlet flow. The cyclone inlet velocity was reduced by opening the bypass air valve until the size distribution of the ash that passed the cyclone was as desired: 100 percent below 20 microns. The cyclone outlet dust was collected in a large filter bag. This proved to be a much more efficient way of generating quantities of sub-20 micron fly ash than sieving. For the purposes of this report, the sub-20 micron fly ash produced by cyclone classification will be referred to as

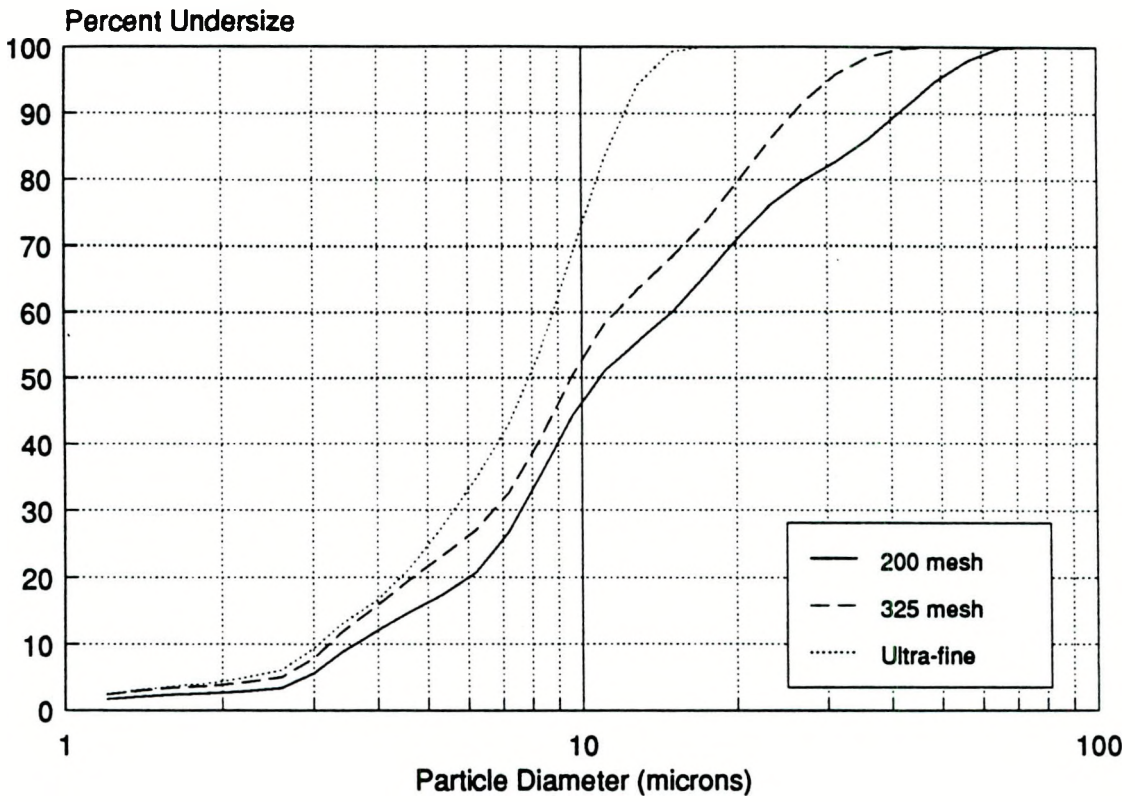

Figure 4-7 Size Distributions of Three Fly Ash Grinds Used In Cleanup Experiments

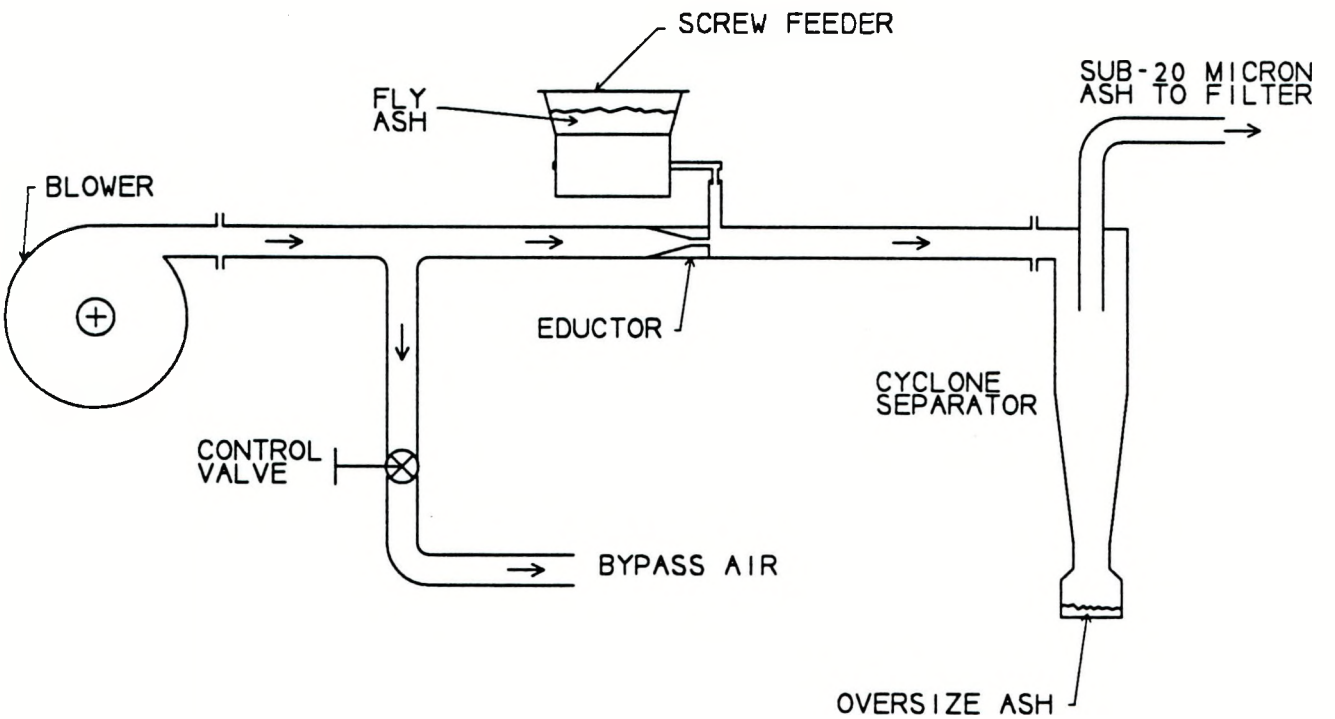

Figure 4-8 Schematic Diagram of Fly Ash Classification System

"ultra-fine fly ash." The size distribution of the ultra-fine fly ash as generated is also shown in Figure 4-7.

There is considerable evidence that the ultra-fine fly ash size distribution changes as it is fed from the fluidized bed feeder. The ultra-fine ash as classified is agglomerated: its size distribution changes quite considerably after being treated in an ultrasonic bath for about 30 minutes. For the ultra-fine ash the values of d_{10}, d_{50} and d_{90} change from 4, 8 and 13 microns to 1, 3 and 8 microns as the ash is ultrasonically treated, see Figure 4-9. The dust size distribution was also measured as fed from the fluidized bed feeder. This was accomplished by using the Malvern particle sizer on-line downstream of the ash injection location in the main air inlet duct. This result is shown in Figure 4-9: the ash size distribution as fed into the CVS reflects the de-agglomerated size distribution rather than the as-classified size distribution.[2] No evidence of size changes was observed for the larger ash sizes. This difference in behavior is presumed to be related to the different methods of generating these ashes.

Figure 4-10 shows various ash size distributions from Test #62, which was made with the ultra-fine fly ash. Four size distribution curves are shown (1) the ultra-fine fly ash as fed to the CVS; (2) the ash as found in the CVS recycle water; (3) the ash as found in the CVS recycle water and ultrasonically treated; and (4) fly ash from the downstream air filter. The size distribution of the ash in the water leaving the CVS is very different to that of the as-fed fly ash. Considerable agglomeration is observed, with the mean size of the ash in the water approaching 20 microns. Ultrasonic treatment, however, results in a size distribution which is very close to that of the de-agglomerated ultra-fine fly ash feed. For most tests not enough fly ash is passed by the CVS to allow a size distribution analysis to be made of the ash collected in the filter. Test

[2] There exists the possibility that only fines are being fed from the fluidized bed. The fact that the size distribution of the ash as fed was independent of the duration of the feed, the position of the offtake tube above the bed and of the fluidizing gas flow rate would suggest that this is not the case.

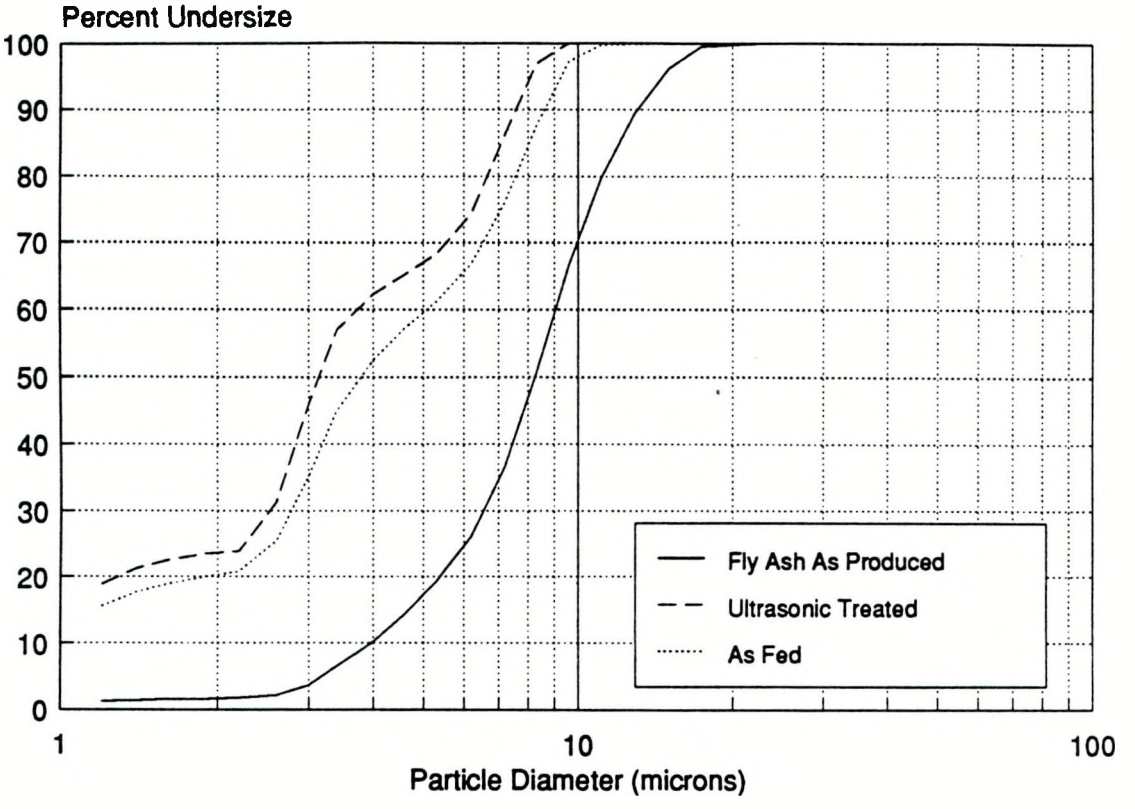

Figure 4-9 Size Distributions of Ultra-fine Fly Ash (1) As Generated; (2) After Ultrasonic Treatment; and (3) As Fed to CVS

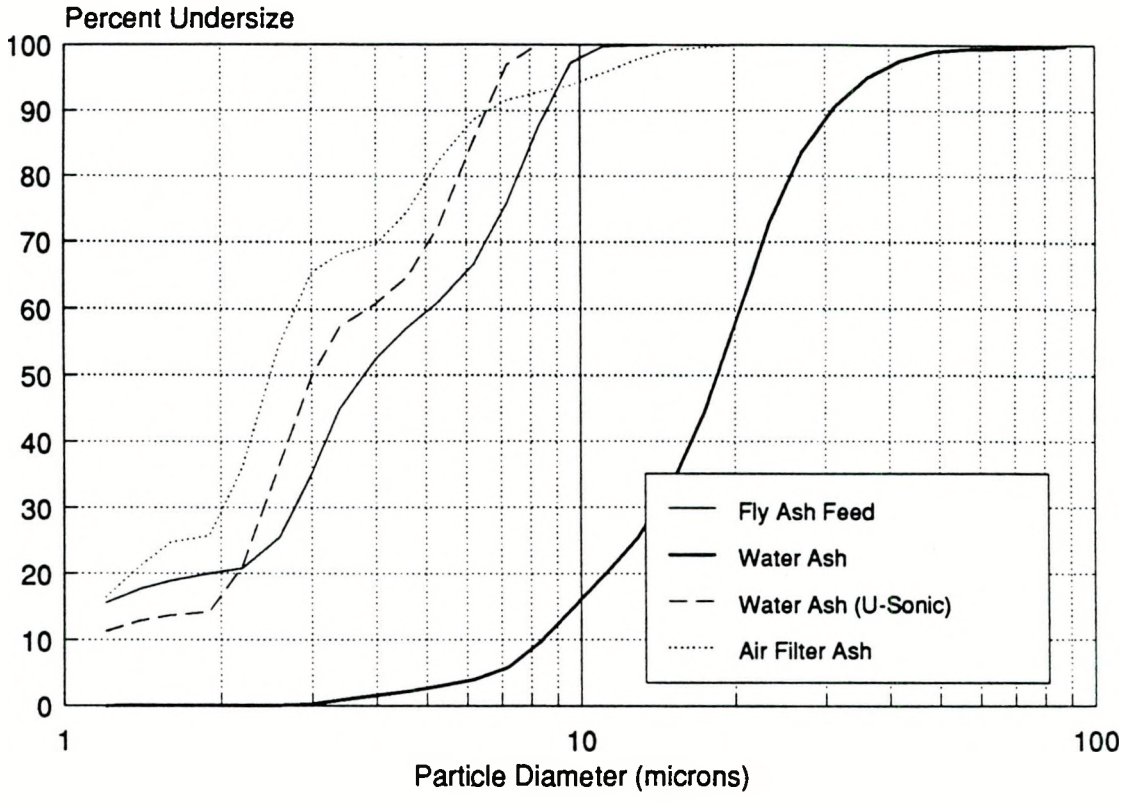

Figure 4-10 Comparison of Fly Ash Size Distributions from One Test, (1) As Fed to CVS; (2) From CVS Outlet Water; (3) From CVS Outlet Water After Ultrasonic Treatment; and (4) From Downstream Air Filter

#62 was made at a low air mass flow rate and hence at a lower CVS efficiency, and such an analysis was possible. The results are also shown in Figure 4-10: the ash from the downstream filter is also very similar to the de-agglomerated fly ash feed.

Thus it can be concluded that (1) the size distribution of the ash entering the CVS is considerably smaller than the size distribution measured for the as-classified ash; and (2) the size distributions of the ash entering the CVS, the ash collected in the water and the ash collected in the downstream filter are very similar. The latter suggests that the CVS does not have a classic inertial separator type grade efficiency curve, with high efficiency for larger particles and significantly lower efficiency for smaller particles. Rather, it suggests that the CVS has a uniformly high collection efficiency for particles of all sizes (in the range exhibited by the fly ash used) and the mechanism by which a very small fraction of the inlet ash is passed through the CVS is connected with either failure to contact all the inlet air with the water or with re-release of a small fraction of the separated ash from the water. At present there is insufficient evidence to determine the precise mechanisms involved.

4.2.2 Effects of Air Inlet Velocity

The measured Mark I CVS cleanup efficiency is plotted as a function of the inlet air mass flow rate in Figure 4-11. As the air inlet geometry is fixed, this plot shows essentially the effect of air tangential inlet velocity on cleanup performance. The nominal design air mass flow rate is approximately 0.1 kg/s. At or above this flow rate the measured collection efficiencies were greater than 99.5 percent. There is a very weak dependence of efficiency on fly ash size: at the same air mass flow the collection efficiency for ultra-fine ash is only approximately 0.1 percent lower than that for the 325 mesh ash. The dependence of efficiency on air mass flow is much more pronounced. This is to be expected, since for a given geometry the inlet air mass flow rate sets the inlet tangential velocity, which sets the radial acceleration produced and hence the

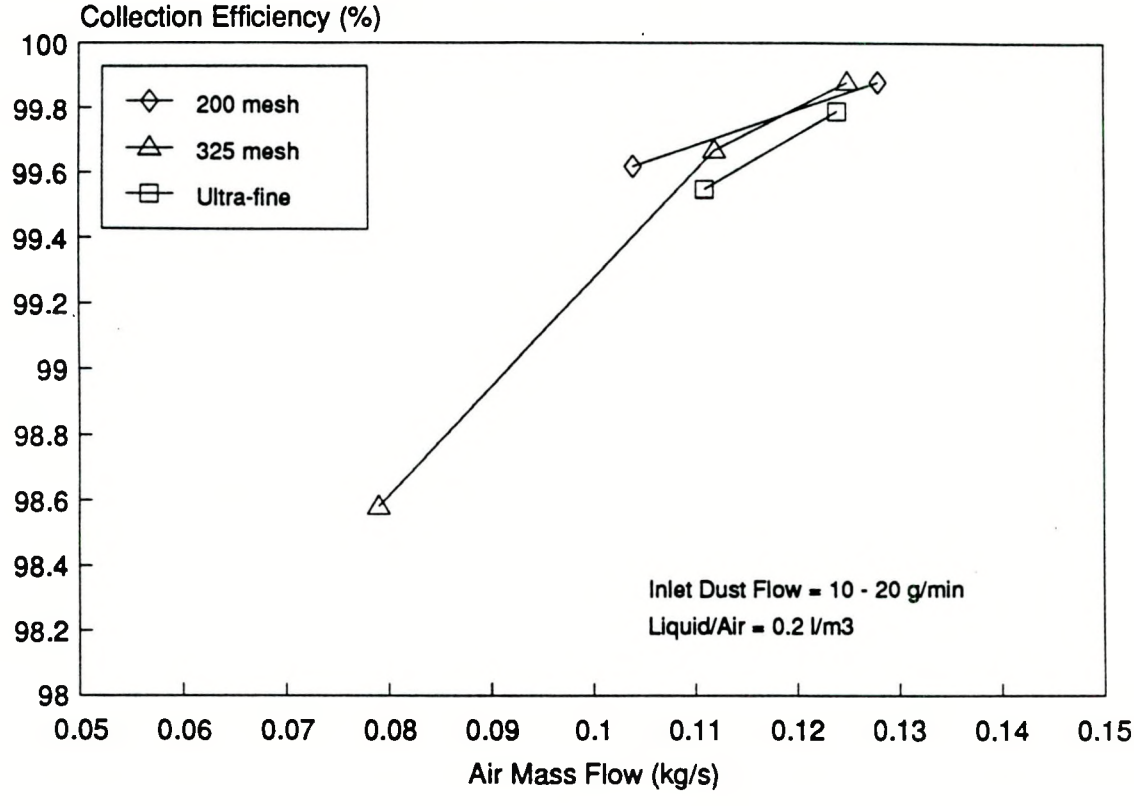

Figure 4-11 Measured Cleanup Performance for Mark I CVS as a Function of CVS Inlet Air Mass Flow Rate for Three Fly Ash Sizes

particle separation forces generated. This can be explained in the following manner.

For the bubbling flow which exists in the CVS, parameters of primary importance are the mean bubble size and velocity. Bubble sizes and velocities set the magnitude of the inertial separation forces which are produced in the CVS, and hence the cleanup performance of the device. Bubble motion in the confined, rotating liquid layer is essentially dictated by a balance between buoyancy and aerodynamic drag forces. A generalized graphical correlation for bubbles rising in an infinite medium is presented in Figure 4-12. This correlates bubble shapes in terms of the bubble Reynolds Number (Re) and the Eotvos Number (Eo), where:

$$Re = \frac{\rho u_b D_b}{\mu}$$

$$Eo = \frac{g\ \Delta\rho\ D_b^2}{\sigma}$$

where for gas bubbles in liquid, ρ is the liquid density, D_b is the bubble Eotvos diameter, or equivalent spherical diameter, u_b is the bubble velocity, μ is the liquid viscosity, g is the acceleration due to gravity, $\Delta\rho$ is the density difference between the phases, and σ is the liquid surface tension.

In order to apply this correlation to conditions present in the CVS, the acceleration due to gravity, g, is replaced by the radial acceleration in the chamber, a_r. The radial acceleration used in this first order analysis (u^2/r) is that obtained from the bulk gas tangential inlet velocity and the chamber radius. The bubble shape regime in the CVS is marked by the cross-hatched area in Figure 4-12. Under the strong accelerations produced in the CVS, the bubbles tend not

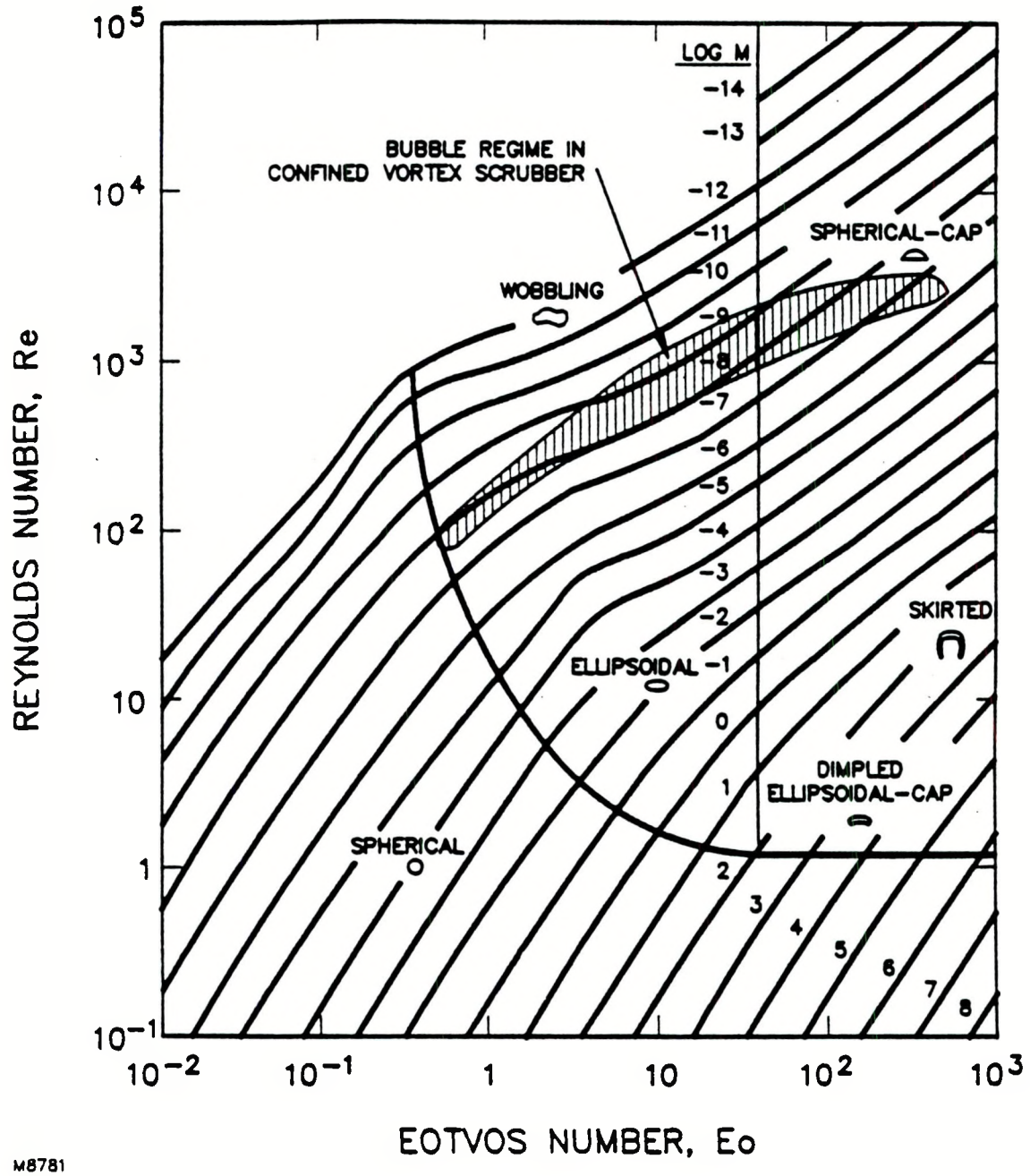

Figure 4-12 Shape Regimes for Bubbles and Drops (Clift et al., 1978)

to be spherical, but are ellipsoidal or spherical cap and may be wobbling.

Maximum stable bubble sizes are characterized by a particular value of Eo. The maximum stable size of an air bubble in water at atmospheric conditions and 1g acceleration is of order several centimeters in diameter (Clift et al, 1978): mean bubble sizes tend to be up to an order of magnitude smaller than the stable maximum size. Scaling considerations indicate that the maximum stable bubble size in the CVS is of order 1 mm, see Figure 4-13. It may be assumed that typical mean sizes will be in the range one tenth to one fifth the maximum stable size, which gives typical bubble sizes of order several hundred microns. This estimate generally agrees with stroboscopic flow visualization of the liquid layer in the CVS, though given the extremely vigorous air/liquid interaction in the CVS, it is difficult to visualize the flow effectively.

Given the order of magnitude of bubble sizes, estimates may be made of the bubble velocities. This is done by balancing the buoyancy forces in the radial acceleration field with the aerodynamic drag on the bubbles. Drag coefficients for gas bubbles in a liquid are considerably different from those of either liquid droplets in a gas or solid particles in either phase. An important parameter here is the phase to phase viscosity ratio, κ, defined as the ratio of the viscosity of the dispersed phase to that of the continuous phase. For gas bubbles in a liquid, $\kappa << 1$, whereas for liquid droplets in a gas, $\kappa >> 1$. For small values of κ, internal circulation will exist in the bubble or droplet. Thus for gas bubbles in a liquid, there is a recirculating internal flow set up due to the bubble's motion through the liquid. A much weaker internal flow exists in a falling droplet. This internal flow affects the aerodynamic drag of the bubble considerably. The internal flow, and hence the bubble drag, can also be affected by the presence of very small quantities of impurities in the liquid. This phenomenon is due to a variety of interfacial effects, which are not yet fully understood (Clift et al, 1978). Drag coefficients of air bubbles in water

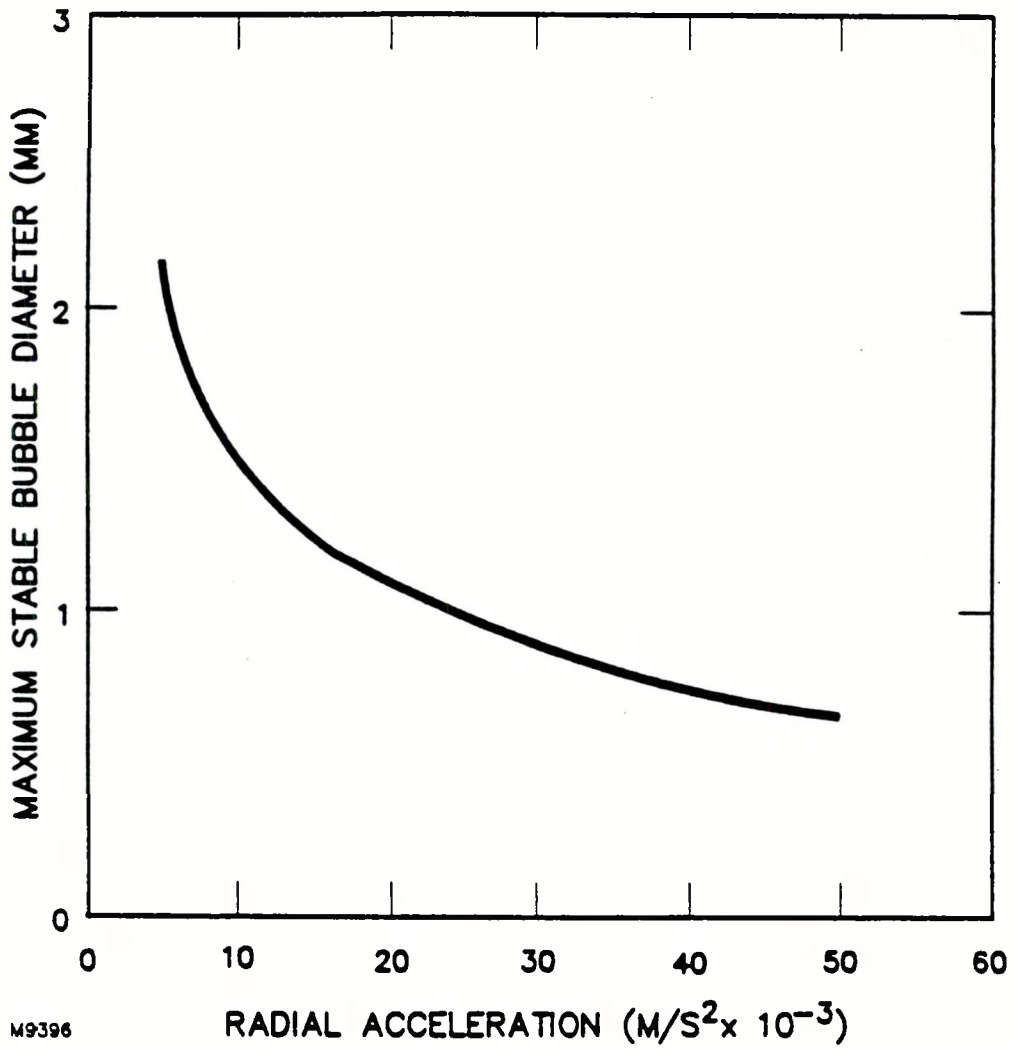

Figure 4-13 Maximum Stable Bubble Size as a Function of Radial Acceleration

are given in Figure 4-14. The effects of impurities can easily be seen. This drag coefficient curve may be used in order to estimate mean bubble velocities in the CVS.

Mean bubble velocities are presented in Figure 4-15, as a function of radial acceleration and bubble size. The bubble velocity increases both with radial acceleration and with bubble size. The curves are not similar in shape because of the highly non-uniform variation of drag coefficient with Reynolds Number. The calculations show that typical bubble velocities are on the order of a few meters per second.

A second estimate of bubble velocities may be obtained from continuity considerations. If the bubble velocities estimated from continuity are in excess of those obtained from bubble buoyancy calculations, then the bubble flow will break down to give a droplet flow. The bubble velocities obtained from continuity calculations are close to the buoyancy values for vortex chambers of small length to diameter (L/D) ratios, indicating a possible break down of the bubbling flow, whereas as the L/D ratio is increased beyond unity, the continuity velocities fall below the buoyancy velocity, indicating a regime of stable bubbling flow. All tests were conducted with CVS chambers of aspect ratios of unity or greater.

There are at least three mechanisms for inertial separation of particles in the confined vortex scrubber: (1) centrifugal forces, (2) inertial separation of particles on liquid droplets, and (3) inertial separation of particles from within bubbles in the liquid. The latter two mechanisms are of primary importance for separation of fines, whereas the first mechanism will be important for separation of larger particles and for liquid confinement. The ratio of the aerodynamic drag on a particle contained within a bubble to the centrifugal separating force on a particle may readily be estimated. For the range of velocities indicated in Figure 4-15 and for particles below about 20 microns in diameter, the particle Reynolds Number is low enough for Stokes flow to hold. Figure 4-16 shows the value of the ratio of aerodynamic to centrifugal forces as a function

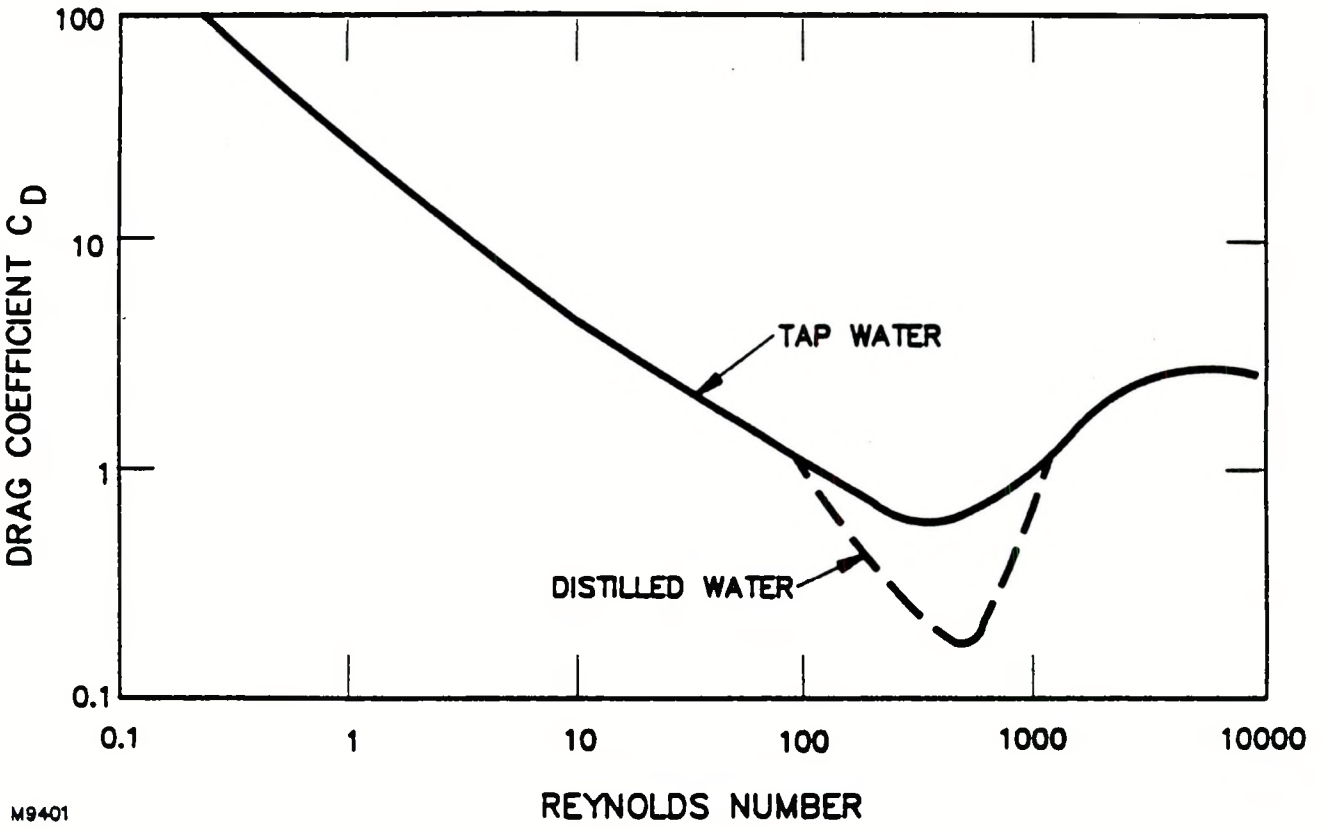

Figure 4-14 Drag Coefficients for Air Bubbles Rising in Water (Haberman and Morton, 1953)

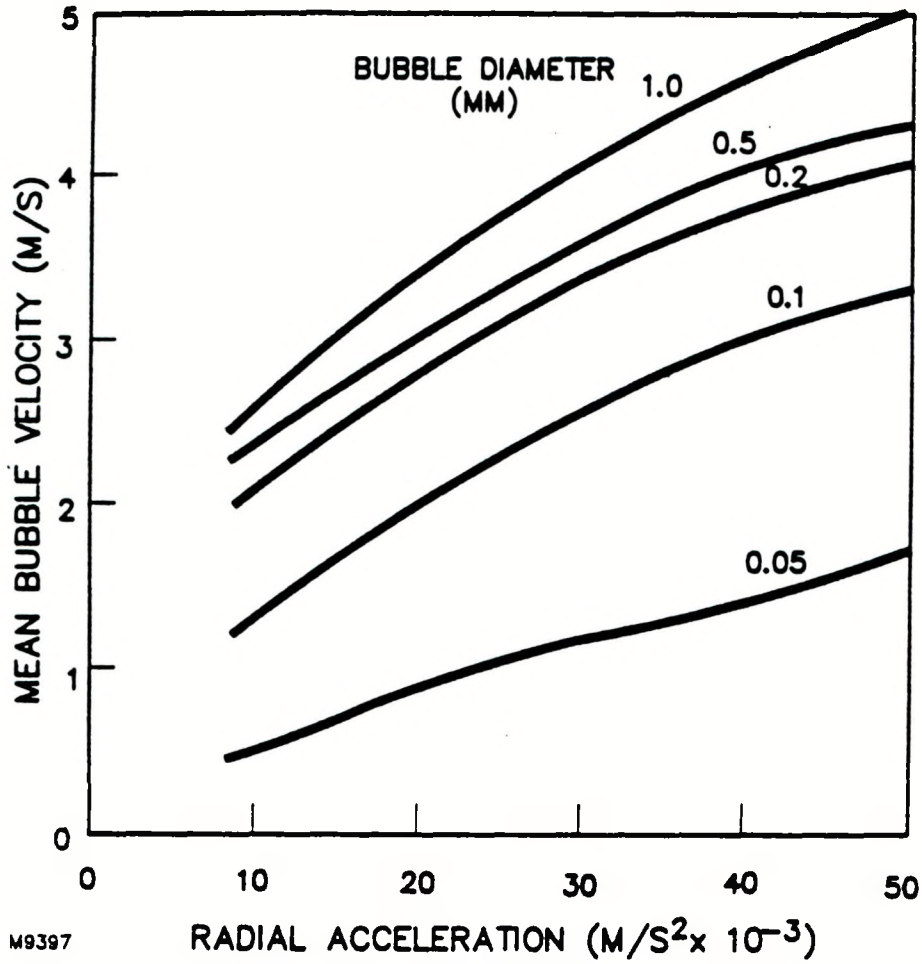

Figure 4-15 Mean Bubble Velocities in the CVS as a Function of Radial Acceleration and Bubble Diameter

of particle diameter for fly ash particles. Curves are plotted for a bubble size of 0.2 mm; there are slight changes of this ratio with bubble diameter, principally because of the different terminal velocities of different sized bubbles, see Figure 4-15.

From Figure 4-16, it can be seen that for particles greater than approximately 4 microns in diameter, the centrifugal forces are considerably greater than the aerodynamic forces in the internal bubble flows, and these particles will be centrifuged to the walls. For fine particles of diameter less than approximately 2 microns, the aerodynamic forces within the bubble flows are considerably larger than the centrifugal forces, and inertial separation inside the bubble is important. In effect, each bubble acts as a miniature cyclone separator.

In order to obtain a first order estimate of the separation efficiencies in such a flow field and examine the expected trends, the separation mechanism may be idealized as in Figure 4-17. A fine particle of diameter d_p is entrained in the re-circulating gas flow inside a bubble of diameter D_b, which is moving through the liquid at a velocity u_b. The particle is inertially separated by the internal bubble gas flow into the surrounding liquid. Typically, the bubble diameter is two orders of magnitude greater than the particle diameter. The gas velocities in the bubble internal flows will be of the same order as the bubble translation velocity. Thus in order to estimate separation performance, the bubble velocity may be assumed as a characteristic separation velocity.

Inertial impaction of particles from gas streams has been the subject of many studies. A good review of impactor design and performance is given by Marple and Willike (1976). Impactor performance is typically characterized in terms of a critical Stokes number. For the geometry under consideration, the Stokes Number is defined as

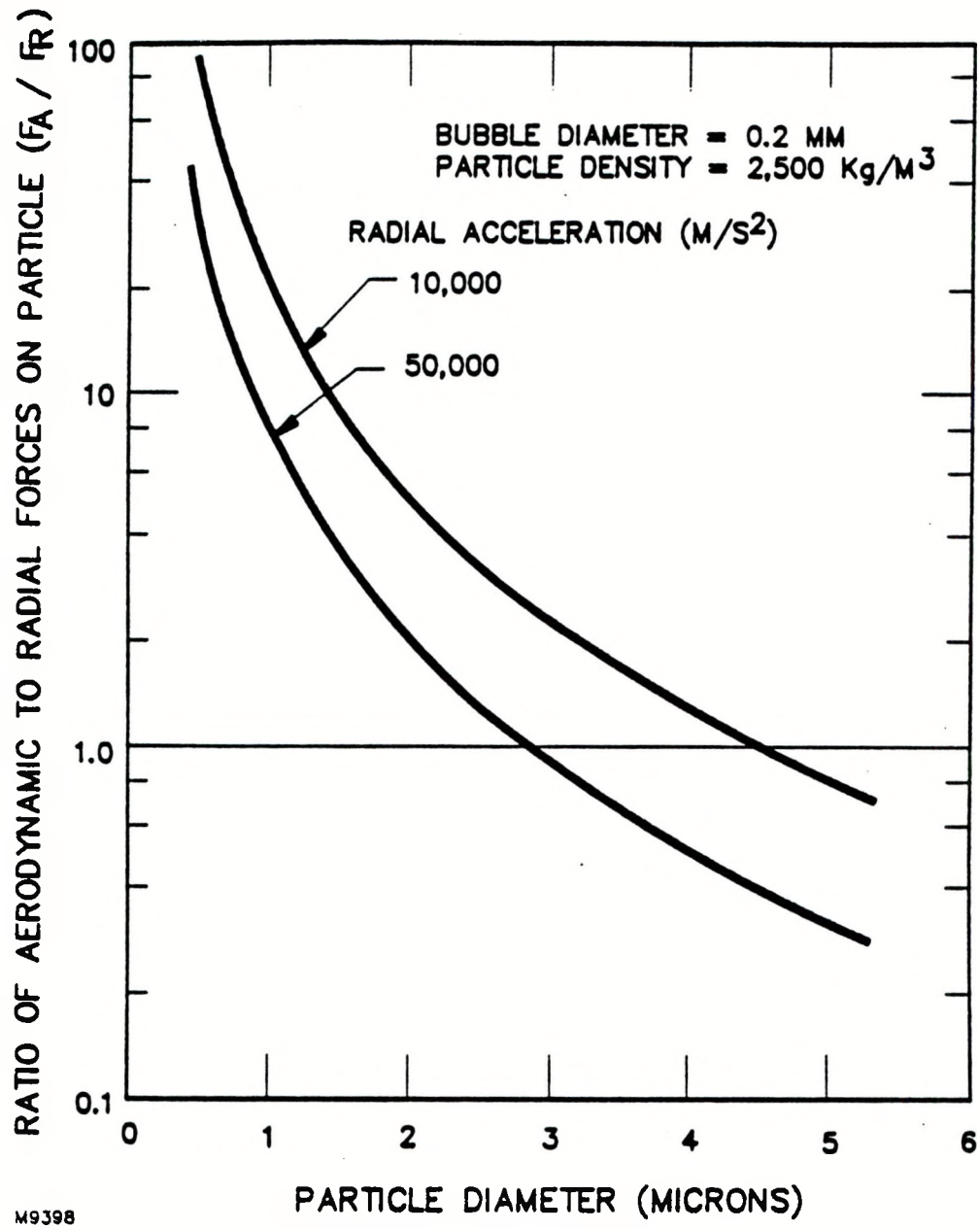

Figure 4-16 Ratio of Aerodynamic to Centrifugal Forces Experienced by Ash Particles in a Bubble in the CVS Liquid Layer

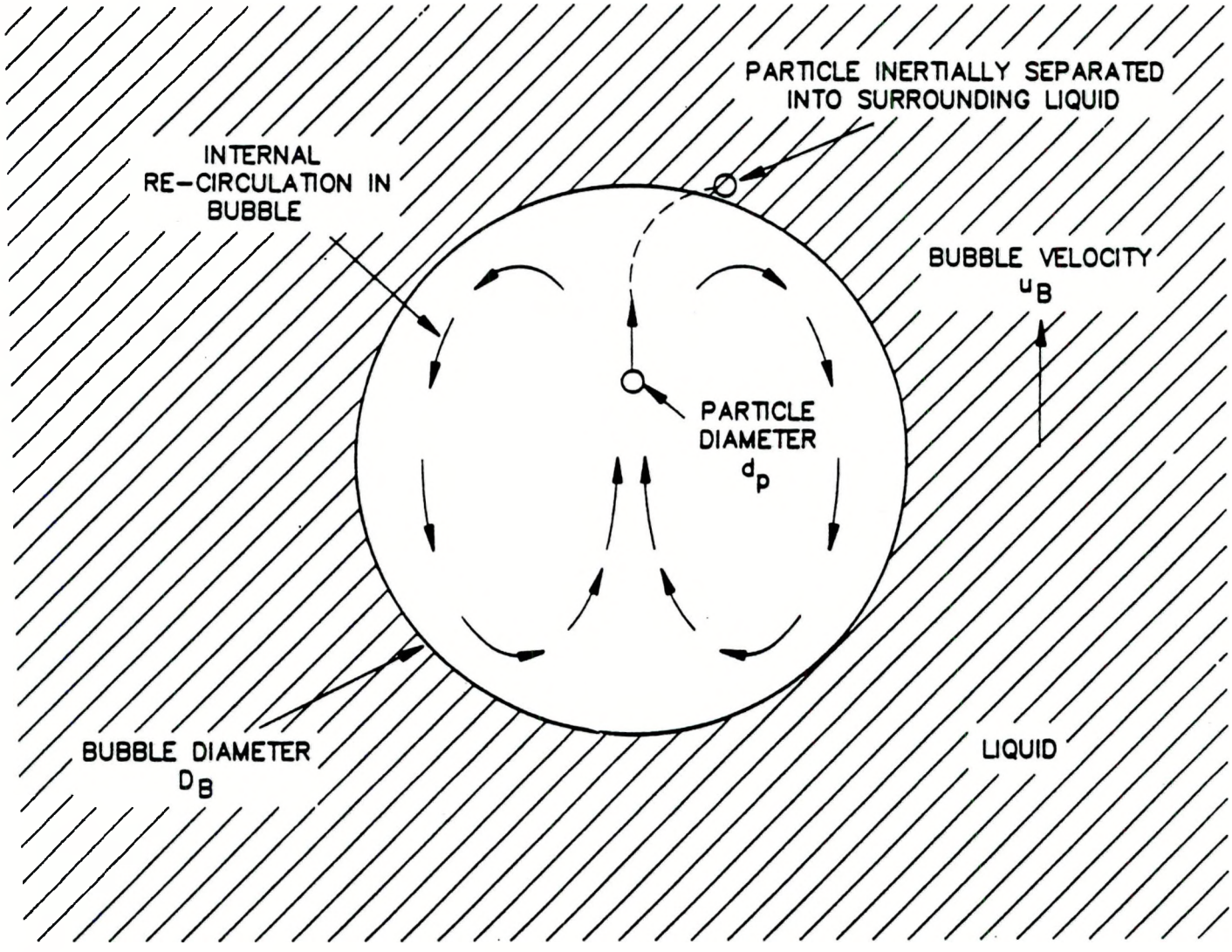

Figure 4-17 Idealized Bubble Internal Flow Field

$$Stk = \frac{\rho_p u_b d_p^2}{18 \mu D_b}$$

where ρ is the particle density and μ is the gas viscosity. Values for Stk_{50} (the Stokes number corresponding to the particle size for which 50% impaction efficiency is achieved) are available for the impaction of a round jet on a plane surface (see, for example, Marple and Willike, 1976). Obviously, for the case of a round jet directed at a plane surface, particles at the edge of the jet are much more likely to escape impaction than those near the jet centerline. Published values of Stk_{50} may be used to estimate the size ranges for particles that will be separated from the internal bubble flow into the surrounding liquid. However, it should be noted that because of the re-circulating flow in the bubble, the particles will undergo repeated impaction events (preliminary estimates are 20 to 50, depending on bubble size and liquid layer thickness) and thus will eventually all be separated into the surrounding liquid. The analysis therefore indicates the particle cut size, i.e. the particle size above which all particles will be separated from the gas stream. The results of this analysis are shown in Figure 4-18, for a variety of bubble sizes. The smaller the bubble size, the smaller the particle cut size. This is because the radius of curvature of the internal flow is reduced, and hence the separating force is increased. The results indicate that for the sub-millimeter bubbles which exist in the CVS two-phase flow, near 100% collection efficiency for sub-micron particles should be achieved. (Typical values of radial acceleration (u^2/r) for the CVS as tested are of order 20,000 m/s^2.)

The foregoing is a simple, first-order analysis of the separation mechanisms in the CVS, but nonetheless highlights some important trends. Increasing the radial gas injection velocity increases the radial acceleration, leading to smaller gas bubbles with higher internal velocities, thereby leading to a smaller particle cut diameter and increased separation efficiency. This trend

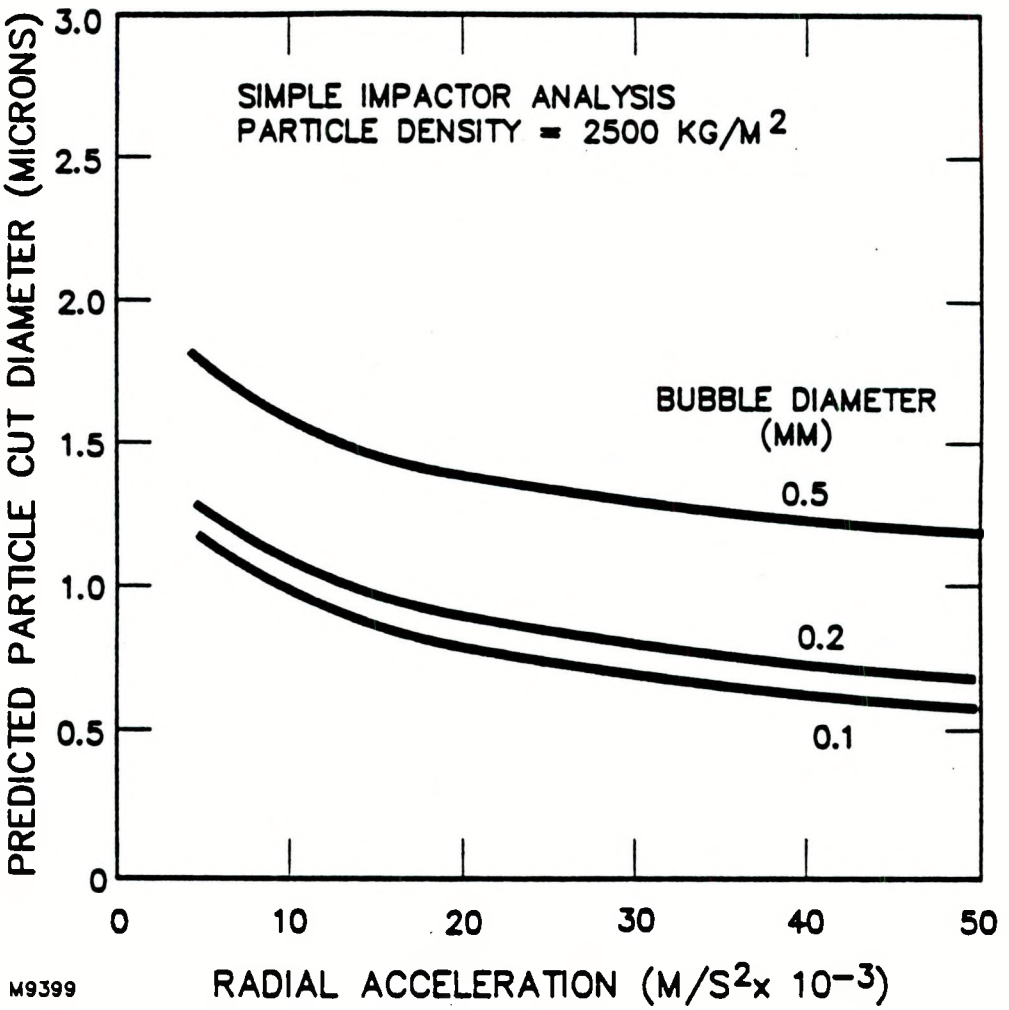

Figure 4-18 Predicted Particle Cut Diameters in CVS

agrees with the experimental data shown in Figure 4-11.

A small number of tests were made with one third of the 24 tangential inlet slots obstructed. This allows comparison of cleanup performance at the same gas mass flow rate but at a different tangential inlet velocity. The results showed no change in cleanup performance, despite the fact that the local gas inlet tangential velocity was increased by some 50 percent. While the inlet jet velocity was increased by blocking off one third of the inlets, the total air mass flow was held constant. The air/liquid interaction and momentum exchange is different in the two cases, and it is possible that competing effects may account for the fact that the cleanup efficiency did not change. It is possible that the change in the number of air inlet slots at the same air mass flow did not result in a significant change in the bulk liquid layer tangential velocity. The foregoing analysis includes a radial acceleration parameter: it may be that the velocity which should be used in this parameter is indeed the bulk rotating liquid layer tangential velocity, rather than the local slot air injection velocity. These arguments would account for the fact that the cleanup performance did not change significantly in this experiment. Direct measurement of the liquid layer velocity by a suitable non-intrusive means would confirm this hypothesis.

For a given inlet geometry, the collection efficiency increases with increasing air inlet velocity. However, the device pressure drop also increases with air inlet velocity. This can be seen in Figure 4-19. The CVS experimental data is plotted in terms of outlet emissions in grains per standard cubic foot as a function of pressure drop in inches of water, in order to allow a comparison to be made between the CVS data and published venturi scrubbers data (Roeck and Dennis, 1979). The Mark I CVS has pressure drops in the range 10-30 inches of water column, which is the same range as that for venturi scrubbers. However at the same pressure drop the CVS gives superior cleanup performance, even for very fine fly ash.

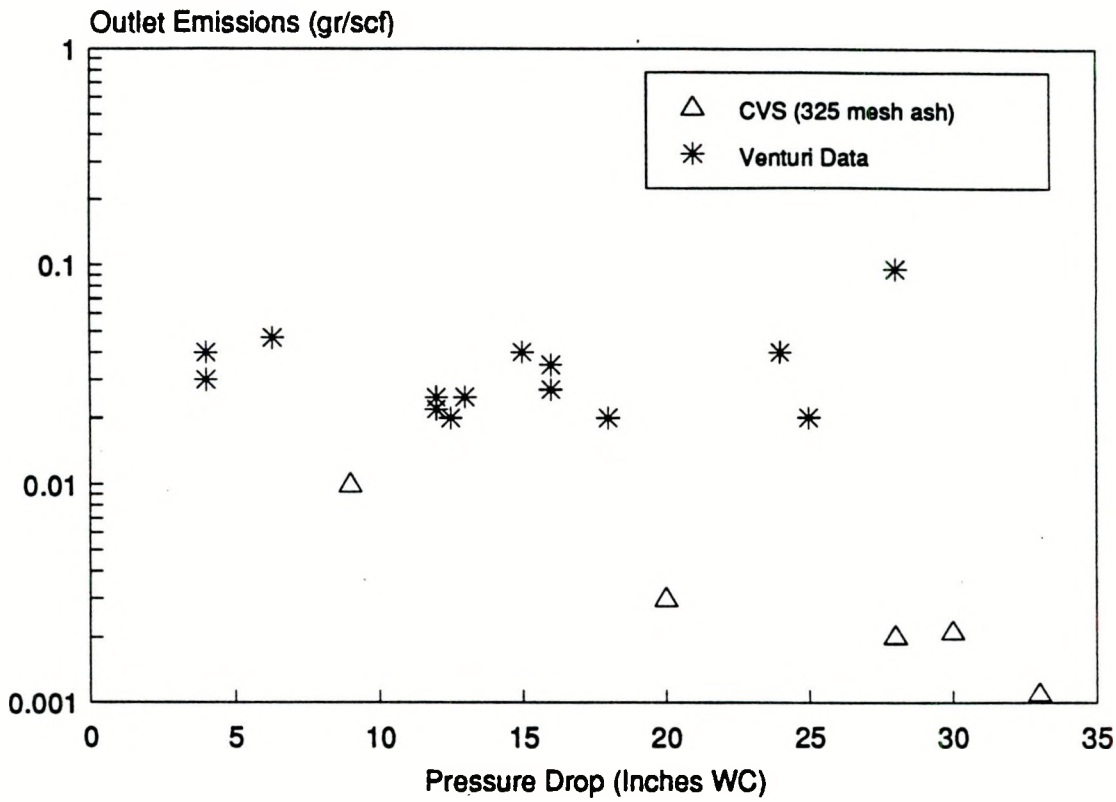

Figure 4-19 Comparison of Mark I CVS Fly Ash Outlet Emissions and Pressure Drop with Published Venturi Scrubber Data for Industrial Coal-Fired Boilers (Venturi Data from Roeck and Dennis, 1979)

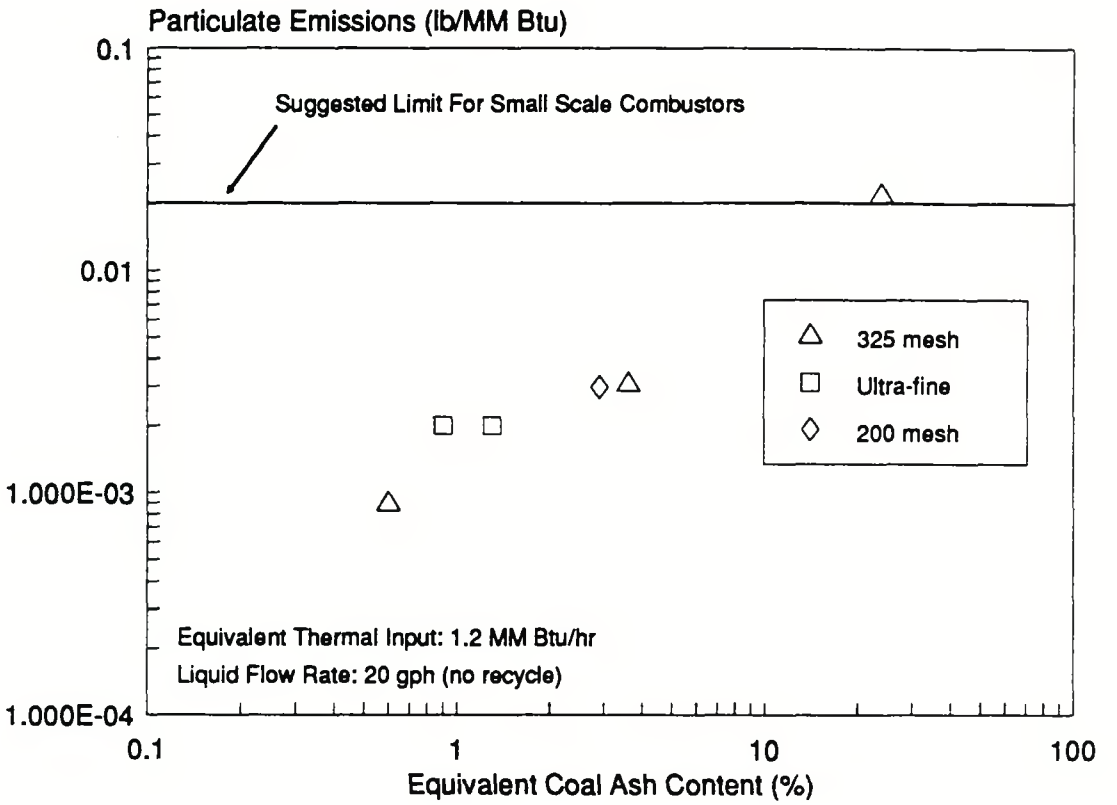

Figure 4-20 Projected Particulate Emissions from a Small-Scale Coal Combustor Equipped with a Confined Vortex Scrubber (Based on Mark I CVS Data)

Based on the measured inlet ash flows and ash removals, particulate emissions from a small-scale coal combustor equipped with a CVS may be projected. This projection is shown in Figure 4-20, for the three ash sizes tested. The proposed small-scale combustor emissions limit of 0.02 lb/MM Btu is also shown for reference. The projected emissions are plotted as a function of the equivalent coal ash content, derived from the measured ash flow rate in the cleanup tests. For 1 to 2 percent ash coals, the projected emissions are approximately 0.002 lb/MM Btu, well below the proposed limit of 0.02 lb/MM Btu.

4.2.3 Effect of Liquid Flow Rate

Figure 4-21 shows the effect of liquid flow rate on measured collection efficiency. In order to obtain this data, the air flow rate was held constant and the liquid flow was varied. This was necessary in order to avoid the quite strong effects of changing air inlet velocity on collection efficiency (see Section 4.2.2). The measured collection efficiency is plotted against the liquid/air flow ratio expressed in liters of water per cubic meter of air. For two different dust sizes, 325 mesh and ultra-fine, the collection efficiency is almost independent of liquid air/ratio. This is true provided that the liquid flow is sufficient to establish a thick and stable liquid layer, see Section 3.2.2. This results is not unexpected: tests conducted during the Vortex Flow Experiments showed that the degree of liquid confinement did not increase significantly with increasing liquid flow rate. Increasing the input flow rate simply caused the output flow rate to increase so as to preserve an essentially constant liquid mass in the CVS chamber. The mass contained was set by the air flow rate and CVS chamber geometry. Thus there is no reason to suppose that increased liquid flow rate will lead to enhanced fine particle collection performance.

It should be noted that the liquid/air ratios in the Mark I CVS are in the range 0.1 to 0.3 l/m^3, approximately 10 percent of those typically employed in venturi scrubbers (Martin, 1981).

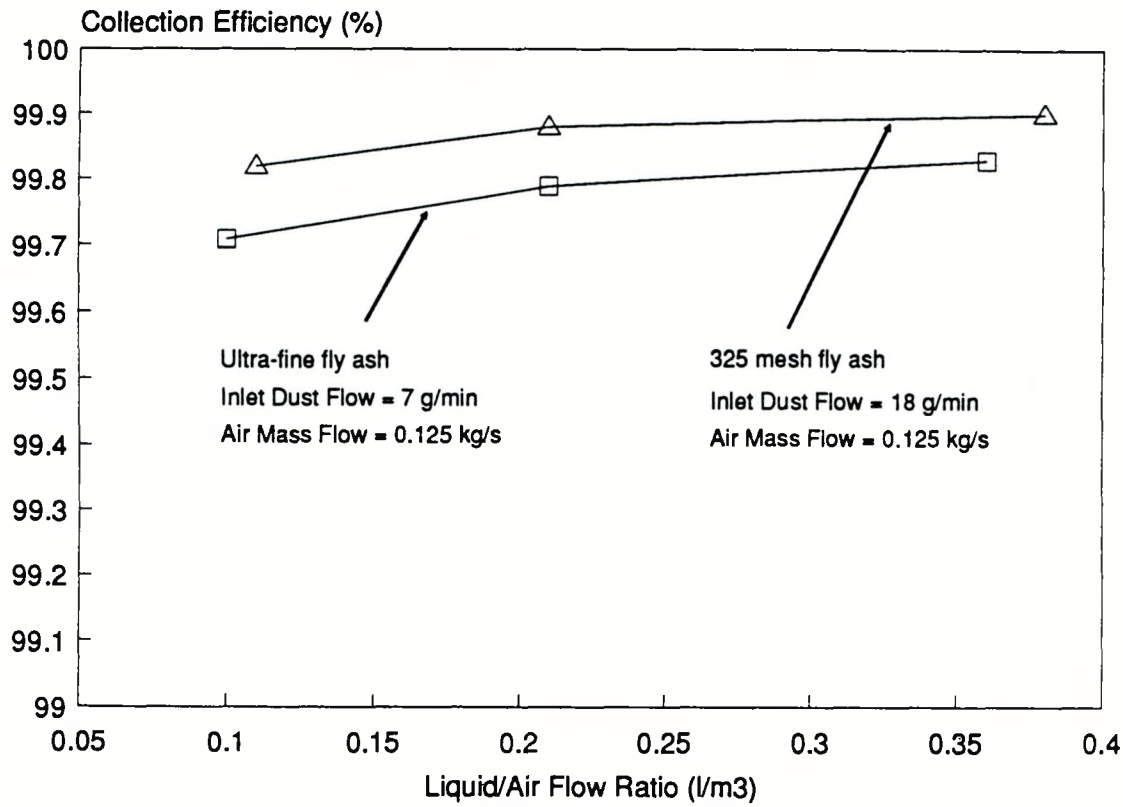

Figure 4-21 Measured Cleanup Performance for Mark I CVS as a Function of Liquid/Air Flow Ratio

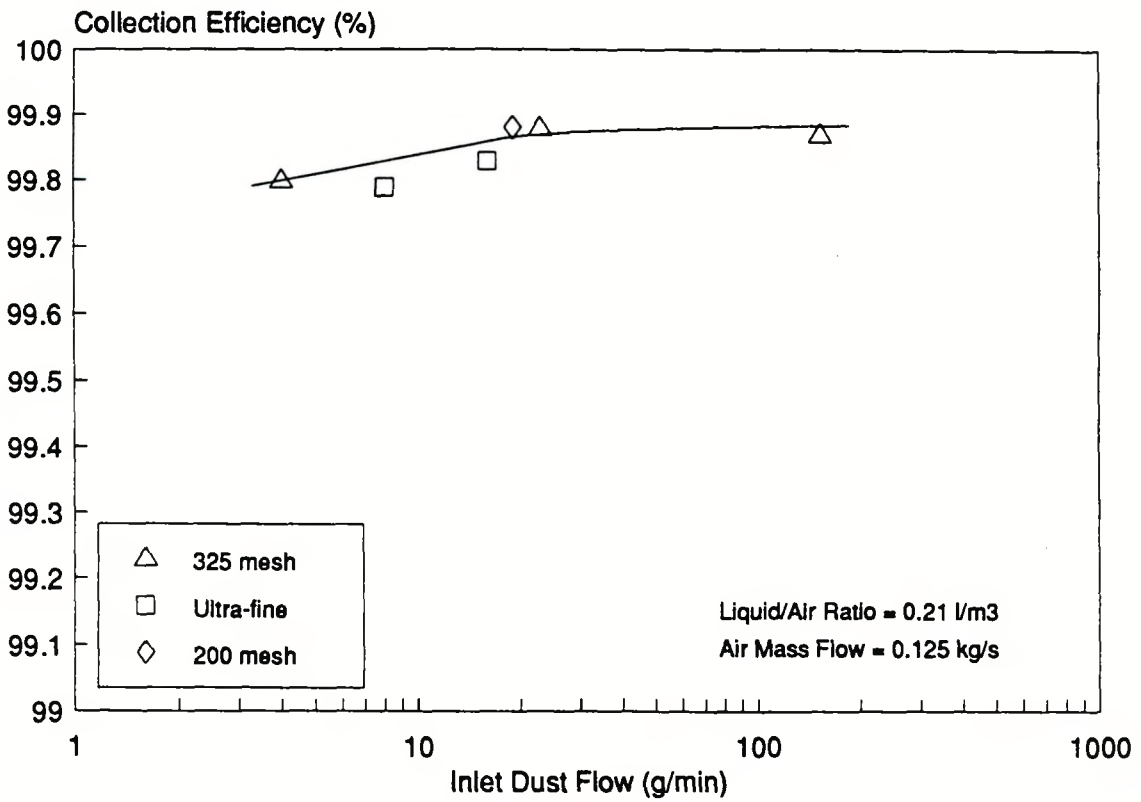

Figure 4-22 Measured Cleanup Performance for Mark I CVS as a Function of Inlet Dust Flow Rate

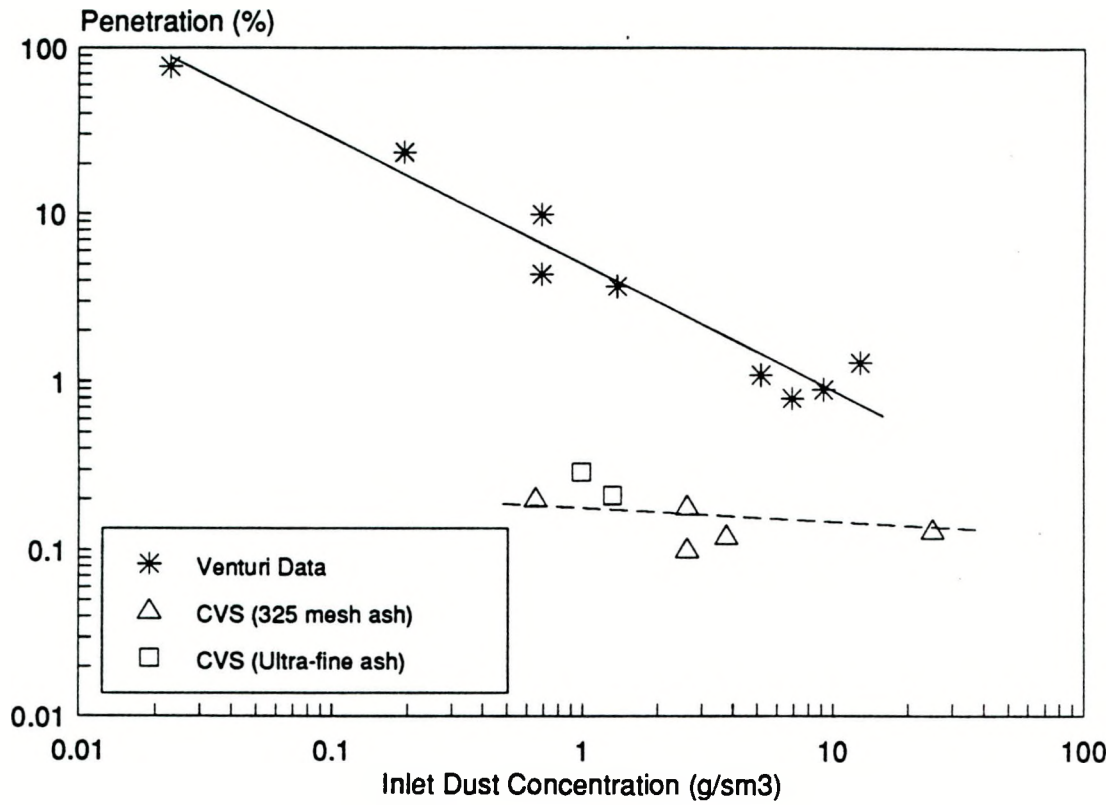

Figure 4-23 Comparison of Mark I CVS Fly Ash Cleanup Performance with Published Venturi Scrubber Data for Industrial Coal-Fired Boilers (Venturi Data from Roeck and Dennis, 1979)

4.2.4 Effect of Dust Loading

It was noted during the shakedown testing with fine alumina powder that the CVS performance seemed insensitive to dust loading. This was examined systematically using fly ash. The results are shown in Figure 4-22. The measured collection efficiency shows only a very slight increase over the range of a factor of 50 in dust flow (from ~3 to ~150 g/min). This is in contrast to the strong dependence of venturi scrubber performance on dust loading (Roeck and Dennis, 1979). The CVS data is compared to that for venturi scrubbers operated on various coal-fired industrial boilers in Figure 4-23. The venturi scrubber data was obtained from Roeck and Dennis (1979). Performance is expressed in terms of penetration, a penetration of 1 percent corresponding to a collection efficiency of 99 percent, and so on. As the dust loading is reduced the venturi performance falls off rapidly. This is because dust removal in a venturi scrubber relies on collisions between dust particles and water droplets. The lower the particle concentration, the lower the collisional frequency and the poorer the collection performance. The CVS, on the other hand, shows a very weak dependence on dust loading.

4.2.5 Comparison of Results for Three CVS Designs

The collection performance of all three CVS designs for ultra-fine fly ash is shown in Figure 4-24 as a function of pressure drop and in Figure 4-25 as a function of air flow rate. The Figure 4-24 indicates that at the same collection efficiency the Mark II and Mark III CVS designs have a substantially lower pressure loss than the Mark I CVS design, as desired. The reduction in pressure drop believed to be due primarily to a reduction in the clean gas outlet velocities, and consequently a reduction in lost outlet swirl-related kinetic energy.

The data in Figure 4-25 indicates that for a given air mass flow rate an increase in collection efficiency is obtained as the squirrel cage diameter is decreased. (The CVS chamber diameter and the collection efficiency at a given air flow increase in the order Mark I, Mark III

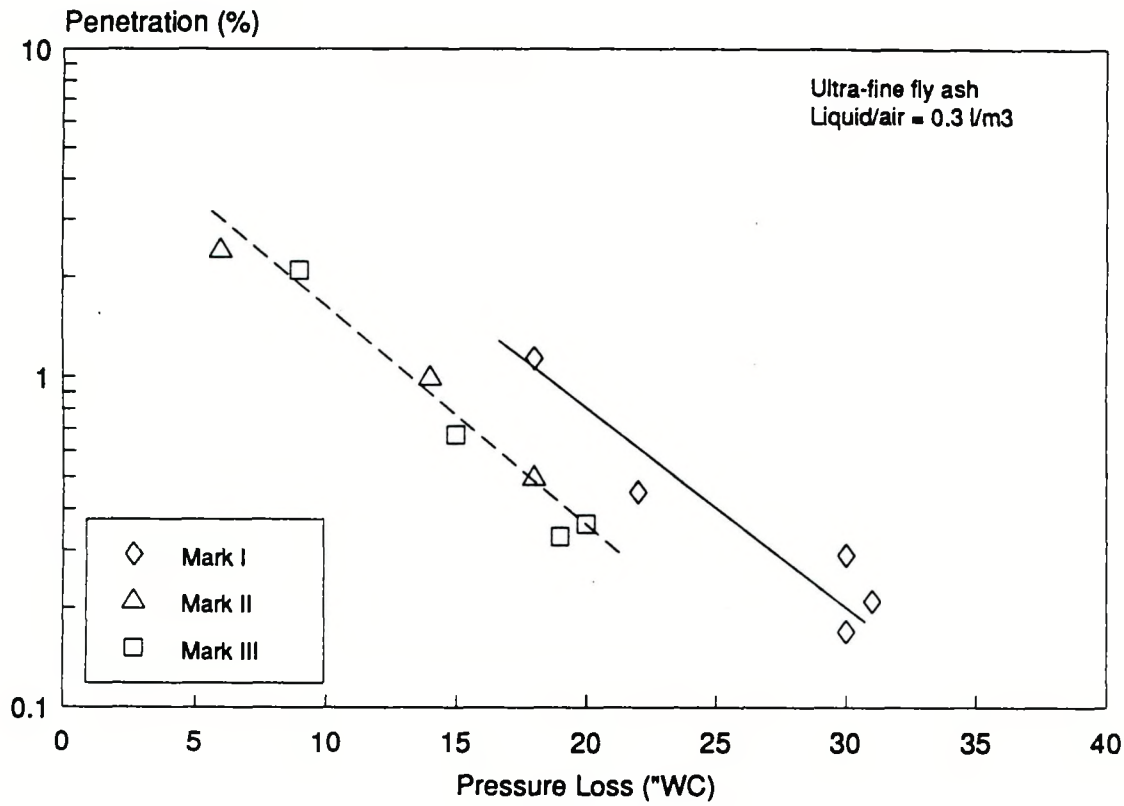

Figure 4-24 Comparison of Ultra-Fine Fly Ash Cleanup Performance for Three CVS Designs as a Function of Pressure Drop

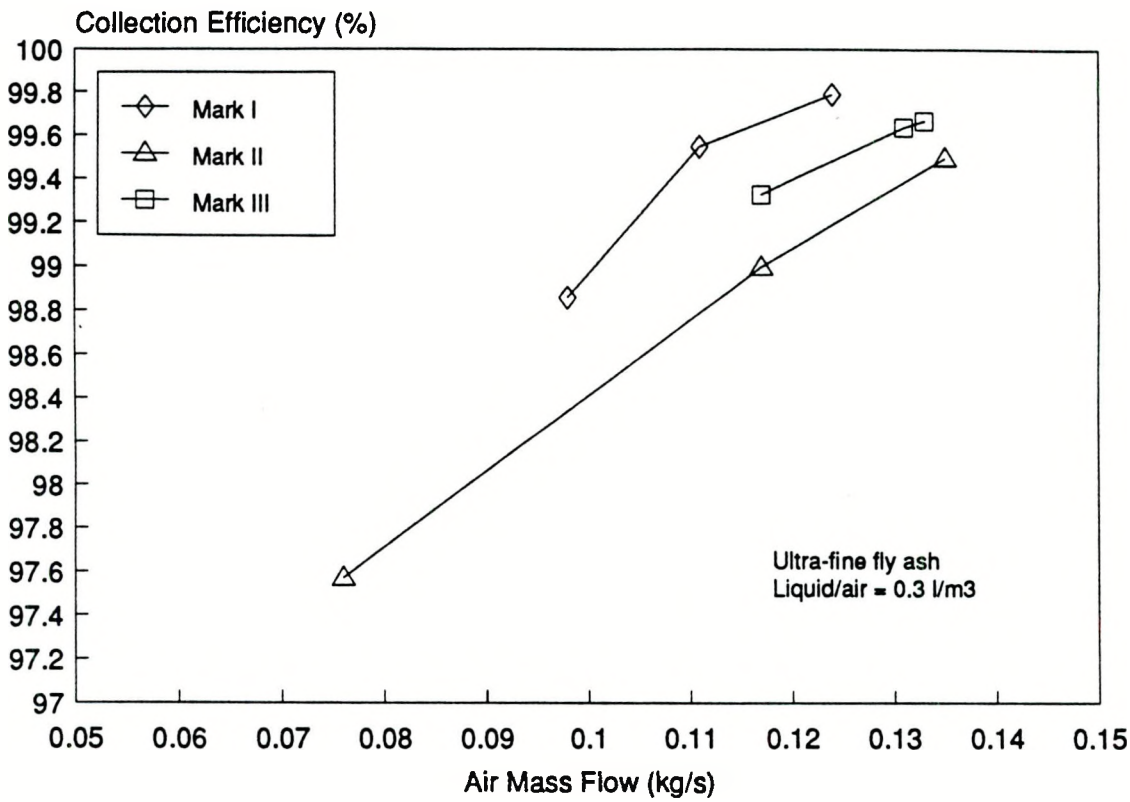

Figure 4-25 Comparison of Ultra-Fine Fly Ash Cleanup Performance for Three CVS Designs as a Function of Air Mass Flow Rate

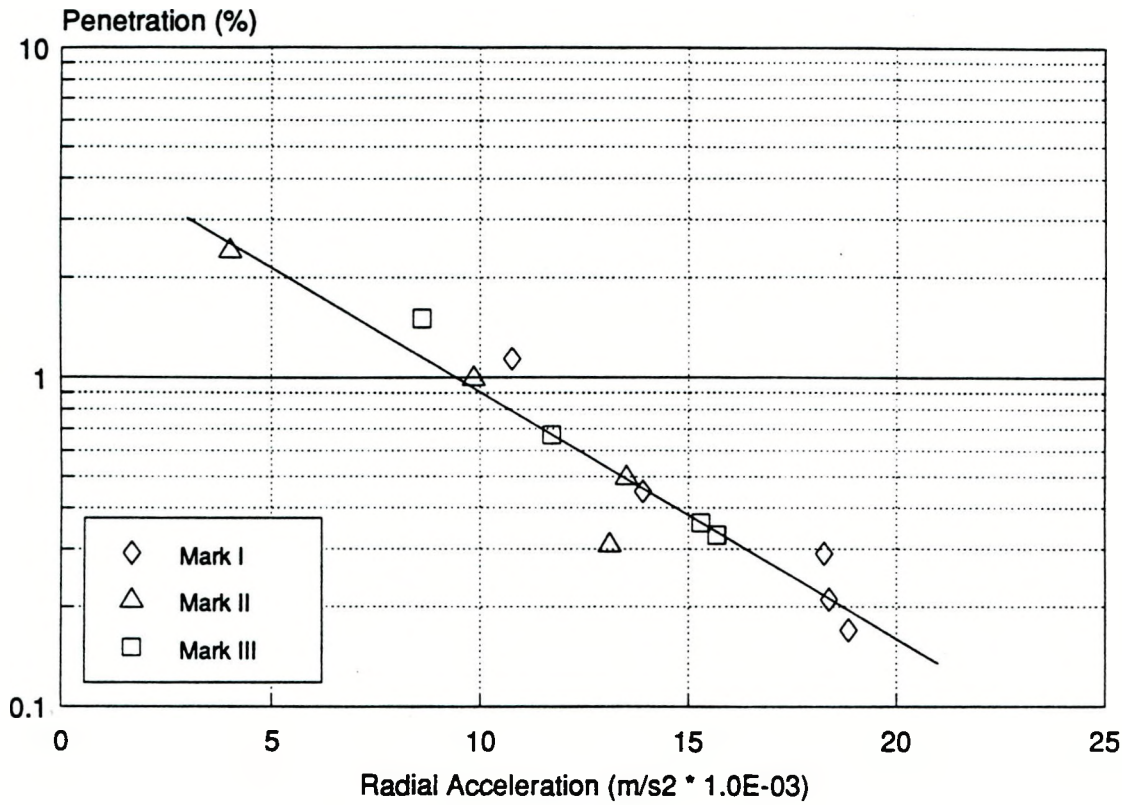

Figure 4-26 Correlation of Cleanup Data for Three CVS Designs

and Mark II.) This trend is confirmed in Figure 4-26, which is a semi-log plot of penetration against the inlet radial acceleration. The radial acceleration used here is based on the nominal tangential inlet velocity (obtained from the measured air mass flow and the total slot inlet area) and the squirrel cage radius. The penetration data for all three CVS designs from Figures 4-24 and 4-25 collapse well when plotted in this manner, indicating an exponential relationship between collection efficiency and radial acceleration of the form:

$$\eta(\%) = 100 - A \exp(-\frac{a_r}{B})$$

where η is the collection efficiency in percent, A and B are constants and a_r is the radial acceleration defined as above. If the data for the coarser fly ash tests (200 and 325 mesh) in the Mark I CVS are examined in the same manner, a slightly different correlation is obtained, see Figure 4-27. The results for the larger dust show slightly but consistently higher collection efficiency than for the ultra-fine ash.

4.2.6 Effect of Liquid Layer Type

Two distinct types of liquid layer have been observed in the squirrel cage CVS chamber. These may be characterized in qualitative terms as follows:

Thick Layer: The liquid layer was 1 - 1.5 cm in thickness and appeared very frothy. Foamy water flowed out of the main CVS chamber into the liquid out-take chamber. The CVS clean air exit flow had almost zero observable swirl and any liquid in the main air outlet tube flowed along the bottom of the tube.

Thin Layer: The liquid layer was much thinner, approximately 0.1 - 0.3 cm, and did not appear frothy. The water flowing out of the main CVS chamber into the liquid out-take chamber was not foamy. The CVS clean air exit flow had significant observable swirl

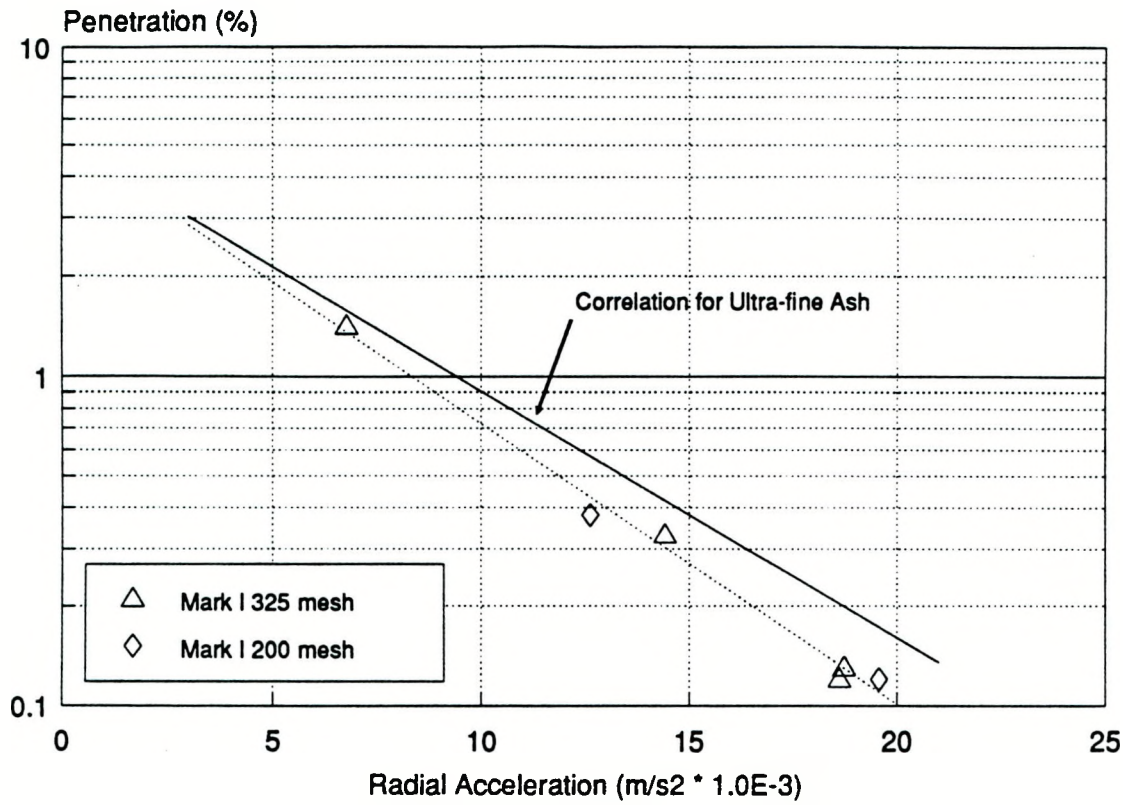

Figure 4-27 Comparison of Correlations for Ultra-Fine Fly Ash and for Larger Fly Ash

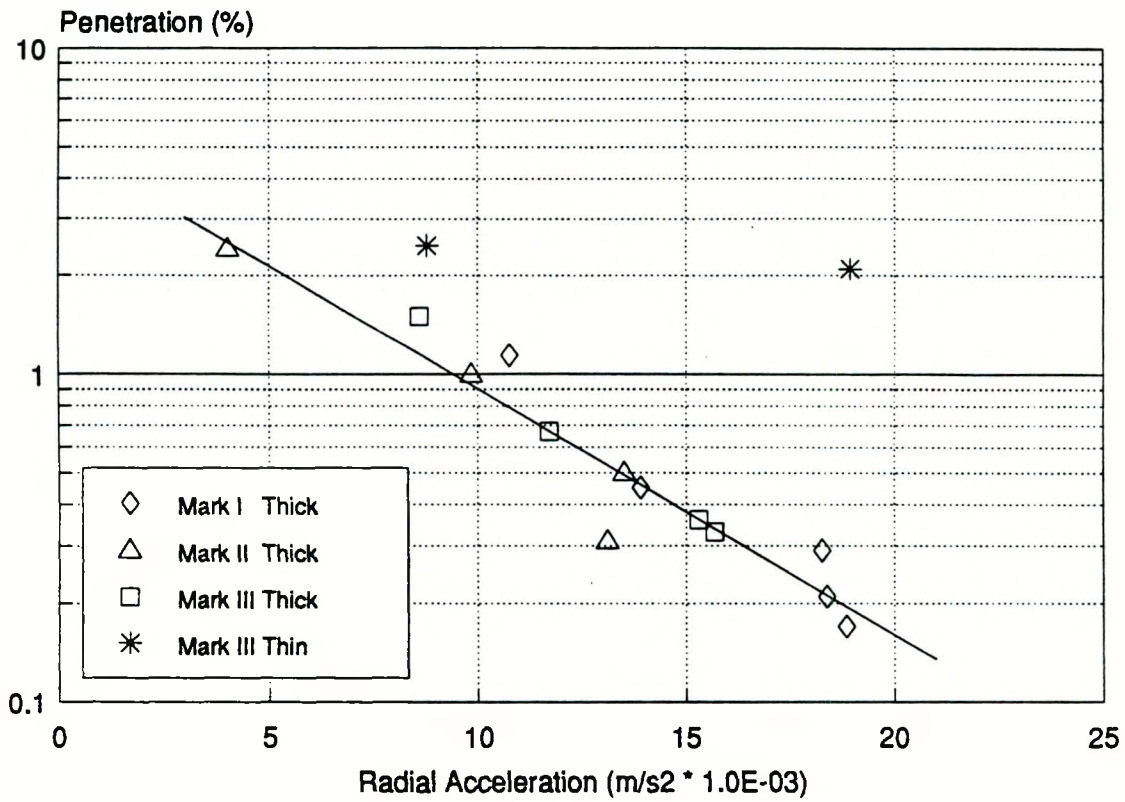

Figure 4-28 Comparison of Cleanup Performance of Thick and Thin Liquid Layers in Mark III CVS

and any liquid in the main air outlet tube flowed in spirals on the tube walls.

All cleanup experiments were made with a thick layer, which was seen as the desired configuration. It was (qualitatively) obvious that the degree of air/water interaction in the thick layer was greater than in the thin layer (this is evidenced not only by the degree of bubbling/foaming, but also by the fact that the inlet tangential momentum of the air was effectively reduced to zero). On occasion a thick layer would break down and form a thin layer: this could happen if the air flow was quickly and significantly reduced and then increased to the original value, or if the inlet water flow was not uniformly distributed across the CVS chamber. In such a situation it was necessary to increase the water flow to a high value (say three to four times the design flow) for a short time until the thick layer was re-established, at which point the water flow could be reduced to its normal value.

A series of experiments were conducted to determine the relative cleanup performances of the two layer types. The results are shown in Figure 4-28. Though there is a clear performance improvement with a thick liquid layer, the thin liquid layer still gave better than 97 percent collection of the ultra-fine fly ash. Pressure drops for the two layer types were comparable.

One cleanup test was also made using the ultra-fine fly ash with no liquid layer present in the CVS. The measured collection efficiency was 75.2 percent. This is comparable to the result obtained for the fine alumina powder with no liquid layer, see Section 4.1.1 above.

4.2.7 Effect of Liquid Inlet Arrangement

The deposition problem that had been observed with the Mark II CVS was again noticed with the Mark III design. A longer duration test was run to examine this problem. After 30 minutes of ultra-fine fly ash feed the CVS pressure drop began to increase due to squirrel cage inlet slot plugging. After 40 minutes the CVS pressure drop had doubled and considerable

deposition was observed in the annular plenum chamber. The deposits appeared to start building up in the plenum corners and appeared to be growing counter to the main flow in the plenum, probably in secondary flow regimes. The overall collection efficiency for this test was still 99.52 percent, despite the inlet slot plugging that occurred.

In order to control this problem, the water inlet arrangement was modified. The water input system was revised so as to allow water to be introduced into either the CVS chamber and/or the annular plenum feeding the squirrel cage inlet slots. The water introduced into the plenum was inertially separated onto the walls and then flowed into the CVS chamber via the inlet slots. The water in the annular plenum eliminated the deposition problem. It was also discovered that once a stable, thick liquid layer was established in the CVS chamber, the water could be introduced into the system only via the plenum with no deterioration of device collection performance or pressure drop. Thus the CVS has great flexibility as far as liquid inlet arrangement is concerned.

4.2.8 Cleanup Performance for Sub-Micron Particles

The first-order inertial separation analysis outlined in Section 4.2.2 predicts close to 100 percent separation for sub-micron particles, depending on the degree of radial acceleration and the mean bubble size in the CVS. In addition, the fact that better than 99 percent cleanup was measured for ash in which 10 percent or more of the mass was present in particles of less than 1 micron in diameter implies that the CVS has extremely efficient collection performance for sub-micron particles. This was tested explicitly by feeding 0.3 micron alumina particles into the Mark III CVS.

As discussed above, the filter material used to filter the CVS outlet flow in these experiments is rated at 99.8 percent collection down to 1 micron particles. Accordingly, the filter collection performance for the 0.3 micron alumina particles was checked by feeding a known

quantity of the alumina dust directly into the CVS outlet piping and hence into the filter. Between 80 and 90 percent collection was measured in repeat tests. The lower of these values was then used to correct the CVS cleanup data for two tests made with the 0.3 micron alumina. The corrected data showed 98.2 and 97.9 percent capture of 0.3 micron alumina particles in the CVS for the two tests. This confirms the implied result from the ultra-fine fly ash cleanup tests and again proves the CVS concept for cleanup of very fine particulate material. The measured CVS performance is significantly better than would be predicted by the inertial separation analysis used in Section 4.2.2, giving a cut diameter of less than 0.3 microns at a radial acceleration on the order of 20,000 m/s^2. Thus these inertial mechanisms do not seem to explain the extremely efficient separation of such fine particles. One possible explanation may lie in the consideration of the unsteady bubble motion in the liquid layer. The particles in the gas bubbles in the liquid layer have a finite stopping distance, which is on the order of several thousand particle diameters. The stopping distance for a 0.3 micron particle is of order 0.6 mm. It is therefore possible that an abrupt acceleration of the gas bubble due to turbulent motion and/or bubble collisions in the liquid layer could result in the particle impacting the liquid boundary of the bubble, with consequent capture of the particle.

4.2.9 Effect of Liquid Properties

It has been postulated that decreasing the liquid surface tension in the CVS may lead to enhanced fine particulate collection because of the increased wettability of the fly ash in a low surface tension liquid. This hypothesis was tested in the Mark III CVS using three different surfactant solutions. The surfactants evaluated were liquid soap, Emcol 4500 (sodium dioctyl sulfosuccinate) and Witconate 1430X (fatty acid sulfonate, sodium salt). The latter is a low-foaming surfactant.

In order to feed surfactant solutions to the CVS a pressurized liquid feed system was

TABLE 4-4
SUMMARY OF SURFACTANT EXPERIMENTS PERFORMED
(ULTRA-FINE ASH, MAXIMUM AIR FLOW RATE)

Test	Solution	Pressure Loss ("WC)	Collection Efficiency (%)	Comments
91	Water	19	98.9	Baseline test for soap runs.
92	0.2% Soap	17	98.9	No foaming, observable changes in liquid flow patterns.
93	0.8% Soap	12	N/A	Extreme foaming, test stopped, no collection data obtained.
118	Water	18	99.0	Baseline test for Emcol & Witconate runs.
119	0.1% Emcol	13	95.3	Some foam entrained in outlet.
120	0.01% Emcol	16.5	98.2	Less foamy, much less entrainment.
121	0.1% Witconate	15	97.9	No foaming, very high dust flow rate.
122	0.1% Witconate	18	98.5	No foaming.
123	0.5% Witconate	16.5	97.4	Very slight foaming, no entrainment in outlet.
124	Water	20	99.2	Repeat baseline test.

fabricated. Nitrogen was used to pressurize a 13 gallon cylinder containing the solution. Table 4-4 presents a summary of the results obtained together with brief comments. As can be seen from Table 4-4, foaming was a serious problem except for the 0.1 percent Witconate 1430X surfactant solution. The 0.8 percent soap solution foamed so much that the CVS itself, the clean air outlet ducting, the water knockout chambers and the outlet ducting filled completely with foam in a matter of tens of seconds. All the surfactant tests were made at full air flow rate and with the ultra-fine fly ash. It can be seen from Table 4-4 that in no case was a collection efficiency improvement obtained with a surfactant solution. On the contrary, significant performance deteriorations were observed. On the other hand, the pressure drop was always reduced when a surfactant solution was used. These two effects appear to be related: in Figure 4-29 the measured penetrations and pressure losses from Table 4-4 are plotted in the same

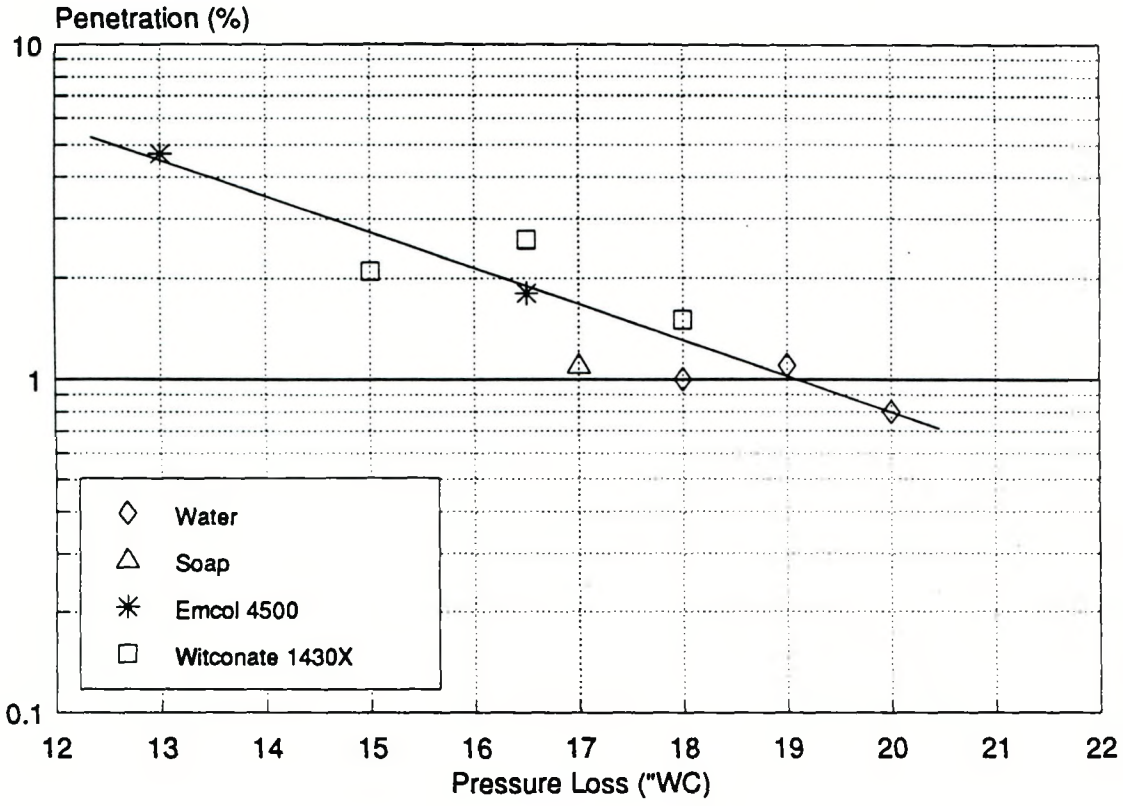

Figure 4-29 Measured Penetration for Surfactant Tests at Full Air Flow Rate as a Function of Pressure Drop

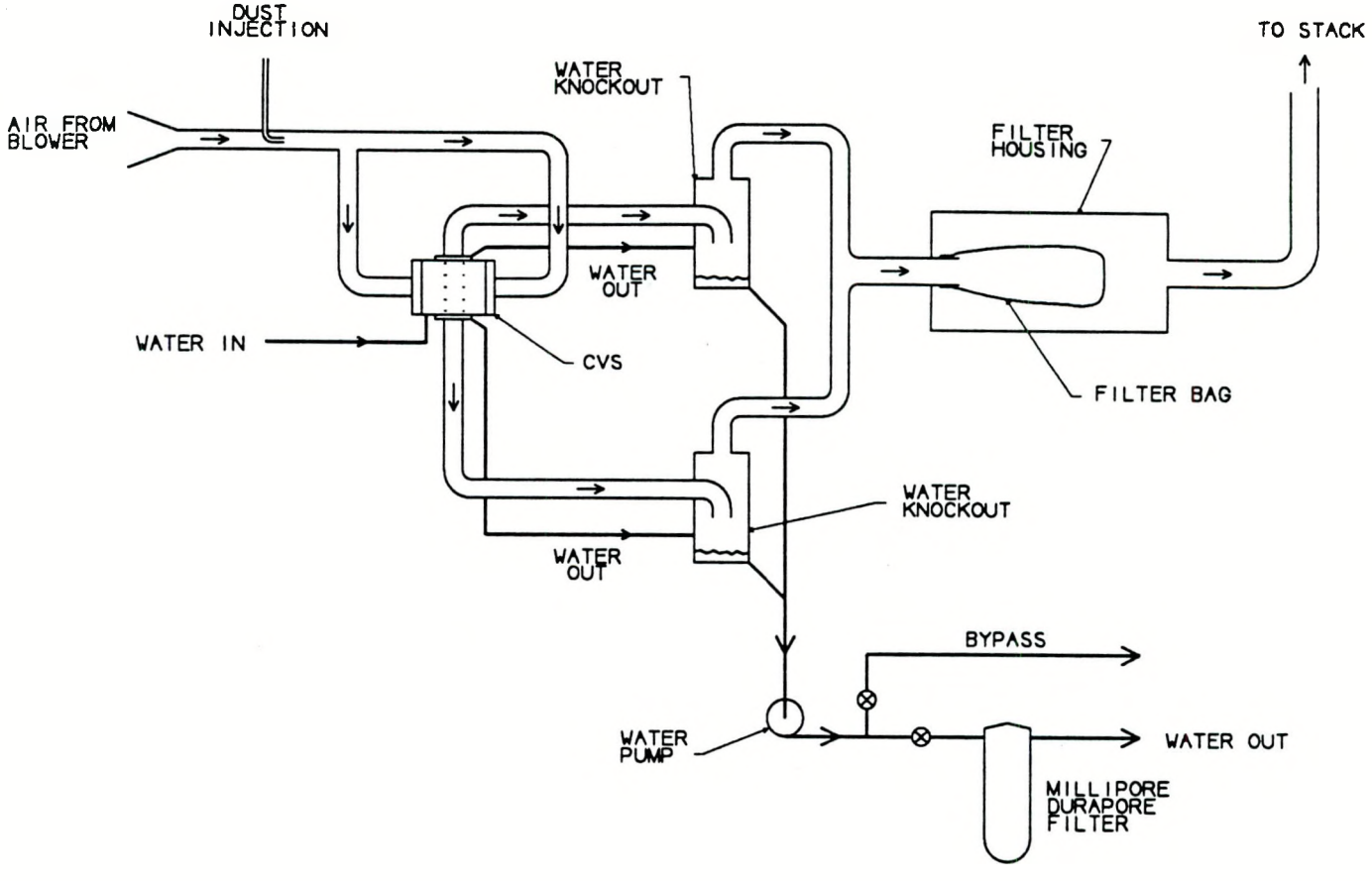

Figure 4-30 Schematic Diagram of Experimental Arrangement for Ash Mass Closure Experiments

manner as the other CVS collection data in Section 4.2.2. Irrespective of the particular surfactant used, there appears to be a fair correlation between the CVS pressure drop and the collection efficiency obtained.

4.2.10 Ash Mass Closures

A liquid filtration system was installed in order to allow the captured ash in the water leaving the CVS to be collected and an ash mass balance to be completed. The system is illustrated in Figure 4-30. The filter used was a Millipore Durapore hydrophilic cartridge filter. This filter was rated down to 0.6 microns. In a typical test the filter has to collect 100 to 200 g of ash. This is a significant quantity, and leads to rapid filter plugging. A liquid pump was therefore required in order to force the outlet water through the filter. The filter inlet pressure was on the order of 25 psig at the end of a test.

Before running any mass balance experiments, the filter was checked by dispersing a known mass of ultra-fine fly ash in water and then pumping that water through the filter. 94 percent recovery of the dispersed ash was obtained. This test was repeated and this time the filtered water was retained and allowed to evaporate. This test gave 98 percent ash recovery, indicating that a substantial fraction of the fly ash was either water soluble of below 0.6 microns in diameter. This is not unexpected: up to 20 percent of fly ash can be water soluble, depending on the parent coal ash chemistry (Santhanam et al., 1981).

Results from initial CVS cleanup experiments with the liquid filtration system showed that 86 to 89 percent of the input ash was present in both the water filter and the downstream air filter at maximum air mass flow rate. At a very low air mass flow rate only 74 percent of the input ash could be accounted for in these two filters. It seemed likely that ash deposition in the feed lines was responsible for this discrepancy, as the deposition would be expected to decrease as the air velocity in the inlet lines was increased.

Accordingly the CVS test rig was completely disassembled and cleaned so that a carefully controlled mass balance experiment could be performed. On disassembly some 75 g of ash was recovered from all the CVS components, indicating that deposition has been occurring during the previous tests. Each CVS component was cleaned and weighed. The CVS was re-assembled and a known mass of ultra-fine fly ash was introduced into the CVS main air inlet line. The CVS rig was then again completely disassembled and each component was re-weighed. Of 150 g input to the system, 130 g was accounted for in the water filter, 2.4 g was accounted for in the air filter and 8 g was accounted for by deposits in the CVS inlet lines and plenums. This accounts for 94 percent of the input mass. Allowing for the solubility effects described above an essentially complete ash mass balance was obtained for this test.

5.0 CONCLUSIONS

5.1 SUMMARY OF RESULTS

The following is a summary of the key experimental observations made during the Vortex Flow and Cleanup Experiments:

- The CVS gave better than 99 percent collection for ultra-fine fly ash (mean size 3 microns) at modest pressure drop (10 - 20 "WC). Collection efficiencies of up to 99.8 percent have been measured.
- The CVS gave 98 percent collection for 0.3 micron alumina particles.
- The collection efficiency increases with increasing air mass flow (and hence tangential inlet velocity). This trend agrees with that predicted from a first order inertial separation analysis.
- Provided the liquid flow is sufficient to establish a thick liquid layer, the collection performance is insensitive to liquid flow rate.
- The collection performance is insensitive to inlet particulate loading.
- The results from three different CVS designs can be correlated using a simple exponential relationship between the penetration and the radial acceleration in the chamber.
- Two distinct liquid layer types ("thick" and "thin") were observed in the CVS. The thick liquid layer can give up to 99.5 percent collection for ultra-fine fly ash whereas the thin layer gave approximately 97 percent collection for the same ash.
- CVS performance is insensitive to liquid inlet arrangement. In order to control deposition in the plenum which feeds the inlet slots, liquid can be introduced via the plenum instead of directly into the CVS chamber. This has no effect on ash collection

performance.

- The size distributions of the ultra-fine ash as fed to the CVS, in the CVS outlet water and in the CVS air filter are all essentially the same.
- Reducing the surface tension of the liquid in the chamber by introducing surfactants produced a drop in both collection efficiency and pressure drop. These two effects appear to be correlated.
- A complete ash mass balance was obtained by accounting for ash found in the CVS inlet lines and plenum, in a liquid filter and in the downstream air filter.
- The CVS pressure drop can be well controlled by suitable choice of air inlet and outlet geometries.
- The dual-inlet CVS design gave adequate radial accelerations and low pressure drop, but had low liquid containment. The liquid layer was thin and was penetrated by the incoming air jets.
- The squirrel cage CVS design produced high radial accelerations and excellent liquid confinement at low pressure drop. The degree of liquid/air interaction was much higher than in the dual-inlet CVS.
- The vortex finder exits were superior to the slotted exit tube, producing lower pressure drop and higher liquid containment .
- The device pressure drop was some 50 percent lower with a thick and stable liquid layer in the CVS chamber than without such a layer.

5.2 CONCLUSION

A novel fine particulate cleanup concept, based on a Confined Vortex Scrubber, has been proven by experiment. The CVS design retains the mechanical simplicity of conventional reverse

flow cyclone separators, but has far superior collection performance for fine particulates. A simple, modular and compact CVS was designed, fabricated and tested at a flow rate equivalent to the exhaust flow from a 1 MM Btu/hr coal combustor. Performance objectives which had been established for a set of Vortex Flow Experiments were accomplished: low pressure drop, high liquid confinement, a stable two-phase flow field and controllable end-wall outlet flows were obtained.

A comprehensive series of simulated flue gas cleanup experiments were made. Greater than 99 percent capture of extremely fine fly ash (mean particle size of 3 microns) at low pressure drops (10 - 20 "WC) and liquid flow rates (0.3 l/m^3) was demonstrated. 98 percent collection was demonstrated for 0.3 micron particles. Device operation was simple and reliable - the two-phase flow field in the device proved to be very stable. Projected particulate emissions from a small-scale coal combustor equipped with a confined vortex scrubber would be well below the proposed emissions limit of 0.02 lbs/MM Btu.

The size distributions of the ash entering the CVS, the ash collected in the water and the ash collected in the downstream filter are very similar. This suggests that the CVS does not have a classic inertial separator type grade efficiency curve, with high collection efficiency for larger particles and progressively lower collection efficiency for smaller particles. Rather, it suggests that the CVS has a uniformly high collection efficiency for particles of all sizes (in the range exhibited by the fly ash used) and the mechanism by which a very small fraction of the inlet ash is passed through the CVS is connected with either failure to contact all the inlet air with the water or with re-release of a small fraction of the separated ash from the water. At present there is insufficient evidence to determine the precise mechanisms involved.

Results from the cleanup experiments show an exponential relationship between the cleanup performance and the radial acceleration in the device. This relationship correlates

measured cleanup data from three different diameter scrubbers over a wide range of radial accelerations. This together with physical considerations of the two-phase flow field suggest that the bubble size in the liquid layer is a key parameter in obtaining highly efficiency fine particle removal. The bubble size is reduced as the radial acceleration field in the CVS is increased. The radial acceleration can be increased by either reducing the device radius or increasing the inlet tangential velocity. Both of these tend to increase the device pressure drop. This suggests that although the CVS has a much more favorable scaling characteristic than most inertial separation devices, there may be a physical limit to the flow that could be handled by a single CVS at a reasonable pressure drop. At flows greater than this multiple CVS units can be employed to given efficient cleanup at low pressure drop. The device also has the potential for controlling SO_x emissions by suitable choice of the liquid scrubbing medium.

Under this contract the CVS concept has been verified at room temperature conditions and at small scale using a simulated coal flue gas. In order to allow further development of the device, tests should be carried out both at realistic flue gas temperatures and at larger scales. In addition, the potential for SO_x and NO_x removal should be evaluated. Future development work could be divided into the following areas (1) Conduct cleanup tests at high temperature coal flue gas conditions at the same small scale as the tests reported here; (2) Develop and test a larger scale device (capable of cleaning 25 times the flow-rate of the small unit) to be tested initially at ambient conditions and subsequently at realistic flue gas conditions; and (3) Test the potential of the CVS for SO_x (and possibly NO_x) removal.

6.0 REFERENCES

Avco Research Laboratory, 1982, " A Novel Hot Gas Cleanup Device," Internal Research and Development Reports, Avco Research Laboratory, Everett, Massachusetts.

Clift, R., Grace, J. R., and Weber, M. E., 1978, *Bubbles, Drops and Particles*, Academic Press.

General Electric, 1980, *Advanced Hot Gas Cleanup Concept Evaluation, Volume B: Developmental Cyclone Evaluation*, US DOE FE-2357-39-B.

Goldstein, R. J., 1971, "Film Cooling," in *Advances in Heat Transfer*, Academic Press, 1971.

Gyorke, D. F., 1987, "Emphasis, Goals and Participants of the DOE Advanced Combustion Technology Program," in *Proceedings: Emissions Control For Small-Scale Combustors Workshop*, Pittsburgh, Pennsylvania, November, 1987.

Haberman and Morton, 1953, David W. Taylor Model Basin Report No. 802.

Lewellen, W. S., and Stickler, D. B., 1972, "Two Phase Vortex Investigation Related to the Colloidal Core Nuclear Reactor," ARL TR 72-0037, Aerospace Research Laboratory, Wright Patterson Air Force Base, Ohio.

Marple, V.A., and Willike, K., 1976, "Inertial Impactors: Theory, Design and Use," in *Fine Particles*, edited by B. Y. Liu, Academic Press.

Martin, A. E., 1981, *Emission Control Technology for Industrial Boilers*, Noyes Data Corporation, Park Ridge, New Jersey.

Roeck, D. R., and Dennis, R., 1979, *Technology Assessment Report on Industrial Boiler Applications: Particulate Collection*, US EPA 600/7-79-178h, December 1979.

Santhanam, C. J., Lunt, R. R., et al., 1981, *Flue Gas Cleaning Wastes: Disposal and Ultilization*, Noyes Data Corporation, Park Ridge, New Jersey.

Schmidt, P., 1986, "New Results in Cyclone Design, Especially for High Pressure and Temperature Application" in *Gas Cleaning at High Temperatures*, I.Chem.Eng. Symp. Ser. No. 99, pp. 67-72.

Smith, J. L., 1962, "An Analysis of the Vortex Flow in the Cyclone Separator", ASME *Journal of Basic Engineering*, 84, pp 602-608.

Stickler, D. B., Lakshmikantha, H., and Lewellen, W. S., 1974, "Heat Transfer and Containment Processes in Two Phase Cavity Nuclear Reactor," ARL TR 74-0007, Aerospace Research Laboratory, Wright Patterson Air Force Base, Ohio.

Yellott, J. I., and Broadley, P. R., 1955, "Fly Ash Separators for High Pressures and Temperatures," *Industrial and Engineering Chemistry*, 47, pp. 944-952.